REGULATION OF MINERALOCORTICOID RECEPTOR AND ITS DOWNSTREAM TARGETS BY ESTROGEN AND ALDOSTERONE IN BREAST CANCER

A THESIS SUBMITTED TO
THE GRADUATE SCHOOL OF ENGINEERING AND SCIENCE
OF BILKENT UNIVERSITY
IN PARTIAL FULFILLMENT OF THE REQUIREMENTS FOR
THE DEGREE OF
MASTER OF SCIENCE
IN
MOLECULAR BIOLOGY AND GENETICS

By
Bircan ÇOBAN
November 2016

REGULATION OF MINERALOCORTICOID RECEPTOR AND ITS DOWNSTREAM TARGETS BY ESTROGEN AND ALDOSTERONE IN BREAST CANCER

By Bircan ÇOBAN

November, 2016

We certify that we have read this dissertation and that in our opinion it is fully adequate in scope and in quality, as a thesis for the degree of Master of Science.

_____

Özlen KONU

(Advisor)

_____

Murat Alper CEVHER

_____

Sreeparna BANERJEE

Approved for the Graduate School of Engineering and Science

_____

Ezhan KARAŞAN

Director of the Graduate School of Engineering and Science

Abstract

REGULATION OF MINERALOCORTICOID RECEPTOR AND ITS DOWNSTREAM TARGETS BY ESTROGEN AND ALDOSTERONE IN BREAST CANCER

Bircan ÇOBAN
M.S. in Molecular Biology and Genetics
Supervisor: Özlen KONU
November, 2016

Many women suffer from breast cancer worldwide thus accurate diagnosis of this disease has become an important issue for treatment options and improved clinical outcomes. Members of steroid hormone receptors, are a subfamily of nuclear receptors can serve as biomarkers in molecular classification of breast cancer. One of these, Mineralocorticoid Receptor (MR) takes part in many physiological processes in epithelial tissues including mammary epithelia, yet it is not well studied in the context of breast cancer. In this thesis, we investigated expression patterns of MR together with Glucocorticoid Receptor (GR) across multiple breast cancer cell lines at the protein level. Our study revealed that expressions of MR and GR were modulated in breast cancer as a subtype specific manner. We then enquired regulation of MR and its downstream targets, SGK1, NEDD4-2 and subunits of ENaC i.e., α, β and γ, by estrogen (E2) and aldosterone (ALDO) treatment in breast cancer via qPCR and Western Blotting. We found differential responses in expression of MR and its downstream targets to E2 and ALDO suggesting ER status was an important mediator of MR action. We also overexpressed MR in MCF7 cells and then showed that MR, NEDD4-2, β and γENaC mRNA levels increased in response to ALDO only when MR was overexpressed.

Keywords: Diagnosis, GR, MR signaling, downstream targets, SGK1, NEDD4-2, ENaC subunits, Estrogen, Aldosterone, breast cancer.

Özet

MEME KANSERİNDE MİNERALOKORTİKOİD RESEPTÖR VE MİNERALOKORTİKOİD RESEPTÖRÜN ALT AKIŞINDA YER ALAN HEDEFLERİNİN ÖSTROJEN VE ALDOSTERON TARAFINDAN DÜZENLENMESİ

Bircan ÇOBAN
Moleküler Biyoloji ve Genetik Bölümü Yüksek Lisans
Tez Danışmanı: Özlen KONU
Kasım, 2016

Dünyada pek çok kadın meme kanserinden mustarip olduğundan meme kanserinin kesin tanısı, hastalığın tedavi seçenekleri ve klinik sonuçları açısından önemli hale gelmektedir. Nükleer reseptörler ailesinin bir alttipi olan steroid hormon reseptörlerinin üyeleri, meme kanserinin moleküler sınıflandırmasında biyomarkör olarak kullanılmaktadırlar. Nükleer reseptör ailesinin bir üyesi olan mineralokortikoid reseptör (MR) meme epitelyal dokusunun da dahil olduğu epitelyal dokularda, pek çok fizyolojik süreçte görev almaktadır, henüz meme kanseri bağlamında yeterli olarak çalışılmamıştır. Bu tezde, MR ve GR'ın ekspresyon modelini protein seviyesinde farklı meme kanseri hücre hatlarında araştırdık. Çalışmamız MR ve GR'ın ekspresyonlarının meme kanserinin alt tiplerine özgü bir şekilde düzenlendiğini ortaya çıkarmıştır. Daha sonra, MR'ın ve MR'ın alt akışındaki hedefleri olan SGK-1, NEDD4-2 ve ENaC'ın α, β ve γ alt ünitelerinin estrojen (E2) ve aldosteron (ALDO) tarafından regülasyonlarını meme kanserinde, qPCR ve Western Blot aracılığıyla inceledik. MR ve alt akışındaki hedeflerin E2 ve ALDO'ya yanıtlarında, ER ekspresyon durumunun MR'ın aktivitesinde önemli bir aracı olduğunu belirten farklı cevaplar sergilediklerini bulduk. Ayrıca, MCF-7 hücrelerinde MR'ın ekspresyon seviyesini arttırdık ve sonra sadece MR'ın

ekspresyon seviyesi arttırıldığı zaman, MR, NEDD4-2, βENaC ve γENaC mRNA seviyelerinin ALDO maruziyetine yanıt olarak arttıklarını gösterdik.

Anahtar kelimeler: Diagnoz, GR, MR sinyal yolağı, alt akış hedefleri, SGK1, NEDD4-2, ENaC subunits, Östrojen, Aldosteron, meme kanseri.

Bana emeğin değerini öğreten canım babama…

Acknowledgement

First of all, I would like to thank my supervisor Dr. Özlen Konu, who has given me the chance to be a part of this project. I would like to thank COST ADMIRE (BM1301) action for supporting my Short Term Scientific Mission (STSM) through a collaboration between the Konu and Staub labs. I have special thanks to Dr. Olivier Staub and his lab members for all their support and hospitability. I thank the members of the jury, Dr. Sreeparna Banerjee and Dr. Murat Cevher, who were kind to spend their valuable time reviewing my thesis.

I would like to thank all members of Konu Lab, but especially Seniye Targen for her support and friendship. I am happy that I met her and have worked with her in the same project. I also would like to thank Erçağ Pinçe for his support and relieving coffee break conversations.

I owe special thanks to my dearest friends Ece Kartal, Ulduz Sobhiafshar, İlknur Çoban and Yağmur Ersoy, whose efforts made me forgot the distance between them and me; and to Aslı Taşpolatoğlu and Dilara Özkan, who have tried to be with me as much as possible.

I'm grateful to Erdem Akın Temel for all his support. My life in Bilkent would unbearable without him, since he tried to solve each problem of mine with kindness and love.

Finally, and most importantly, I'm deeply grateful to my father, who have thought me the value of endeavor and being respectful to my work, and to my mother who have always supported me, unconditionally.

This project was supported by a research grant (to OK) funded by The Scientific and Technological Research Council of Turkey (TUBITAK) (114S226) and COST

Action ADMIRE (BM1301). I was supported by Bilkent University Molecular Biology and Genetics department, and TUBITAK for my graduate studies.

Table of Contents

List of Figures

List of Tables

Abbreviations

11β-HSD1 / 2	11β-Hydroxysteroid dehydrogenase 1/2
ALDO:	Aldosterone
AR:	Androgen receptor
BRCA-1 / 2	Breast cancer 1/2
BSA	Bovine serum albumin
Dex	Dexamethasone
DBD	DNA binding domain
DMSO	Dimethyl sulfoxide
EGTA	Ethylene glycol-bis(β-aminoethyl ether)-N,N,N',N'-tetraacetic acid
ENaC	Epithelial sodium channel
ER/ESR1	Estrogen receptor
ERC	EnaC regulatory complex
ERE	Estrogen response element
Her2	Human epidermal growth factor receptor 2
FBS	Fetal bovine serum
GAPDH	Glyceraldehyde 3-phosphate dehydrogenase
GEO	Gene Omnibus database
GFP	Green fluorescent protein
GPL / GSE	Platform or Series accession number
GR	Glucocortioid Receptor
GRE	Glucocorticoid response element
HCC	Hepatocellular carcinoma
HEPES	4-(2-hydroxyethyl)-1-piperazineethanesulfonic acid
hrs	Hours
hGR	Human glucocorticoid receptor
hMR	Human mineralocorticoid receptor
HRE	Hormone response element
Hsp90	Heat shock protein
IGF-1	Insulin-like growth factor-1

LB	Luria broth
LBD:	DNA binding domain
LogFC	Log fold change
MR	Mineralocorticoid receptor
mTORC	Mammalian target of rapamycin
NEDD4-2 or	Neural Precursor Cell Expressed, Developmentally Down-
NEDD4L	Regulated 4-Like
PBS	Phosphate buffered saline
PDK1:	Phosphoinositide-dependent protein kinase-1
PGR / PR	Progesterone receptor
PI3K	Phosphatidyl-inositol 3-kinase
PKB	Protein kinase beta
PVDF	Polyvinylidene difluoride
RT	Room temperature
SDS	Sodium dodecyl sulfate
SGK1	Serum and glucocorticoid kinase-1
SHR	Steroid hormone receptor
SOB	Super optimal broth
TBS	Tris buffered saline
TEMED	Tetramethylethylenediamine
TFF1/pS2	Trefoil factor 1
TPT-1	Tumor Protein, Translationally-Controlled 1

Chapter 1

Introduction

1.1. Breast cancer

Breast cancer is a common cause of death for women. Although many prevention strategies and treatment options were developed over time, approximately 1 out of 10 women still face breast cancer throughout their lives[1]. The most important obstacle in front of forming successful therapies for breast cancer is its complexity that arises from genetic heterogeneity[2] among breast tumors. Therefore, researchers focus on understanding the molecular basis of this heterogeneity by categorizing breast cancer into types, based on histological, pathological and molecular features of breast tumours[3].

Broadly, breast cancer can be categorized under two histological types, which are *in situ* carcinoma and invasive (infiltrating) carcinoma[3]. *In situ* carcinomas are divided into two sub-types by being either ductal or lobular. Invasive carcinoma has six main sub-types: Tubular, ductal lobular, invasive lobular, infiltrating ductal, mucinous (colloid), medullary and infiltrating ductal[3]. Breast cancer arises from hyper-proliferative ductal cells and differentiates into ductal carcinoma *in situ* and may become metastatic at final stages[1-2]. Many breast cancer cases are invasive ductal carcinomas[1].

Pathological classification of breast cancer relies on histological features of breast tumours[4]. Grade of tumor is defined by differentiation and proliferation potential of

breast tumours[4-5] and grading scores (from 1 to 3) are finalized by adding each feature as points into the grading scores[6].

Molecular subtypes of breast cancer are defined by molecular expression profiles of three hormone receptors: Estrogen receptor (ER), Progesterone receptor (PR) and human epidermal growth factor receptor 2 (Her2). A sub-type classification based on these hormonal status forms the five molecular subtypes of breast cancer: Luminal (A and B), Basal, Her2 overexpressing, Claudin-low, Normal like- breast cancers[7].

Many genes are also dysregulated in breast cancer and classifications can be generated by using mutations that occur in tumors. Mutations in BRCA1 and BRCA2 genes disrupt the cell cycle progression involved in DNA damage thereby leading to genomic instability. P53 as a tumor suppressor gene in breast cancer also takes a crucial part in regulation of cell cycle, growth and apoptosis[1].

1.2. Steroid Hormone Receptors and cancer

As a member of nuclear receptors, Steroid Hormone Receptors (SHRs) are synthesized from cholesterol and transported to the blood circulation via proteins such as albumin and transcortin.[8]

Steroid receptor family is composed of five members: Androgen, Estrogen, Glucocorticoid, Progesterone and Mineralocorticoid receptors. Receptors with corresponding ligands are listed in Table 1.2.

Table 1.1: Steroid hormone receptors, specific nomenclatures and ligands.

Steroid receptors	Abbreviation	Nomenclature	Ligand
Androgen receptor	AR	NR3C4	Testosterone
Estrogen receptor	ERα	NR3A1	Oestradiol-17β
	ERβ	NR3A2	
Glucocorticoid receptor	GR	NR3C1	Cortisol
Mineralocorticoid receptor	MR	NR3C2	Aldosterone (ALDO), cortisol
Progesterone receptor	PR	NR3C3	Progesterone

All members of the steroid receptor family resemble each other in terms of structure. They possess an N-terminal domain also called as ligand binding domain (LBD) for ligand-dependent transcriptional activity, and a DNA binding domain (DBD) recognizing the hormone response element (HRE) of target genes in a sequence specific manner. There is a link between DBD and LBD provided by hinge region responsible for forming sites for posttranslational modifications of the receptors and interfaces for dimerization[9-10-11].

SHRs function in many physiological processes such as metabolism, inflammation and lipid signaling[12-13-14]. Functions of SHRs rely on their action as transcription factors in response to certain types of ligands (e,g, glucocorticoids, estrogen[15]/17-ß Estradiol (E2).) or signal molecules (e.g., retinoid, vitamin D3, thyroid hormone[15]) within cells. Therefore, SHRs are called as ligand-dependent transcription factors in the literature.

Genomic actions of SHRs are triggered by binding of steroid hormone/ligand to their cognate receptors either in the cytosol or membrane. SHRs undergo conformational changes upon ligand binding thus they are released from chaperons which are bound to receptors in their inactive state. SHRs translocate into nucleus and then make homodimers. They act as transcription factors by binding to sequence specific recognition elements/hormone response element (HRE)/enhancer sequences within regulatory region of target genes and recruit general transcription factors and

coregulatory proteins to target DNA resulting in either transcriptional activation or repression of target genes[15-16-17].

Considering the physiological roles of SHRs, disruption of SHR signal transduction may contribute to growth and development of various types of cancers. Alterations in steroid hormone receptor signaling affect breast cancer since it is hormone dependent. Certain members of SHR family have pivotal roles in progression, development and maintenance of tumor growth in breast cancer[18]. For example, it has been previously shown that E2 signaling acts a mitogen thereby activating several cyclin genes resulting in cell cycle progression of breast cancer cells[19]. It also takes part in activation of major signaling pathways related to growth and progression of breast cancer by cross-talking with other growth factor receptors[19]. On the other hand, glucocorticoids possessing an anti-inflammatory feature, induce apoptosis in lymphomas and leukaemia[20] whereas androgen receptor signaling (AR), a key regulator of normal prostate development, is disrupted in prostate cancer[21]. Since they have crucial roles in initial stages and progression of cancers, SHRs are used as targets for drug therapy against many hormonally-responsive cancers[22].

1.2.1. Mineralocorticoid Receptor (MR) signalling

NR3C2 gene localized on chromosome 4q31.1-4q31.2 encodes the Mineralocorticoid Receptor (MR) in human[23]. Human MR (hMR) is composed of 10 exons of which first two are called as "1α and 1β", and are not translated into protein. Transcripts of hMR, hMRα and hMRβ are constituted by these two untranslated exons while promoters located in these exons regulate gene expression of MR[24]. A 107kDa MR protein is translated from hMR mRNA in target tissues of mineralocorticoid hormone[25]. MR shares a common structure with other members of steroid hormone receptor family (Figure 1.2).

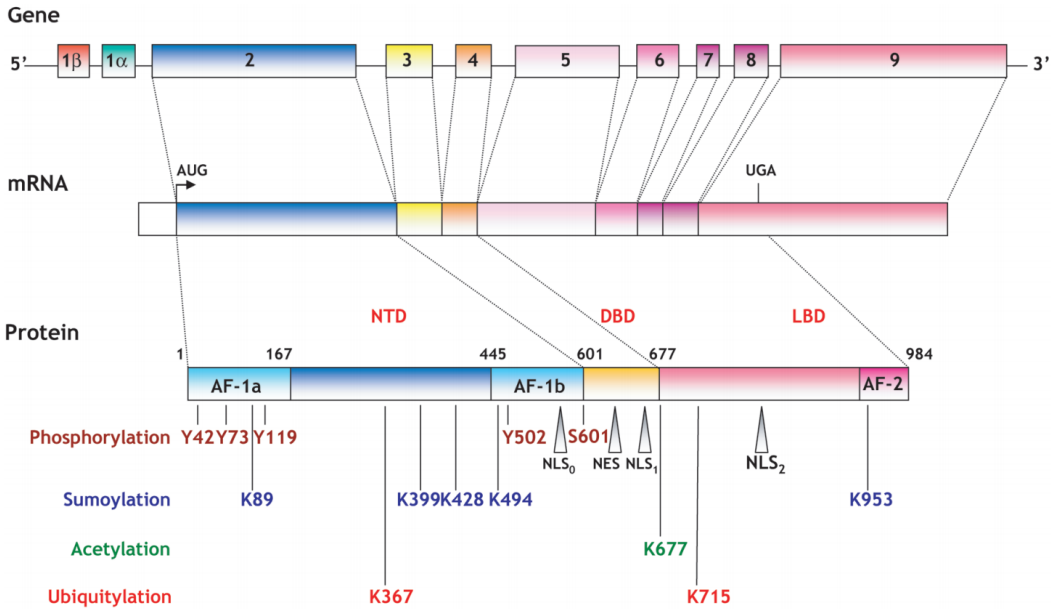

Figure 3.1: Genomic structure of human mineralocorticoid receptor.
*Figure was taken from "Viengchareun et. al. The mineralocorticoid receptor: insights into its molecular and (patho) physiological biology. Nucl Recept Signal 2007 30; 5:e012"

Expression of MR is seen in various epithelial and non-epithelial tissues. MR is mostly known as a regulator of salt and water balance in kidney, colon and skin[26]. MR expression is also reported in the ducts and secretory tubules of mammary epithelia[27]. MR exhibits tissue specific functions in non-epithelial tissues[28] such as adipocyte differentiation[28-29], regulation of blood pressure, hemodynamic homeostasis, salt appetite[30] in cardiovascular system and behavioral responses like memory[31] in brain. A pro-inflammatory role of MR has also been demonstrated in cardiovascular system in the Rickard et. al.[32] study.

Tissue specific ligands of MR decide the genomic actions of MR that has two main physiological ligands, ALDO (mineralocorticoids) and cortisol (glucocorticoids) [33].MR possesses higher affinity towards its ligands in both the epithelial and non-epithelial tissues besides both ligands exhibit same affinity to MR in epithelial tissues.[33-34] Ligand selectivity of MR in epithelial tissues relies on activity of 11β-hydoxy-steroid dehydrogenase type 1 (HSD11B1) and 11β-hydoxy-steroid dehydrogenase type 2 (HSD11B2) enzymes[35]. Type 1 enzyme possesses a reductase function thereby producing active cortisol/glucocorticoid from inactive 11-dehydro metabolites (corticosterone). As a result of this reaction, level of circulating

glucocorticoids in blood increase and receptor becomes occupied by glucocorticoids. Type 2 dehydrogenase/11β-HSD2 converts cortisol into cortisone, which is an inactive form of the ligand, thereby decreasing the circulating level of cortisol and making the ligand binding site of the receptor available for aldosterone binding in epithelial tissues[35-36-37].

Once MR is occupied by its tissue specific ligand, a conformational change is triggered. In the inactive state, MR makes a hetero-oligomeric complex with heat shock protein 90 (Hsp90) in the cytosol and conformational change of MR results in disruption of this complex[38-39]. After dissociation, MR translocates to the nucleus; receptor homodimerization occurs; and MR binds to the hormone response element of its target gene(s). All these results in transcriptional activation or repression of target gene(s) [32-39-40-41] (Figure 1.2).

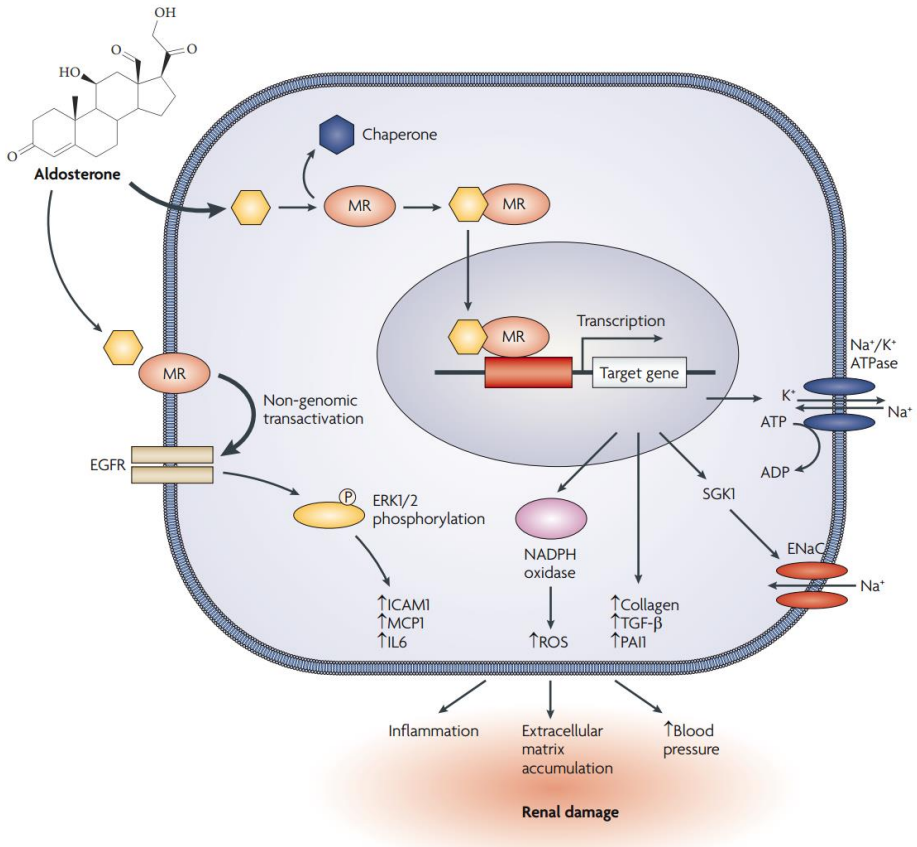

Figure 1.4: Genomic actions of mineralocorticoid receptor.

*Figure was taken from "Norberto Perico et. al, Nature Reviews Drug Discovery, 2008 vol 7 no 11."

Non-genomic actions of MR are mediated through its activation by its tissue specific ligand, aldosterone (ALDO) for most of the epithelial tissues, and then transactivation of epidermal growth factor receptor (EGFR). EGFR further phosphorylates and activates extracellular signal-regulated kinases (Erk 1/2) thus stimulates tissue-specific non-genomic actions of ALDO induced-MR[40].

MR activity and signaling is regulated by post-translational modifications such as phosphorylation, ubiquitination, methylation and other modifications. Receptor stability and turnover of MR are modulated by phosphorylation and ubiquitination[42]. It has been previously demonstrated that MR is a phospho-protein and commonly, phosphorylated at the serine/threonine residues within ligand binding domain. Phosphorylation leads to an upward shift in molecular weight of MR in immunoblots[43]. On the other hand, ubiquitination also affect MR activity. Receptor activation upon ligand binding triggers poly-ubiquitination of MR that remains in a mono-ubiquitiylated form in the cytosol[44] and later, the MR receptor is degraded by proteasomes[45].

1.2.2. MR signalling in cancer

Members of steroid receptor family are commonly dysregulated in hormonally responsive cancers such as lung, breast, colon, prostate. As mentioned earlier, expression patterns of these receptors could be utilized in categorization of hormone-dependent diseases. However, there are only a few studies showing importance of MR function and its potential dysregulation in cancer.

MR has been considered as a biomarker for lung cancer and increased MR expression is linked with better patient prognosis[45]. MR also participates in development of hepatocellular carcinoma (HCC) by regulating energy metabolism of the liver. In fact, the downregulation of MR expression results in poor prognosis in HCC[46]. On the other hand, decreases in expression level of MR might influence tumor growth and progression by inducing angiogenic pathways as shown in colorectal cancer.[47-48] Moreover, research has shown that glucocorticoid receptor expression decreases in breast tumor progression. Due to the possible interactions of

glucocorticoid and mineralocorticoid receptors in the breast tissue, it is suggested that MR expression may be lower in breast tumorigenesis[49].

1.2.3. Glucocorticoid Receptor (GR) signalling

Human glucocorticoid receptor (hGR) is another member of SHR family and encoded by NR3C1 gene (located in 5q31Y32) that is constituted by 9 exons[50]. Two alternative splices in Exon 9 form two isoforms of hGR protein which are hGRα and hGRβ having 97kDa and 94kDa molecular weights, respectively[51]. There are 13 identified variants of hGR formed by multiple promoter regions within exon 1[52-53]. HGR is generated by common domain structures of steroid hormone receptors. HGR has functions in almost all tissues and organs in human body. Many cellular processes i.e., cell differentiation and proliferation, glucose metabolism, maintenance of homeostasis as response to stress[54], and regulation immune system[55], are controlled by GR.

Genomic action of GR is initiated by binding of glucocorticoids/cortisol to the receptor and then continues with GR's dissociation from heat shock proteins and its shuttling to nucleus. After nuclear translocation, GR binds to glucocorticoid response element[56] (GRE) in the promoter site of target genes and mediates transactivation of these genes[57-58-59].

GR exhibits its activity as a transcription factor via either DNA-dependent or independent actions which are through either crosstalk with other transcription factors like other members of steroid receptor family, NF-κB[60-61] or interactions with kinases[62]. GR also make interactions with other members of SHR family and this results in various tissue-specific actions. For example, ALDO and synthetic agonist of glucocorticoids called as Dexamethasone (Dex) interact with PR, mimicking the progesterone functions and leading to growth inhibition and focal adhesion in breast cancer cells[63]. In another study, GR antagonist exerts its effects on ER transcriptional activity through direct protein-protein interactions in the E2-induced ERα + breast cancer cells[64]. A recent work by Karmakar et. al shows that coexpression of GR and ER results in better survival in the ER + breast cancer patients[65].

1.2.4. GR signalling in breast cancer

Glucocorticoids are commonly used as premedication for chemotherapy in hormonally responsive cancers like breast and prostate to reduce toxicity and side effects of chemotherapeutic reagents[66]. Moreover, studies with normal breast cells revealed presence of anti-proliferative and anti-apoptotic properties of glucocorticoids in mammary epithelia[67-68]. These features of glucocorticoids and GR are also studied in the context of breast cancer. It has been shown that GR protects cancer cells from apoptosis by modulating survival genes like SGK1[69]. There is a recent study indicating inhibitory effect of Dex on proliferation of the breast cancer cell line, MCF-7[70]. On the other hand, GR expression is reduced in parallel with breast cancer progression[71-72]. When the disease becomes more progressive and aggressive, GR expression is downregulated in breast tumours. In addition, expression levels of GR in tumour cells affect patient survival in a molecular subtype specific manner in breast cancer. It has been reported that tumour cells with high GR expression show poor survival in ER – breast cancer[73].

1.3. Downstream targets of MR in epithelial tissues

Mineralocorticoid receptor signalling affects expression patterns of several genes since it is expressed in multiple tissues. Several tissue-specific downstream targets of MR are summarized in Table 1.3.

Table 1.2. Downstream targets of MR in epithelial tissues.

Target genes	Tissues	Functions	References
αENaC subunit	Kidney	Na^+ transport	[Bens et al., 1999; Masilamani et al., 1999]
	Inner ear	Remains to be elucidated	[Teixeira et al., 2006]
β/γENaC subunits	Colon	Na^+ transport	[Epple et al., 2000]
α1/β1 Na^+,K^+-ATPase subunits	Kidney, colon	Na^+ transport	[Kolla and Litwack, 2000]
CHIF	Kidney, colon	Na^+ transport	[Brennan and Fuller, 1999; Wald et al., 1996]
K-ras2	Colon	Remains to be elucidated	[Brennan and Fuller, 2006]
ELL	Kidney	Elongation factor	[Pascual-Le Tallec et al., 2005]
SGK1	Kidney, colon	Na^+ transport/Nedd-4-2 phosphorylation/ENaC trafficking	[Naray-Fejes-Toth et al., 1999] [Chen et al., 1999] [Bhargava et al., 2001]
GILZ	Kidney	Na^+ transport/inhibition of ERK cascade	[Soundararajan et al., 2005]
Usp2-45	Kidney, colon	ENaC deubiquitylation	[Fakitsas et al., 2007]
KS-WNK1	Kidney	Na^+ transport	[Naray-Fejes-Toth et al., 2004]
NDRG2	Kidney, colon	Putative ENaC activation	[Boulkroun et al., 2002; Wielputz et al., 2007]
ET-1	Kidney, colon	Vasoconstriction? Remains to be elucidated	[Wong et al., 2007]
PAI-1	Kidney	Initiation of glomerulosclerosis? Remains to be elucidated	[Yuan et al., 2007]

*Table was taken from "Viengchareun, S., Le Menuet, D., Martinerie, L., Munier, M., Pascual-Le Tallec, L., & Lombès, M. (2007). The mineralocorticoid receptor: insights into its molecular and (patho) physiological biology. Nuclear Receptor Signaling, 5, e012."

1.3.1. Serum Glucocorticoid Kinase-1 (SGK1)

SGK1 is one of the downstream targets of MR in colon and kidney (Table 1.3). It belongs to the AGC protein kinase family, a subfamily of serine/threonine kinases. The members of this subfamily phosphorylate their targets/substrates at serine or threonine residues within the target proteins. The gene controlling SGK1 expression (located in 6q23) consists of 14 exons and encodes 49 kDa protein product[74]. SGK1 has two paralogs expressed in human, named as SGK-2, SGK-3[75]. SGK proteins that have similar structure of protein kinase B (PKB)/Akt family of kinase. The SGK structure is constituted by an N-terminal domain, a kinase domain for its catalytic activities involving threonine residues in its activation loop, and a C-terminal domain involving serine residues[76]. Serine and threonine residues modulate complete activity of SGK1 and phosphorylation of its substrates[76].

SGK1 expression occurs nearly in all tissues. Activation of SGK1 is controlled by external stimuli. SGK1 has transcription factor binding sites for GR as well as MR[77] and its activation relies on its phosphorylation by phosphatidyl-inositol 3-kinase (PI3-K) on serine residues and by 3-phosphoinositide dependent kinase PDK1 on threonine residues. Upon activation, growth factors such as serum and glucocorticoids as well as mineralocorticoids stimulate SGK1 translocation to the nucleus[78-79].

SGK1 facilitates the regulation of cell volume, ion channel activity and thus cell survival and apoptosis. In colon and kidney, epithelial sodium channel (ENaC) activity is modulated by SGK1 expression known to be stimulated upon ALDO induction through MR signaling[80]. It has been reported that SGK1 expression is upregulated during cell shrinkage thus SGK1 induces the activity of ion channels which take part in increase of cell volume[81]. Role of SGK1 in survival relies on its activation by PI3K that belong to a survival signaling pathway- and its relation with Akt, the serine/threonine kinase. SGK1 stimulates the survival signals via phosphorylating the downstream targets in the PI3K-Akt pathway[82]. A study with low and high grade DCIS demonstrates that SGK1 expression is increased in parallel with the disease grades[83]. Another study demonstrated that increases in the expression of SGK1 exerted anti-apoptotic role in breast cancer cells. When knock down study was performed to decrease expression levels of SGK1, breast cancer cells became more sensitive to chemotherapy in response to the decrease in SGK1 expression levels[84].

1.3.2. Neural precursor cell expressed developmentally downregulated gene 4-like (NEDD4-2)

MR signaling modulates the activity of certain genes as its downstream targets. Neural precursor cell expressed developmentally downregulated gene 4-like, NEDD4-2 (NEDD4L) is one of those genes regulated by MR activity in epithelial tissues[85].

NEDD4-2 is a member of NEDD4-like E3 ubiquitin ligases and encoded by NEDD4 gene (located in 15q21.3) which has 30 exons. The NEDD4-2 protein product is

~120 kDa and family consist of 9 members (NEDD4-1, NEDD4-2, WWP1, WWP2, Smurf1, Smurf2, ITCH, NEDD4L1, NEDDL2)[85]. All members share a common structure involving C2 domain for membrane binding WW domains for controlling substrate selectivity through interactions with phospho-serine/threonine residues or PY (PPXY) motif in substrates, and a HECT domain for ubiquitin ligase function[86]. NEDD4-2 is mainly localized in the cytoplasm and exerts its function in tissues such as kidney, lung, and heart[87].

As an E3 ubiquitin ligase, NEDD4-2 tags substrates for ubiquitination mediated proteosomal degradation[85]. NEDD4-2 mainly functions as a regulator of growth factor signaling and ion transport. ENaC is one of the substrates of NEDD4-2; and NEDD4-2 leads to proteosomal degradation of ENaC in epithelial tissues. SGK1 as an ALDO induced gene facilitates the NEDD4-2 mediated alterations in expression and degradation of ENaC in the colon and kidney[88-89]. In addition, cell surface expression of insulin-like growth factor (IGF-1) receptor is modulated through NEDD4-2 actions[90].

Besides its normal physiological role, NEDD4-2 also participates in tumorigenesis. Altered expression patterns of NEDD4-2 are associated with tumour invasiveness and worse clinical outcomes of the disease. Furthermore, copy number loss in the chromosomal location of NEDD4-2 gene appears in many cancer types including the breast cancer and affect tumour aggressiveness[91].

1.3.3. Epithelial Sodium Channel (ENaC)

Epithelial Sodium/Na^+ channel (ENaC) as a transmembrane protein is another downstream target of MR signaling in epithelial tissues. There are four subunits of ENaC (α, β, γ and δ) and trimeric complexes made up of α, β, γ[92-93] constitute the functional epithelial sodium channel. Chromosomal locations of genes encoding β and γ subunits are chromosome 16p while αENaC is on chromosome 12p and δENaC is on chromosome 1p. Subunits have 13 exons and encode 100 kDa, 73kDa, 76 kDa and 70 kDa gene products for α, β, γ and δ, respectively[94].

Subunits of ENaC are the members of Degenerin superfamily. Each subunit is structured by the extracellular loop/domain, two helices crossing the membrane thus forming cytoplasmic N-terminal and C-terminal domains. Cytoplasmic parts of the channel involving PY motifs provide sites for protein-protein interactions and posttranslational modifications for channel trafficking and gating whereas extracellular loop directs the movement of channels to the cell surface[95]. ENaC is also known as amiloride sensitive sodium channel; and amiloride blocks Na^+ transport by binding domains within the extracellular loop of ENaC[96].

ENaC is placed in apical membrane of epithelial cells. All three subunits of ENaC come together in the endoplasmic reticulum, undergo posttranslational modifications through Golgi and then they are delivered to the membrane. Receptor is placed to the membrane in an unstable form and matured by ENaC regulatory molecules. These processes are fundamental for the maximum activity of the channel[93]. ENaC activity depends on the number of channels which is managed by a dynamic relation between degradation and new synthesis of the channel on the cell surface. ENaC activity, expression and its stability on membrane are controlled by ENaC regulatory complex involving SGK1 and NEDD4-2[97-98].

ENaC is expressed in the lung, kidney and mammary epithelial cells as well as in breast cancer cells (MCF-7 and T-47D)[98-99]. The main role of ENaC in epithelial tissues is to facilitate in regulation of Na^+ transport and and the blood pressure in a hormone dependent manner[97]. SGK1 and NEDD4-2 modulates Na^+ transport and ion homeostasis via ALDO induction in colon and kidney[100]. On the other hand, ENaC is post-translationally modified by NEDD4-2. NEDD4-2 binds to PY motifs of αENaC and γENaC by its WW domains and stimulates receptor internalization and further degradation by the proteasome thus functioning in receptor stability and abundance[100]. Another regulatory mechanism influencing the ENaC activity is proteolytic cleavage of α and γ subunits of ENaC. Tissue-specific proteases take part in these cleavage processes. For example, Furin acts as a protease cleaving αENaC and γENaC from their extracellular loops thus functioning in channel maturation and activation[101].

Unlike physiological functions, ENaC is also involved in different mechanisms in cancer. Contribution of αENaC to cell proliferation was shown in hepatocellular carcinoma cells. It has been suggested that ENaC mediated Na^+ influx might act as a mitotic signal triggering cell cycle of cancer cells[102]. Since ENaC modulate Na^+ transport, it affects cell shape and stiffness through regulating cell volume. Therefore ENaC takes part in cell migration and invasion in cancers. Silenced αENaC expression results in decrease migration of melanoma cells[103]. In addition, αENaC and γENaC participate in invasion of glioma cells[104]. As a result of these actions, it has been suggested that ENaC might contribute cancer development. There is also a study showing potential action of ENaC in breast cancer. Increased release of reactive oxygen species is found to be associated with upregulated of γENaC levels in breast cancer[105].

1.4. Regulation of downstream targets of MR

1.4.1. Mechanism of ENaC Regulation by SGK1 and NEDD4-2

Epithelial sodium channel has a pivotal role in regulation of Na^+ homeostasis and blood pressure. Molecular mechanism underlying the ENaC regulation is constituted by an interplay between SGK1 and NEDD4-2 in kidney, colon and cardiovascular disease. ALDO triggers MR-mediated activation of SGK1. Active SGK1 phosphorylates NEDD4-2 by interacting with serine residues in the PY motif of NEDD-2. Phosphorylated NEDD4-2 becomes functionally inactive due to conformational changes in its PY motif and could not be able to interact with ENaC via its WW domains. Therefore, cell surface abundance of ENaC is increased as a result of SGK1/NEDD4-2 pathway[89-100-106-107].

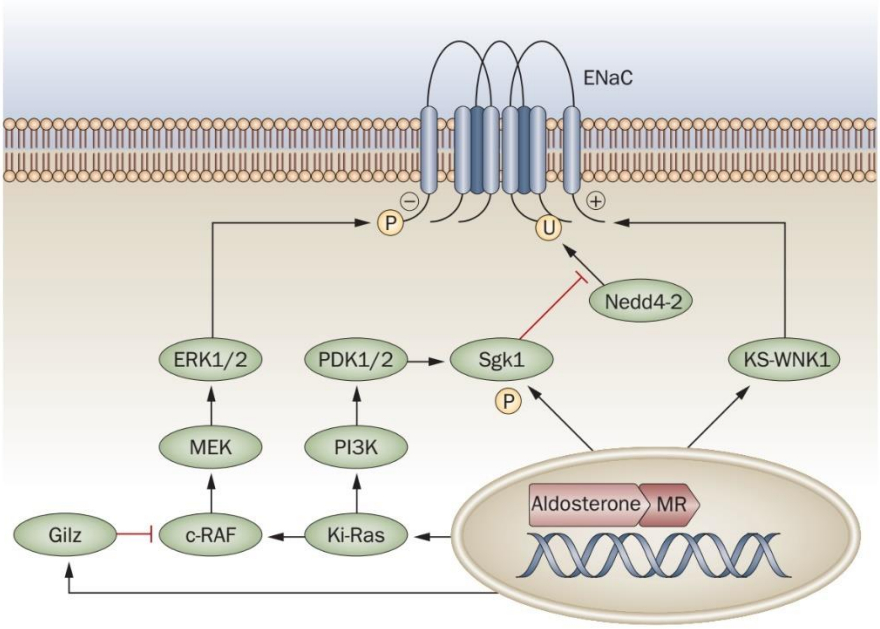

Figure 1.3: Regulation of ENaC in cardiovascular diseases and kidney.
*Figure was taken from "Briet, M., & Schiffrin, E. L. Aldosterone: effects on the kidney and cardiovascular system. Nat Rev Nephrol (2010), 6(5), 261–273."

1.4.2. E2 and ALDO treatments: Effects on MR targets

E2 as a steroid hormone with roles in many physiological processes involving mammary development, fluid balance, and heart diseases in various tissues such as ovary, testis, mammary gland, prostate and heart[108]. Biological functions of E2 are managed by the Estrogen Receptor (ER/ESR1). There are two subtypes of ER, ERα and ERβ in mammals and each is expressed from ESR1 (NR3A1- locating 6q25.1) or ESR2 (NR3A2-locating 14q23-24.1) genes, respectively. ERα and ERβ consist of 8 exons which form splice variants of each gene and producing 67 kDa, 59 kDa protein products for ERα and ERβ[108-109]. Multiple promoter sites control tissue specific action of ER. ER is formed by common structural parts of SHRs. In addition, ER exerts its functions through following the same activation processes occur in the MR and GR activation. ER binds to estrogen responsive elements (ERE) [77] of target genes thereby modulating the expression patterns of its target genes[110].

Genes regulated by MR signaling i.e., SGK1, NEDD4-2 and ENaC are also regulated by E2 in different tissues. SGK1Studies with E2 revealed its regulatory role on

SGK1 in myocardium[111]. In addition, mammalian target of rapamycin complex (mTORC) mediates phosphorylation of SGK1 and studies with ER + breast cancer cells suggest that E2 induction and ER activity might be necessary for the action of mTORC on SGK1[112]. Subunits of ENaC are also modulated by E2 differentially reported in studies with kidney, lung and osteoblasts. E2 treatments result in increases in expressions of αENaC and βENaC in kidney and lung at the mRNA level whereas no change is detected in the expression levels of γENaC [113-114]. In contrast, both mRNA and protein expressions of αENaC and γENaC are upregulated in response to E2 in osteoblasts[115]. E2 effect also investigated in MLE-12 cells (murine lung epithelial cells). E2 exposure caused no change in mRNA expression levels of ENaC subunits (namely α, β and γ) after LPS induction in MLE-12 cells[116]. On the other hand, there is a published study indicating E2-activated ERα receptor blocks the transcriptional activities of MR via making inhibitory complex with MR in nucleus in kidney cells[117].

Another regulator of SGK1, NEDD4-2 and ENaC in epithelial tissues is the ligand of MR, ALDO. ALDO facilitates ion transport by regulating interaction of SGK1 and NEDD4-2 thus changing the cell surface expression and abundance of ENaC. Increases in circulating aldosterone levels induce the protein abundance of αENaC while no effect occurs in other subunits in kidney[118]. As explained in 1.4.1 part of the Introduction, a rapid upregulation in expression of SGK1 occurs in response to ALDO and activities of SGK1 through NEDD4-2 leading to decreased abundance and cell surface expression of ENaC[77-80-106].

1.4.3. MR overexpression

MR downstream targets can also be modulated by alterations in MR transcriptional activity. Since MR is a phospho-protein and it is hard to detect it in stable form due to its further proteosomal degradation, overexpression of MR has been performed in various tissues including kidney, cardiomyocytes to study tissue specific actions of MR. Alnemri et. al[119]. established the first study on MR overexpression, by using *Spodopteru frugiperda* (Sf9) insect cells. Human renal mineralocorticoid receptor was overexpressed in insect cells and its phospho-protein feature, activity and nuclear translocation upon ALDO stimulation were shown[119]. Most of the studies

involving MR overexpression have been performed by using *in vivo* mouse models. In addition, MR has been overexpressed in mouse cortical collecting duct kidney cell line ($mmCCD_{cl1}$) to study ubiquitination process of MR protein[43]. Two MR expression vectors, i.e., Pcmv4-hMR and pcDNA3.1-S-tag MR, have been used in this study. In another study, MR has been overexpressed in rat cardiomyoblast cell line to decipher downstream targets of ALDO in cardiomyocytes[120].

1.5. Aim of the Study

Patients with breast cancer have high mortality rates so that the diagnosis of this cancer plays a pivotal role for better clinical outcomes. Some members of nuclear receptor family are commonly used as biomarkers for disease diagnosis and prognosis. Recently, Jeong et.al. (2010) demonstrated that MR as a member of nuclear receptor family members, is downregulated in lung cancer. Accordingly, higher MR expression is associated with better patient survival and good prognosis in lung cancer[121]. Furthermore, there are other studies performed in HCC and colorectal cancers supporting the decreased expression pattern of MR and its relation with cancer progression[46-47].

The first hypothesis of this study is that expression of MR and GR, both being from the same receptor family and share ligands, might exhibit a similar pattern in breast cancer. There is no study in literature that shows the correlation of MR and GR at the protein level in breast cancer. Furthermore, an *in-silico* analysis of laser dissected epithelial tissues from breast tumour and non-tumour tissues (GSE54002) showed that non-tumour tissues exhibited relatively low MR expression compared to tumors (Study performed by Huma Shehwana, Konu Lab, Bilkent University). This phenomenon results in worse clinical outcomes and poor prognosis in breast cancer patients (kmplot.org). Similary GR also exhibited prognostic significance (Hazard ratio= 1.09 (0.98-1.22). Thus, our first aim was to experimentally validate our *in-silico* analysis by investigating expression patterns of MR at protein level, using protein samples extracted from various subtypes of breast cancer cell lines. In addition, we also investigated expression patterns of GR and enquired possible correlations in expression patterns of MR and GR proteins in the same set of breast cancer cell lines. We hypothesized that MR and GR might display similar expression

patterns across breast cancer cells since both receptor share structural and ligand similarities. This will reveal the significance of MR and GR in breast cancer subtyping for better diagnosis and prognosis of the disease and provide in vitro cell line models for further study in breast cancer.

Our second motivation was to decipher regulatory role of ALDO and E2 on downstream targets of MR signaling which were previously established in epithelial tissues as being modulated by MR. Results of this study will help identify whether there are similarities between breast tissue and other epithelial tissues and cancers. Three subunits of ENaC and its regulators, SGK1 and NEDD4-2 have been well-studied in terms of their regulations by ALDO stimulated MR signaling in kidney, cardiovascular diseases and the colon[77-80-106]. While some of these genes such as SGK1 and γENaC individually function in breast cancer, regulation and expression profiles of all these molecules remain unknown for breast cancer in the literature.

We performed an *in-silico* analysis of breast cancer microarray datasets by using Gene Expression Omnibus (GEO) database in line with our aims. We have found studies that reveal E2 (or Estrogen Receptor (ER), ESR1) dependency of ENaC (its three subunits) and its regulators[122-123-124-125].
Thus, this lead us to study interactions among these proteins in relationship to the ER status in breast cancer and compare our *in vitro* results with the *in silico* findings in the context of this aim. In addition, there is only one study in the literature showing ER inhibitory action on MR transcriptional activity in kidney cells[118]. E2's effect on expression levels of MR in breast cancer is also a missing point in the literature. Therefore, expression modulation in response to E2 and/or ALDO exposures need to be further investigated to reveal regulation of MR and its targets in breast cancer.

Last aim in this study was to perform an overexpression of MR in breast cancer cells. Since MR was downregulated in breast cancer, the overexpression of MR will help functional studies to find out novel signaling pathways and MR effects on the transcriptome in breast cancer. Moreover, future studies may analyze MR activity in relation with its downstream targets using this overexpression model.

Chapter 2

Materials and Methods

2.1. Materials

2.1.1. General Laboratory reagents and materials:

Laboratory materials, reagents and kits used in this study are listed in Table 2.1.

Table 2.1: General laboratory reagents, materials, and kits.

Name	Company	Catalog number
Cryovial	Grenier-Bioone, Germany	122280
Hemocytometer	Interlab, Turkey	Neubauer Improved
6-well plate	Grenier bio-one, Germany	657160
96-well plate	Grenier bio-one, Germany	655180
100 mm dish	Grenier bio-one, Germany	664 160
T-25 flask	Grenier bio-one, Germany	690175
T-75 flask	Grenier bio-one, Germany	658175
Serological pipettes	Corning, USA	4487-88-89
Cell scraper	Corning, USA	CLS3010

Trypan Blue	Sigma Aldrich, USA	T8154
QIAzol lysis reagent	Qiagen, Germany	79306
RNase ZAP	Sigma Aldrich, USA	R2020
Nuclease free water	Lonza, Switzerland	BE-51200
LightCycler 480 Multiwell plates-96, White	Roche, USA	04 729 692 001
LightCycler SYBR Green I Master	Roche, USA	4707516001
iScript cDNA synthesis kit	BioRad, USA	17008891
Complete EDTA-free protease inhibitor cocktail tablets	Roche, UK	11873580001
PhosSTOP easypack phosphatase inhibitor cocktail tablets	Roche, UK	4906845001
BCA Protein Assay kit	Thermo Scientific, USA	23227
4X Laemmli Sample Buffer	BioRad, USA	161-0747
Ponceau S solution	Sigma Aldrich, USA	P-7170
Page Rule Prestained Protein Ladder	Thermo Scientific, USA	26616
PVDF membranes	Roche, UK	3010040001
TGX Stain-Free™ FastCast™ Acrylamide Kit, 12%	BioRad, USA	1610185
TGX Stain-Free™ FastCast™ Acrylamide Kit, 7.5%	BioRad, USA	1610181
TGX Stain-Free™ FastCast™ Acrylamide Kit, 10%	BioRad, USA	1610183

Blue medical X-ray film	Carestream, USA	8143059
Western Bright Quantum Western Blotting Detection kit	Advansta, USA	K-12042-D10
Super RxN medical X-ray film	Fujifilm, Japan	4741019318
Hypercassette Autoradiography cassette	GE healthcare, UK	RPN11643
NucleoSpin MiniPrep plasmid isolation kit	Macherey-Nagel, Germany	740588.50

2.1.2. Chemicals

Chemicals used for buffer and solution preparations for protein, RNA, plasmid studies etc. are listed in Table 2.2.

Table 2.2: Chemicals used in protein, RNA, plasmid, and cell culture studies.

Name	**Company**	**Catalog number**
Ethanol	Sigma Aldrich, USA	32221
Methanol	Sigma Aldrich, USA	24229
Chloroform	Sigma Aldrich, USA	24216
Isopropanol/2-propanol	Sigma Aldrich, USA	24137
Trizma base	Sigma Aldrich, USA	T1503
Tween-20	Merck, USA	822184
Sodium chloride	Carlo Erba, Italy	479687
Hydrogen chloride	Sigma Aldrich, USA	07102
Sodium hydroxide	Carlo Erba, Italy	480507
BSA	Sigma Aldrich, USA	A7905

Ammonium persulfate	Carlo Erba, Italy	420627
TEMED	BioRad, USA	1610800
6-aminocaproic acid	Sigma Aldrich, USA	A2504
EGTA	AppliChem, Germany	A0878
Glycerol	Sigma Aldrich, USA	15524
Glycine	Sigma Aldrich, USA	G4392
HEPES	Sigma Aldrich, USA	H-1016
Triton x100	Sigma Aldrich, USA	T8787
2-mercaptoethanol/ß-	AppliChem, Germany	A1108,0100
Sodium dodecyl sulfate (SDS)	Sigma Aldrich, USA	71725
Agar, microbiology grade	Sigma Aldrich, USA	05039
Bacto-Tryptone	Conda, Spain	1612
Bacto-Yeast extract	Conda, Spain	1702
KCl	Sigma Aldrich, USA	P4504
KOH	Sigma Aldrich, USA	P6280
MgSO4	Sigma Aldrich, USA	M2773
CaCl2	Sigma Aldrich, USA	C3306
MgCl2	Merck, Germany	A406233
MnCl2	Merck, Germany	1,05917
Pipes	Merck, Germany	1.102.200
Ampicillin	Roche, UK	835 269
Kanamycin	Sigma Aldrich, USA	K1876
DMSO	AppliChem, USA	A3672,0100

17ß-Estradiol	Sigma Aldrich, USA	E2758
Aldosterone	Sigma Aldrich, USA	A9477

2.1.3. Cell culture media and reagents:

Media and reagents used in routine cell culture studies and cell treatments are listed in Table 2.3.

Table 2.3: Cell culture media, reagents and chemicals used in the study.

Name	**Company**	**Catalog number**
DMEM, Low Glucose	Lonza, Switzerland	BE12-707F
RPMI 1640, Low Glucose	Lonza, Switzerland	BE12-702F
DMEM w/o phenol red	Thermo Scientific, USA	11880-028
RPMI w/o phenol red	Lonza, Switzerland	BE12-918F
PBS	Lonza, Switzerland	BE17-516F
Fetal Bovine Serum (FBS)	Biowest, France	S181H-500
Trypsin	Lonza, Switzerland	BE-17-161E
L-Glutamine	Lonza, Switzerland	BE17-605E
Sodium pyruvate	Lonza, Switzerland	BE13-115E
Penicillin/Streptomycin	Lonza, Switzerland	DE17-602E
Opti-MEM	Thermo Scientific, USA	31985-070
Lipofectamine® 2000	Thermo Scientific, USA	11668027
HiPerFect	Qiagen, Germany	301704

2.1.4. Primers

Primers sequences and regarding product sizes and annealing temperatures are listed in Table 2.4.

Table 2.4.: Primer list.

Gene	Sequence (5'-3')	Product size	Tm (°C)
NR3C2/MR F:	AGTGGAAGGGCAACACAACT	175	60
NR3C2/MR R:	CTGCTCCTCGTGAATCCCTTT		
SGK1 F:	AACCCTTCTCCTCCACCAAG	118	59
SGK1 R:	TTCCAAAACTGCCCTTTCCG		
NEDD4-2 F:	CATCAGCGAAGACTTGGAGC	220	59
NEDD4-2 R:	GCTGAACTGTTCCCCATTGG		
αENaC F:	GGTTTCTCACACCAAGGCAG	138	59
αENaC R:	AGCCCTTACCCATCTTGCTT		
βENaC F:	TCCTACCCTCGTCCCTACCT	151	59
βENaC R:	CCAGGAAGGAGAAAACCACA		
γENaC F:	AAGGTGACACAGTGAGGAGG	183	59
γENaC R:	GGAAGGGTCAGCTCTGTCTT		
PGR F	GGAGGAGGAGGGAGGTATCA	210	58
PGR R	CTGCTTGGAAGACTCAGGGA		
TPT-1 F	GATCGCGGACGGGTTGT	100	58/ 59/ 60
TPT-1 R	TTCAGCGGAGGCATTTCC		
PS2/TFF1 F	CCATGGAGAACAAGGTGATCTGC	208	58
PS2/TFF1 R	TTAGGATAGAAGCACCAGGGGAC		

2.1.5. Antibodies

Antibodies used in Western Blot studies provided with antibody dilutions, appropriate gel running percentages, catalog numbers and company names are listed in Table 2.5.

Table 2.5. List of antibodies used in this study.

Antibody	**Catalog number**	**Company**	**Dilutions**
Mouse-anti MR	rMR1-18 1D5	DSHB/ University of Iowa	1:100
Rabbit-anti GR	12041S	Cell Signaling	1:3000
Mouse- anti SGK1	S5188	Sigma	1:2000
Rabbit-anti NEDD4-2*	300-376; A27 (AP)	Cocalico/Dan	1:500
Rabbit-anti αENaC*	JL**- #1132	JL	1:5000
Rabbit-anti βENaC*	JL- #135	JL	1:10.000
Rabbit-anti γENaC*	JL- #552	JL	1:10.000
Rabbit-anti Actin	ab1801	Abcam	1:2000
Rabbit anti-GAPDH	sc-25778	Santa Cruz	1:10.000
Anti-rabbit secondary	7074P2	Cell Signaling	1:5000
Anti-mouse secondary	7076P2	Cell Signaling	1:5000

* denotes that it was a kind gift from Prof. Olivier STAUB, Department of Pharmocology and Toxicology, University of Lausanne.

** JL denotes Johannes Loffing from Institute of Anatomy, University of Zurich.

2.1.6. DNA constructs

DNA constructs used for overexpression studies; pcDNA3.1 and pcDNA3.1-Stag MR were kind gifts of Dr. Nourdine Faresse, University of Zurich. P-EGFP N2 construct was a kind gift from Assist. Prof. Dr. Ebru ERBAY.

2.1.7. Buffers

Buffers commonly used in Western blot, protein, plasmid studies are listed in Table 2.7.

Table 2.6: Buffers commonly used in Western blot, protein, and plasmid studies.

Name	Components
10X TBS	24 g Tris, 88 g NaCl dissolve in 900 ml ddH_2O. PH adjusted to 7.6, volume bring up to 1000ml.
1X TBS-T (Tween 0.1%)	100ml from 10X TBS, 900 ml ddH_2O, 1ml Tween-20.
10X Running Buffer	10.08 g SDS, 30.3 g Tris, 144g Glycine, volume up to 1000ml with ddH_2O. Keep at °C after dissolving.
1X Running Buffer	100 ml from 10X Running Buffer, 900 ml ddH_2O. Stored in aliquots at 4 °C.
Anode Buffer I	300 mM Tris, 20% Methanol, volume up to 500 ml with ddH_2O.
Anode Buffer II	25 mM Tris, 20% Methanol, volume up to 500 ml with ddH_2O.
Cathode Buffer	40 Mm 6-aminocaparoic acid, 20% Methanol, volume up to 500 ml with ddH_2O.
4X SDS Loading dye	900 µl BioRad Laemmli Buffer, 100 µl
Protein Lysis Buffer	25 ml from 1M HEPES, 15 ml from NaCl, 2.5 ml from 200 mM pH:8.0 EGTA, 57.4 ml from 87% Glycerol, 50 ml from 10% Triton x100, volume up to 500 ml with

	ddH_2O. Stored at 4 °C.
Mild Stripping Buffer	15g Glycine, 1g SDS, 10ml Tween-20 volume up to 800 ml with 900 ml ddH_2O. PH adjusted to 2.2 and volume bring up to 1000ml with ddH_2O (Freshly prepared).
SOB (Super Optimal Broth) Medium	20 g Bacto-tryptone, 5 g yeast extract, 0.584 g NaCl, 0.186 g KCl, 2.03 g $MgCl_2$, 2.465 g $MgSO_4$ dissolved in 1L ddH_2O. Prepare just before autoclave.
Transfer Buffer	0.6048 g Pipes, 0.441 g $CaCl_2$, 3.727 g KCl, 1.7806 g $MnCl_2$. All components except $MnCl_2$ were dissolved in 100 ml ddH_2O. PH adjusted to 6.7 with 1M KOH. If it became more than 6.7, prepare the solution again. Then add $MnCl_2$, bring the volume to 200 ml with ddH_2O and filter sterilized with 0.45 μm filter. Store at 4 °C.
Glycerol stock	10 ml LB media, 10 ml Glycerol. Vortexed and filter sterilized by 0.45 μm
LB (Luria broth) agar	2 g Bacto-tryptone, 1 g yeast extract, 1g NaCl dissolved in 200 ml ddH_2O. Prepare just before autoclave.
LB media	5 g NaCl, 5 g Bacto-tyrptone, 2.5 g Bacto-yeast extract, volume up to 500 ml with ddH_2O. Prepared just before autoclaving.

2.2. Methods

2.2.1. Cell Culture studies

2.2.1.1. Cell lines:

Multiple breast cancer cell lines were used throughout this study, i.e., MCF-7, MDA-MB-231, MDA-MB-453, T-47D, ZR75-1, BT-20, CAL-51, HCC-1937 (ATCC; Manassas, USA). HEK (Human embryonic kidney cell line) and $mCCD_{c11}$ (mouse cortical collecting duct cell line) cell lines were used as positive controls in Western Blot studies. $MCCD_{c11}$ cells whole protein extract was a kind gift from Dr. Nourdine Faresse, Institute of Anatomy, University of Zurich. HEK-293 cells were a kind gift of Assist. Prof. Dr. Ebru ERBAY.

Breast cancer cell lines used in this study are listed with regard to their molecular subtypes and hormonal status in Table 2.7.

Table 2.7: Gene expression profiles and molecular subtypes of breast cancer cell lines.

Cell line	ER	PR	Her2	Molecular subtype
MCF-7	+	+	-	Luminal
MDA-MB-231	-	-	-	Basal B
MDA-MB-453	-	-	+	Luminal
T-47D	+	+	-	Luminal
ZR75-1	+	-	-	Luminal
BT-20	-	-	-	Basal A
CAL-51	-	NA*	-	Basal B
HCC-1937	-	-	-	Basal A

Data provided from "Kao J, Salari K, Bocanegra M, Choi Y-L, Girard L, et al. (2009) Molecular Profiling of Breast Cancer Cell Lines Defines Relevant Tumor Models and Provides a Resource for Cancer Gene Discovery. PLoS ONE 4(7): e6146".

*"NA" denotes not available.

2.2.1.2. Growth conditions:

All cell lines were grown in 37 °C incubator with 5% CO_2. MCF-7, MDA-MB-231, MDA-453, BT-20, HEK cells were grown in DMEM, supplemented with 10% FBS, 2% L-Glutamine, 1% Sodium pyruvate, 1% Penicillin/Streptomycin, 1% Non-essential amino acids.

T-47D, HCC-1937 and ZR75-1 cell lines were maintained in RPMI 1640, supplemented with 10% FBS, 2% Sodium pyruvate, 1% Penicillin/Streptomycin, 1% Non-essential amino acids.

CAL-51 cell line was grown in DMEM with 20% FBS, 2% L-Glutamine, 1% Sodium pyruvate, 1% Penicillin/Streptomycin, 1% Non-essential amino acids.

Each cell type was grown in T-75 flasks before any experiment. All estrogen, aldosterone treatments and transfection studies were carried out in 6-well plates. For protein studies, investigating the expressions of MR and GR across multiple breast cancer cell lines, cells were grown in 100 mm plates.

2.2.1.3. Passaging cells:

Cells were passaged when confluent at 80-90%. As a first step, medium was aspirated and cells were washed with 1X PBS. PBS was then aspirated and 0.25 ml, 0.50 ml, and 1 ml of Trypsin-EDTA were used per well at 6 well plates, T-25 flask and T-75 flask, respectively. Trypsinization of cells for 2 minutes in incubator at 37°C with 5% CO_2 was reversed by addition of complete medium (at least twice the volume of used trypsin) onto detached cells. Cells were re-suspended in medium by pipetting up and down thus cell clamps were disrupted to homogenize cell suspension. Cells were distributed into new flasks or plates in various dilutions depending on the following experiments.

2.2.1.4. Thawing cells:

Cryovial containing frozen cells were taken from liquid nitrogen and kept on ice in order to carry to cell culture room, immediately. The vial was placed in a pre-heated 37 °C water bath until the small amount of frozen cells remained. Thawed cells were added into a falcon containing 10 ml complete medium, dropwise in the cell culture hood. Cells were re-suspended in medium gently, and then centrifuged at 1500 rpm for 3 minutes. Supernatant was aspirated; cell pellet was dissolved in 7 ml medium and placed in T-25 flask. The day after thawing, if adherent cells were attached to the flask and reached at least 70% confluency, then the cells were split into T-75 flask.

2.2.1.5. Counting cells by haemocytometer:

Cell counting was performed before seeding cells for each experimental procedure and cryopreservation. Trypsinized cells were collected in medium and pipetted up and down to disrupt cell clamps in order to count cells precisely. 10µl from cell suspension and 10µl trypan blue dye were added into a PCR tube and mixed. Hemocytometer chamber cleaned by 70% alcohol was gently filled with this mix and cells were drawn out onto chamber by coverslip. Cells were counted under the light microscope by using 10X objective. Cells in 16 corner squares of hemocytometer were counted in regard to live cells unstained by trypan blue while dead cells were stained by trypan blue. Total counted number of cells were divided by 4 and this number was multiplied by 2 (as dilution factor) and 10^4 (to find cell number in 1 ml). After calculations, cells were centrifuged at 1500 rpm for 3 minutes. Cell pellet was dissolved in complete medium (according to cell type) and diluted into new plates or vials depending on the following experiment.

2.2.1.6. Cryopreservation of cells:

Cells with low passage number and high confluency (almost 90%) were used for freezing. Confluent cells were detached following the protocol used during passaging and collected in a falcon, containing fresh medium that was specific to the studied cell type. Total cell number was determined by using hemocytometer (number of

viable cells should be at least 90%). Then, cells were spun in a pre-cooled centrifuge (+4 °C), at 1500 rpm for 5 minutes. 'Freezing medium' was prepared using 10% DMSO and 90% FBS (filter sterilized). After centrifuge step, supernatant was removed and cell pellet was dissolved in freezing medium. Cell suspension were gently mixed by pipette to have a homogenous cell suspension. 1 ml of freezing medium containing 1 x 10^6 cell were dispensed to each screw-capped cryovials. Cell freezing process was performed by gradually decreasing the temperature. Cryovials were placed in -20°C for 1 hour, then stored in -80°C freezer, overnight (frozen cells can be stored in -80°C up to 1 month). As a last step, the vials were stored in liquid nitrogen tanks for extended period of time.

2.2.1.7. Cell pellet collection for RNA isolation:

All centrifuge steps of this protocol were carried on centrifuges, precooled to 4 °C. Experiments were finalized by detaching cells with trypsin. Cells were collected with medium into falcon tubes and centrifuged at 1500 rpm for 3 minutes. Then, medium were aspirated and cell pellets were dissolved in ice cold PBS and centrifuged at 1500 rpm for 3 minutes. This step was performed once more and small volume of PBS was remained on cell pellets. Each cell pellet was snap-frozen by using liquid-nitrogen. Samples were stored in -80°C.

2.2.1.8. E2 treatments:

MCF-7, T-47D and MDA-MB-231 cell lines were treated with 10nM and 100nM Estrogen/ 17ß –Estradiol/ E2, separately, and control (containing only medium) for 24 hours. 27.238 mg estrogen was dissolved in 50 ml 100% ethanol/EtOH (filter sterilized) for the E2 stock solution. The concentration of the stock was 2mM and it was filtered, aliquoted and stored at -20 °C.

In the first day of the experiment, cells were counted as described in counting cells by hemocytometer section and seeded as 150.000 cell/well for MCF-7, 200.000 cell/well for T-47D and MDA-MB-231 in 6-well plates. The day after, media were changed to phenol red-free medium (DMEM or RPMI 1640), supplemented with 5%

Charcoal FBS. Cells were grown in the cell-specific 5% Charcoal FBS - phenol red-free medium for 72 hours. Then, for the cell synchronization before E2 treatment, cells were incubated in phenol red-free medium supplemented with 0.1% Charcoal FBS for 24 hours.

After synchronization, cells were treated with 10nM and 100nM E2, separately. E2 doses and all dilutions were prepared in phenol red free complete medium with 5% Charcoal FBS. 2mM stock solution was diluted to 1:1000 times to have 2μM E2 solution. For MCF-7 and MDA-MB-231 100nM E2 dose, 450 μl from 2μM E2 solution was added into 8.550 ml phenol red free DMEM with 5% Charcoal FBS. For T-47D, 250 μl from 2μM E2 solution was added into 4.750 ml phenol red free RPMI 1640 with 5% Charcoal FBS. For the 10nM E2 dose, 100nM solutions were diluted as 1:10 times in control medium containing 0.005% EtOH. For the control wells, appropriate volume of EtOH from 0.1% EtOH were added into phenol red free complete medium with 5% Charcoal FBS to reach 0.005% EtOH in medium as final ratio. 2 ml from each dose specific medium and control medium were added into appropriate 6-well plates with regard to experimental design. Cells were incubated with E2 and experiments for 24 hours. Experiments were finalized with either taking cell pellets for RNA isolation or total protein extraction from cells after 24 hours. Method for estrogen treatments was taken from Sila Ozdemir's thesis on "qPCR validation of in vivo diagnostic importance and regulation by estrogen for CHRNA5 isoform expression in breast cancer". Studies conducted at mRNA levels include only 100 nM dose of E2 whereas protein studies have two doses of E2 treatment; 10 nM and 100 nM.

2.2.1.9. Aldosterone treatments:

MCF-7, T-47D and MDA-MB-231 cell lines were treated with 10nM and 100nM aldosterone (ALDO), separately, and control for 24 hours. In order to have 10mM ALDO stock solution, 5 mg ALDO were dissolved in 1.4 ml 100% EtOH (filter sterilized). The stock concentration was 10mM and it was stored in aliquots at -20 °C.

In the first day of the experiment, cells were counted as described in counting cells by hemocytometer section and seeded as 150.000 cell/well for MCF-7, 200.000 cell/well for T-47D and MDA-MB-231 in 6-well plates. All dilutions from ALDO stock solution were prepared in phenol red free complete medium (DMEM or RMPI 1640), supplemented with 5% Charcoal FBS. 10mM ALDO stock solution was gradually diluted; first 2mM and then 2µM. 100nM ALDO doses for MCF-7 and T-47D were prepared by adding 450 µl from 2µM stock into 8.550 µl phenol red free medium complete medium with 5% Charcoal FBS. For T-47D 100nM ALDO dose, 250 µl from 2µM ALDO solution was added into 4.750 ml phenol red free RPMI 1640 with 5% Charcoal FBS. For the 10nM ALDO dose, 100nM solutions were diluted as 1:10 times in control medium (phenol red free medium with 5% Charcoal FBS) containing 0.001% EtOH. Control medium were obtained by adding appropriate volume of EtOH from 0.1% EtOH into phenol red free complete medium with 5% Charcoal FBS. Dose specific medium and control medium were distributed to each well as 2 ml/ well and cells were treated with ALDO for 24 hours. After 24 hours, cell pellets were taken for RNA isolation and total protein extraction were performed for the further analysis. Studies conducted at mRNA levels include only 100 nM dose of ALDO while protein studies consist of two doses of ALDO treatment; 10 nM and 100 nM.

2.2.1.10. Transfection of cells, optimization of MR overexpression:

Optimization studies for overexpression of MR were performed in MCF-7, MDA-MB-231 and T-47D cell lines. Three cell lines were transfected with 1 µg/µl pEGFP vector by using HiPerFect transfection reagent for 48 hours in order to find out whether those cell lines were transfected by HiPerFect reagent or not.

200.000 cell/well for MCF-7 and 300.000 cell/well for MDA-MDA-231 and T-47D cells were seeded in 6-well plates. One day after seeding, GFP containing DNA construct; pEGFP vector and 6 µl HiPerFect transfection reagent were mixed in 100 µl serum and antibiotic free complete medium. This mix was vortexed and incubated at room temperature for 10 minutes. Medium were changed to complete medium without antibiotics before the transfection of DNA construct. PEGFP vector was added to each well drop by drop and plates were shaken well to distribute the

construct equally; then cells were incubated for 48 hours in the incubator. After 48 hours, GFP transfection efficiency of each cell line was checked under the fluorescent microscope and images were taken by using either fluorescent or light microscope from each well.

After GFP transfection study, transfection efficiency of T-47D cells were optimized by changing DNA: transfection reagent ratio as 200 ng/µl DNA: 6 µl HiPerfect, 2 µg/µl: 6 µl HiPerfect, 2 µg/µl:12µl HiPerfect.

After the optimization of T-47D transfection, MCF-7 and HEK-293 cells (used as transfection control) were transfected with 1 µg/µl pcDNA3.1-S-tag MR and pcDNA3.1 empty vector: 6 µl HiPerFect transfection reagent whereas T-47D cells were transfected with 2 µg/µl pcDNA3.1-S-tag MR and pcDNA3.1 empty vector: 6 µl HiPerFect transfection reagent for 48 hours. Transfection protocol of HiPerFect was followed as described above in optimization studies section. Results were finalized with following total protein extraction and Western Blot experiment.

Optimization studies further continued with using an alternative transfection reagent, Lipofectamine® 2000 before proceeding to final MR overexpression experimental setup for microarray studies. MCF-7 cells were transfected with 1 µg/µl pEGFP vector for 48 hours, by using Lipofectamine® 2000 transfection reagent for 48 hours. Cells were seeded as 200.000 cell/well into 6-well plates. The day after, 1 µg/µl pEGFP vector was added into an eppendorf tube containing 250 µl OPTI-MEM and 2 µl Lipofectamine® reagent was mixed in a separate eppendorf tube containing 250 µl OPTI-MEM. Then, two 250 µl OPTI-MEMs were incubated at room temperature (under hood) for 5 minutes. After 5 minutes, eppendorf tubes containing OPTI-MEMs were collected in one tube, vortexed for few seconds and incubated at room temperature for 20 minutes. Before the transfection of pEGFP vector, medium were switched to complete medium without antibiotics as 1.5 ml medium/ well. PEGFP vector was added into wells by dropwise and whole plate were shake with making 8 shape to distribute construct equally in wells. 3 hours after transfection, media were switched to complete media. Cells were incubated with the vector for 48 hours in incubator. After 48 hours incubation, results were finalized by checking the GFP intensity under the fluorescent microscope. No quantitative data were obtained.

2.2.1.11. MR overexpression:

Overexpression of MR were tested in MCF-7 and HEK cell lines by using Lipofectamine® transfection reagent. HEK cells were transfected with 1 µg/µl pcDNA3.1 S-tag MR construct and MCF-7 cells were transfected with 200 ng/µl, 1 µg/µl and 2 µg/µl pcDNA3.1-S-tag MR and pcDNA3.1 empty vector, separately, for 48 hours. Cells were seeded as 200.000 cell/well into 6-well plates. The day after, MR constructs regarding their concentrations were added into 250 µl Opti-MEM, separately, and 2 µl Lipofectamine® reagent were dissolved in a separate 250 µl Opti-MEM. Then, tubes containing 250 µl Opti-MEM were incubated at room temperature for 5minutes; after 5 minutes, collected in one tube, vortexed for few seconds and incubated at room temperature (under hood) for 20 minutes. Before adding constructs, cell medium was changed to complete medium w/o antibiotics as 1.5 ml/well. Each concentration of MR construct was added into wells containing 1.5ml medium by dropwise and whole plate were shake with making 8 shape to distribute constructs equally in wells. 3 hours after transfection, medium was switched to complete medium. Cells were incubated with constructs for 48 hours in incubator. After 48 hours incubation, results were finalized with further protein isolation and Western Blot studies.

2.2.1.12. Aldosterone treatment upon MR overexpression

MCF-7 cells were treated with aldosterone upon MR overexpression. Cells were seeded as 200.000 cell/well into 6-well plates. The day after, overexpression of MR study was conducted with 1 µg/µl S-tag MR and corresponding empty vector by using 2 µl Lipofectamine® reagent as explained in 2.2.2.11. After 24 hours, medium was switched to DMEM w/o phenol red for synchronization for further ALDO treatment. 48hours after overexpression study, 100 nM ALDO were given to the cells as described in 2.2.1.9. Cells were exposed to ALDO for 24 hours. Experiment was finalized with RNA extraction. Changes in response to aldosterone in MR overexpressing cells were analyzed by q-PCR.

2.2.2. Gene expression analyses

2.2.2.1. Primer design

Ensemble genome browser was used to find the transcripts of each gene in *Homo sapiens.* The longest (according to amino acid length) protein coding variant of each gene was chosen for further analysis. FASTA sequence of the longest protein coding variant was copied into "Source sequence" section in Primer3 primer designing tool and PCR product size ranges were changed as 100-250bp in "General primer picking conditions" section. After getting results from Primer3 tools, each primer pairs were also tested by using NCBI Primer Blast tool and again product size range were changed to 100-250bp. Quality of each primer pairs were checked for product length, Tm values, GC content and percentage, self-3'complementarity, self-complementarity, and hairpin formation. Products created by target sequences of each primer were also controlled if primer pairs hit any exon-exon junction or not by using NCBI Primer Blast tool. An *in silico* PCR were run with designed primers on another genome browser called USCS, which shows all exons within transcripts and exon-exon junctions that hit by primer pairs. For this purpose, GRCh37/hg19 genome assembly of UCSC was used.

2.2.2.2. Total RNA isolation:

Trizol method was used for total RNA isolation from cells. Prior to RNA isolation, the working bench and all the equipment used for this protocol were cleaned by RNase Zap solution to avoid possible RNA degradation and contamination. Centrifuges were precooled to 4 °C before starting the RNA isolation.

Cell pellets were thawed on ice and tubes were vortexed for a few seconds to dissolve cell pellets within the remaining PBS. 800 µl Trizol reagent were added on the cells and mix was pipetted up and down under the fume hood. Then, 200 µl Chloroform were added to each tube. Tubes were inverted for 15 times and incubated at room temperature for 10 minutes, centrifuged at 13.200 rpm for 17 minutes at 4 °C. After the centrifuge step, DNA and RNA were separated from each other and

RNA remained in clear upper aqueous layer. These layers were taken in new autoclaved eppendorf tubes with regard to the experiments. Equal volume of isopropanol (filter sterilized with 0.45 µm filter) was added to the colorless part. Tubes were inverted 5 times and incubated at room temperature for 10 minutes, centrifuged at 13.200 rpm for 10 minutes 4 °C. Supernatant was removed from tube by paying attention to the RNA pellet. Remaining supernatant was taken by a small volume micropipette. Pellet was dissolved in 1 ml 75% EtOH (fresh prepared, filter sterilized by 0.20 µm filter) and centrifuged at 8000 rpm for 8 minutes at 4 °C. Ethanol was discarded and RNA pellet was washed with 1 ml 100 % EtOH (filter sterilized by 0.20 µm filter) and centrifuged at 8000 rpm for 8 minutes at 4 °C. Ethanol was removed carefully and pellets were air-dried for 5-10 minutes at room temperature. In the final step of this procedure, each cell pellet was dissolved in 20 µl RNase free water. RNA quantity measurement and quality analysis were done at 280 nm wavelength by using Nano drop one spectrophotometer (Thermo Scientific, USA).

2.2.2.3. CDNA synthesis:

Bio-Rad cDNA synthesis kit was used according to manufacturer's protocol for cDNA synthesis. Required volume of RNA template to have 1 µg total RNA was taken into PCR tubes. 4 µl 5x iScript reaction mix, 1 µl iScript reverse transcriptase were added to tubes and volume adjusted to 20 µl with Nuclease free water. In every cDNA synthesis reaction, one sample was prepared without reverse transcriptase enzyme called "-RT" to find out any DNA contamination in RNA samples. Experiments were run in Techne TC-512 (Bibby Scientific, UK) PCR machine by incubating samples at 42 °C for 1hour, 70 °C for 5 minutes. Then, samples were stored at -20 °C.

2.2.2.4. Q-RT-PCR:

Experiments were performed in Light Cycler® 480 Multiwell plate 96, white by using Light Cycler® 480 PCR Instrument. All experiments were performed by using duplicate samples. Negative controls that have either no cDNA template or no

reverse transcriptase enzyme were always included to the experiments. 1: 10 times diluted cDNA templates (100 ng final concentration) and primer pairs (10nmol final concentration) were used in all experiments. For a single qPCR reaction, 1 µl from each primer pairs and 5 µl from Light Cycler® SYBR Green I Master mix were mixed in a PCR tube and volume adjusted to 8 µl with nuclease free water. This master mix was distributed into 96 well-plates as 8 µl/ well and then 2 µl cDNA templates were added into wells. Reagent volumes given for the master mix were multiplied with the number of wells designed in experimental set-ups. qPCR reaction protocol was as follows: Initial denaturation at 95 °C, 5 minutes, 45 cycles of denaturation (94°C, 20 seconds), annealing (Tm values as in Table 2.4 , 15 seconds) and elongation (72°C, 15 seconds), acquisition (95 °C, 5 seconds; 55 °C, 1 seconds; 95 °C, continuous) and final elongation (40 °C, 30 seconds).

2.2.2.5. Q-RT-PCR expression analyses:

Q-PCR data were analyzed by relative quantification method. Ct values of duplicates were averaged. Average Ct values of control samples were subtracted from average Ct values of treatments samples for target gene and reference gene, separately (ΔCt values). Then efficiencies (2^) of target gene were normalized to efficiencies of reference gene. (ΔΔCt values). Log 2 scale values were taken of each ΔΔCt value and these values used for further statistical analyses.

2.2.2.6. Preparation of Protein Lysis Buffer:

Lysis Buffer for protein extraction was prepared as explained in Table 2.7. Just before protein isolation, one pill of Complete EDTA-free Protease inhibitor cocktail was dissolved in 20 ml lysis buffer at 4°C, on rotator. After dissolving, 10 ml was taken from lysis buffer containing protease inhibitor and 1 pill PhosSTOP Phosphatase inhibitor cocktail was dissolved in this mixture at 4°C on rotator. Complete lysis buffer (including protease and phosphatase inhibitors) was used in further protein extractions. Both mixture including either only protease inhibitor or complete protein lysis buffer were kept at -20 °C.

2.2.2.7. Total Protein extraction:

All experimental steps for protein extraction were performed on ice. Cell-harboring plates were placed on ice and medium was aspirated. Cells were washed with ice cold PBS, twice. Depending on the cell confluency percentage of plates, volume of complete lysis buffer that covers the surface of wells/ plates were added on cells. 90-120 µl complete protein lysis buffer for one well in 6-well plate, 200-250 µl complete protein lysis buffer for 100 mm plates were used. Cells were scraped in lysis buffer and collected in eppendorf tubes. Tubes were incubated on ice for 30 minutes and every 5 minutes, tubes were vortexed, placed back on ice. After incubation, samples were centrifuged at 13.200 rpm for 15 minutes at 4 °C. Since total extracted proteins were in supernatant part, supernatants were taken carefully and placed in a new eppendorf tubes. Protein samples were either used for further quantification analyses or kept at -80 °C for later uses.

2.2.2.8. BCA assay and calculations for protein quantification:

Proteins used in this thesis were measured by BCA method. Protein and standard curve samples were used as duplicates in 96-well plates in BCA assay. Standard curve is constructed for each individual BCA assay. Standards were prepared as explained in manufacturer's guidelines by using 2 mg/ml BSA solution as stock. BSA stock solution was diluted in complete protein lysis buffer for standard curve samples. BCA assay working solution was prepared by taking 50 volume of BCA reagent A and 1 volume of BCA reagent B (50:1). Depending on total number of samples (protein and standard curve), final volume of working solution was calculated. Working solution was distributed into wells as 200 µl/well. Then, 25 µl from standard curve samples were added into wells. Protein samples were used 2 µl/well for BCA assay. Samples were mixed in wells by pipetting up and down. Plates were covered by aluminum and incubated at 37 °C incubator for 30 minutes. Absorbance values were detected at 562 nm by using Synergy HT microplate reader (BioTek, USA).

After getting absorbance values, a standard curve line graph was drawn by using standard curve absorbance values corresponding to each standard dilutions in Excel

program and an equation (y=ax+b, where y= absorbance values, x= concentration) for further protein quantifications was formulized. Absorbance values of protein samples were calculated by using equation found in standard curve graph and each value was multiplied with 12.5 (dilution factor) in order to find final concentration of protein sample.

Protein samples would be used in Western Blot studies were denatured at 95 °C for 5 minutes on Thermolyne 17600 Dri-Bath (Thermo Scientific, USA). All protein concentrations were adjusted to 1 or 2 µg/µl and mixed 4x SDS loading dye and final desired volume was completed with complete protein lysis buffer. Heat-denatured proteins were stored at -20 °C. Remaining protein samples were kept at -80 °C.

2.2.2.9. SDS page and Western Blot

Expression studies at protein level were studied by Western Blot. Bio-Rad Mini-PROTEAN® TGX™ Precast Gels were used. Bio-Rad Mini-PROTEAN® Tetra System Casting Frame and Stand with 1.5mm glass plates were set. Distilled water was used to test if there is any liquid leakage between glasses. 4 ml of each Resolving solutions (Solution A and B) were mixed and 40 µl 10 % APS, 4 µl TEMED were added into mixture under fume hood. Mixture was poured between glasses slowly.. 1.5 ml of each stacking solutions (Solution A and B) were mixed and 15 µl 10% APS, 3 µl TEMED were added into mixture under fume hood. Stacking solution was poured on resolving solution at once. Gels were polymerized in 30-40 minutes. Gel percentages used in this study were listed in Table 2.6. Samples of estrogen and aldosterone treatments were loaded on SDS gels as 20 µg/ µl per well for visualizing proteins other than MR and GR. 30 µg/µl proteins were loaded for MR and GR Western Blots. 3-5 µl page ladder was used for each blot. Empty wells were filled with 4x SDS loading dye. Gels were run at 120 volt with power supply EC 300 XL (Thermo Scientific, USA). Gels were transferred to Polyvinylidene difluoride (PVDF) membranes with semi-dry method by using Bio-Rad Trans Blot® Turbo Transfer system. Two Whatman papers were wet with Anode Buffer-I and settled in the bottom part of transfer cassette. Four Whatman papers were wet with Anode Buffer-II and placed on other two Whatman. PVDF membrane was activated in 100% Methanol for 1 minute and put on those Whatman papers. SDS gel was

placed on top of membrane. Excess amount of buffer and bubbles were removed. Then, six Whatman papers were wet with 1x Cathode Buffer and put on the upper part of the system. Cassette was closed tightly and, Standard SD (up to 1.0A, 25V) for one mini gel was selected from Bio-Rad programs and run for 30 minutes. After transfer, membranes were stained with Ponceau Red at room temperature for 5 minutes on Thermolyne, RotoMix type 50-800 (Thermo Scientific, USA) shaker. Photo of the blots were taken and membranes were washed with distilled water to get rid of Ponceau Red. Blocking was performed with 5 % milk in TBS-T (5% BSA in TBS-T for GR) for 1hour. Membranes were incubated with antibodies diluted in 1% milk-TBS-T (in 5% BSA for GR) at 4 °C, overnight. Antibodies with dilutions, company names and catalog numbers were provided in Table 2.6. The day after, membranes were washed with 1X TBS-T for 15 minutes, three times at room temperature on shaker with high speed. Secondary antibody incubations at 1:5000 dilution was performed at room temperature on shaker with slow speed. Washing steps were repeated with 1X TBS-T after secondary antibody incubations. Membranes were detected with either Amersham ECL prime western blotting detection reagent or Western Bright Quantum western blotting HRP substrate by using solution A and B in 1:1 ratio. Results were taken with medical X-Ray films using hyper processor Amersham (Life Science USA) X-Ray detection machine in dark room.

2.2.2.10. Mild Stripping Protocol:

Stripping protocol was performed in order to study more proteins on same blot. Strip buffer was prepared fresh as described in Table 2.7. Blots were re-stained as follows: Membranes were incubated with a volume of strip buffer that covers membrane at room temperature for 10 minutes, twice. Then, buffer was discarded and washing steps were performed with 1X TBS at room temperature, for 10 minutes, twice. Last washings were done two times, with 1X TBS-T for 5 minutes. Membrane became ready for blocking stage and following procedures for Western blot.

2.2.2.11. Image J Analyses:

Image analysis for Western Blot studies were performed as follows. All Western Blot images were processed by ImageJ. All image types were formatted to 16-bit images. Bands corresponding to protein expression levels were selected one by one and band densities were given as plots in ImageJ. Area of each plot was selected by labelling each peak formed by plots and percentage of these measurements was extracted to an Excel file. Expressions of target proteins were normalized to reference proteins such as GAPDH or Actin. Log2 scale values of each result was used in graphs.

ImageJ analysis was also used in counting the cells in GFP transfection studies. GFP transfected cell images taken under either light or fluorescent microscope were used for ImageJ processing. ImageJ program processed images by subtracting the background and adjusting the image thresholds black and white. Then number of cells in each image was measured by analyze particle option.

2.2.2.12. Preparation of competent cell:

E. coli DH5α strain was used as competent cells in plasmid studies. Initial bacteria stock was obtained from Erbay Lab. Small amount was taken from bacteria stock was by a sterile tip and incubated in 100 ml LB (preparation explained in Table 2.7) on 37 °C Innova 4300 incubator shaker (Eppendorf, USA), overnight (16 hours.). In the morning, 10 ml from autoclaved SOB media super optimal broth media (SOB preparation explained in Table 2.7) was taken in a falcon tube near fire for further blank measurements in spectrophotometer. 1ml from overnight culture were added into 100 ml SOB media near fire and OD measurement were performed at 600nm with Beckman DU 640 (Beckman Coulter, USA) spectrophotometer. OD value should be between 0.3 and 0.6. (If OD value is 0.2 or less, a few amounts of overnight culture is added into SOB media and media is incubated on +4 °C shaker, OD values is checked every 30 minutes. When the proper OD was reached, SOB culture was poured equally into 4x 50 ml prechilled falcon tubes near fire and tubes were incubated on ice for 30 minutes. Cells were harvested by centrifuge at 2500 g for 10 minutes at 4 °C. Supernatants were removed and excess supernatant was discarded by a small volume micropipette. Cells were placed on ice and suspended in

16 ml/per falcon ice cold Transfer Buffer (TB, described in Table 2.7) by pipetting up and down, slowly. Tubes were left on ice for 10 minutes. Then, contents of one falcon were transferred in another falcon, slowly and remaining tube was centrifuged at 2500g for 10 minutes at 4 °C. Supernatant was discarded, cells were suspended in 8 ml of TB containing 7% DMSO and left on ice for 10 minutes. After incubation, 0.2 ml aliquots were made from 8ml of final mixture with prechilled eppendorf tubes in +4 °C cold room and all aliquots were stored at -80°C.

2.2.2.13. Bacterial transformation:

Competent cells were taken out of -80 °C and thawed on ice. Upon thawing, the required quantity of competent cells was used and the remaining cells were discarded. Depending on the DNA concentration of plasmid (up to 1000 ng/µl, 4 µl of plasmid; more than 1000 ng /µl 2-3 µl of plasmid), required volume of plasmids were added in 50 µl competent cells in micro centrifuge tubes. Tubes were incubated on ice for 30 minutes and a heat-shock process was performed to competent cell-DNA mixture in water bath at 42 °C for 30 seconds. Then, tubes were left on ice for 2 minutes. 815 µl LB (without any antibiotics) were added into tubes near fire and tubes were incubated on 37 °C shaker for 1 hour. After 1 hour, 100 µl from competent cell-DNA mixture was spread on agar plates containing 1000X Ampicillin or Kanamycin near fire. Plates were incubated at 37 °C, overnight.

2.2.2.14. Inoculating bacterial culture:

After overnight incubation (16 hours) of bacterial cells, single bacteria colonies were picked from plates by using sterile tips and inoculated in 10 ml LB (Ampicillin for pcDNA3.1 and pcDNA3.1 Stag-MR, Kanamycin for pEGFP) containing falcon tubes. Tubes were incubated at 37 °C shaker, overnight.

2.2.2.15. Preparation of Glycerol stock

Before plasmid isolation, 500 µl from overnight bacteria culture were suspended in 500 µl 50 % Glycerol stock in screw-capped cryovial tubes on ice. Tubes were vortexed for few seconds and stored at -80 °C.

2.2.2.16. Plasmid isolation and quantification:

Plasmid isolations were performed by using MN NucleoSpin Mini-Prep kit according to manufacturer's protocol for isolation of high copy plasmid DNA from *E. coli.* All centrifuge steps were done at room temperature at 11.000 g. 5ml from overnight bacterial culture was taken into new falcon tubes and centrifuged for 30 seconds and supernatants were removed carefully. 250 µl ice cold Buffer A1 was added to tubes and pellets were suspended completely by vortexing for a few seconds. 250 µl Buffer A2 was added to cell mixtures and tubes were inverted 8 times, incubated for 5 minutes until color of lysates became clear. 300 µl Buffer A3 was added and mixed thoroughly by inverting tubes 8 times. Tubes were centrifuged for 5 minutes. Centrifuge step was repeated if supernatant was not clear. Supernatants (max. 750 µl) were placed into NucleoSpin columns containing 2 ml collection tubes and centrifuged for 1 minute. Flow-through was discarded, washing step was performed by adding 600 µl Buffer A4 into columns and centrifuge was performed for 1 minute. After removing flow-through, columns were placed into new collection tubes and centrifuged for 2 minutes to dry membrane inside columns. New collection tubes were used to collect DNA from columns and 50 µl nuclease free water was added directly on membranes inside columns. Tubes were centrifuged for 1 minute. Eluted DNAs were measured by Nano drop one (Thermo Scientific, USA) at 260 nm wavelength.

2.2.3. Statistical analyses:

Statistical analyses were performed in GraphPad Prism 6.0 software. Observed changes at mRNA expression level of each gene in response to treatments were subjected to significancy test by applying two-way ANOVA. Two-way ANOVA is

often used to compare observed changes between either cell lines or treatments. Overexpression studies were tested by applying one-way ANOVA analyses which show statistical differences between cell lines used in each experimental set-up. In addition to ANOVA, Tukey's multiple comparison test was used to compare effect of each treatments or overexpression studies within each cell line in a statistical manner.

2.2.4. GEO2R analyses:

Gene expression omnibus database (GEO) was used to find out possible regulators participating in modulation of downstream targets of MR gene expressions. Breast cancer microarray studies done by other research groups were selected with regard to GPL96 and GPL570 platforms. E2 related studies were found in GEO. For MCF-7 cells GSE11324, GSE4668, for both MCF-7 and T-47D GSE3529 and for MDA-MB-231 cells GSE2251 were selected in order to perform GEO2R analysis. In initial step control versus treatment groups were defined for each microarray data set. Then gene expression changes for all samples used in the study were tested by GEO2R. Data were imported to Excel datasheet and converted to tab-delimited format. Raw P value and log fold changes were used to interpret data.

Affymetrix prob sets with regard to each gene tested in this study were given in Table 2.8.

Table 2.8: Genes analyzed by GEO2 and corresponding Affymetrix prob set names.

Gene name	**Prob set**
SGK1	201739_at
NEDD4-2	212445_s_at
αENaC	203453_at
βENaC	205464_at
γENaC	207295_at

2.2.5. Heat map analyses:

Visual representation of gene expression changes in response to E2 and ALDO at both mRNA and protein levels were demonstrated across breast cancer cell lines via heat map. Log fold change values were used in heat map analyses. Then, data were adjusted to color scale by using conditional formatting in Excel.

2.2.6. Illustrative figures for discussion:

Mechanism proposed for E2 and ALDO activity in ER (+) and ER (-) breast cancer cells were shown by illustrative cell figures drawn by Adobe Illustrator CS6 program.

Chapter 3

Results

3.1. Expressions of MR and GR across multiple subtypes of breast cancer cells

In vitro validation of MR protein expression and its possible correlation with GR expression in various breast cancer cell lines were studied at the protein level. Expression patterns of MR and GR proteins were detected by using Western Blot (WB) in breast cancer cell lines sub-grouped into various types. HEK-293 cell line as a positive control and GAPDH, as reference gene, were used in this study. Experiments were conducted using the same amount of protein and similar experimental procedures as described under the Materials and Methods section, 2.2.2.9. Figure 3.1 represents expressions of MR and GR in eight different breast cancer cell lines. These cell lines included basal and luminal subtypes. Analysis of each blot was performed in the ImageJ program (Materials and Methods, 2.2.2.10).

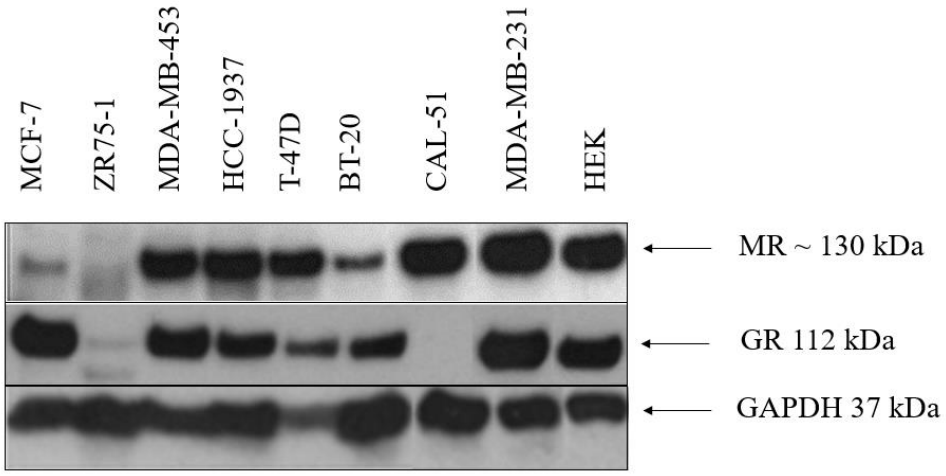

Figure 3.1: Expression patterns of MR and GR in breast cancer cell line protein panel.

According to the Figure 3.2, MR was highly expressed in two triple-negative breast cancer cell lines; CAL-51 and MDA-MB-231 whereas it had low expressions in ER + cell lines such as MCF-7. On the other hand, GR exhibited higher expression in MCF-7 and MDA-MB-231 cell lines compared to other six breast cancer cell lines. Interestingly, CAL-51 cell line had no detectable level of GR expression while MCF-7 had relatively lower expression of MR. No signal for both MR and GR proteins could be detected for ZR75-1, another ER + cell line. For the other cell lines (MDA-MB-453, HCC-1937, BT-20 and T-47D) MR showed higher expression patterns than GR (Figure 3.2A). Two triple negative cell lines, MDA-MB-231 and MDA-MB-453, which belong to the basal subtype, showed relatively high expressions of MR and GR proteins (Figure 3.2B). The protein levels of MR and GR were in accord with each other except two cell lines, i.e., MCF7 and CAL-51. These two represent interesting models in which either MR or GR is under expressed, respectively.

A)

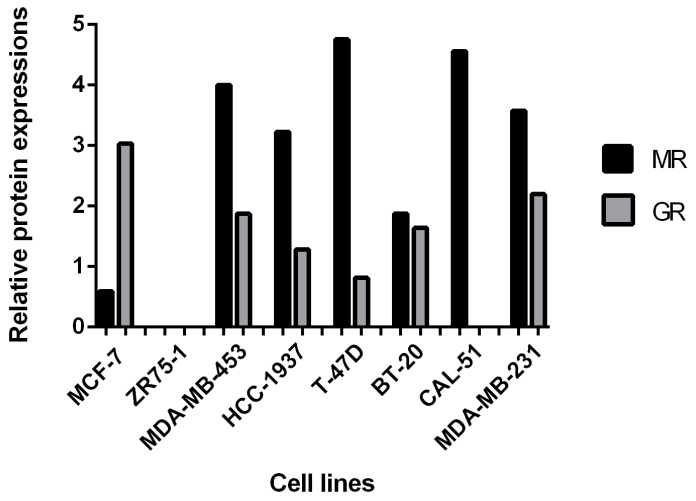

B)

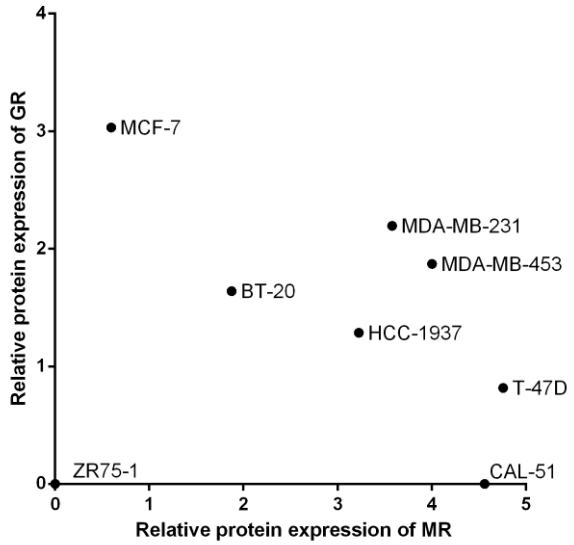

Figure 3.2: Graphical representations of MR and GR expressions in different subtypes of breast cancer. **A.** GR and MR expressions were shown in columns in cell line specific manner. **B.** Comparisons of MR and GR protein expressions for each cell line by scatter-plot.

3.2. Protein expression profiles of MR and its downstream targets in ER (+) and ER (-) breast cancer cell lines

Expression profile of MR protein and its downstream targets i.e., SGK1, NEDD4-2 and three subunits of ENaC i.e., α, β and γ, were analyzed in two ER (+) breast cancer cell lines, MCF-7 and T-47D and one ER (-) breast cancer cell line, MDA-MB-231. $mCDD_{cl1}$ and HEK293 cells were used as controls since they were known to express MR and its downstream targets. Antibodies against all these six proteins

(Table 2.6) were used in Western Blot to detect protein expression levels along with MR protein expression. Beta-Actin was used as a reference protein in the study. Graphs representing expressions of MR and its downstream targets were drawn by taking relative expression of each gene to the reference gene expression.

MR, SGK1 and NEDD4-2 were expressed across breast cancer cell lines studied from low to high levels. MCF7 as shown before did not express MR at highly detectable levels whereas T-47D and MDA-MB-231 cells exhibited higher MR expression when compared to MCF-7 cells (Figure 3.3A). Expression of MR protein was lower in breast cancer cells when compared to control cells (HEK and $mCCD_{C11}$). The predicted size of the MR protein is 107 kDa, while we detected a doublet of bands with apparent molecular weights between 105 and 130 kDa across the breast cancer and control cell lines (Figure 3.3A). SGK1 was expressed in all the breast cancer cell lines used in this study. MDA-MB-231 and T-47D cell lines had similar levels of SGK1 expression and SGK1 expression levels in these cell lines were higher than that in MCF-7 (Figure 3.3B). Moreover, NEDD4-2 proteins exhibiting potentially two different splice variants were also detected in both the ER (+) and ER (-) cell lines. Presence of these splice variants was confirmed by either detecting expressions of those variants in $mCCD_{C11}$ cell line used as positive control in WB study or observing same variants with another antibody against NEDD4-2 in Western blot study. Highest NEDD4-2 expression between breast cancer cell lines was observed in T-47D cells. Both ER (+) and ER (-) breast cancer cells exhibited lower NEDD4-2 expression patterns in comparison to control cells (Figure 3.3C).

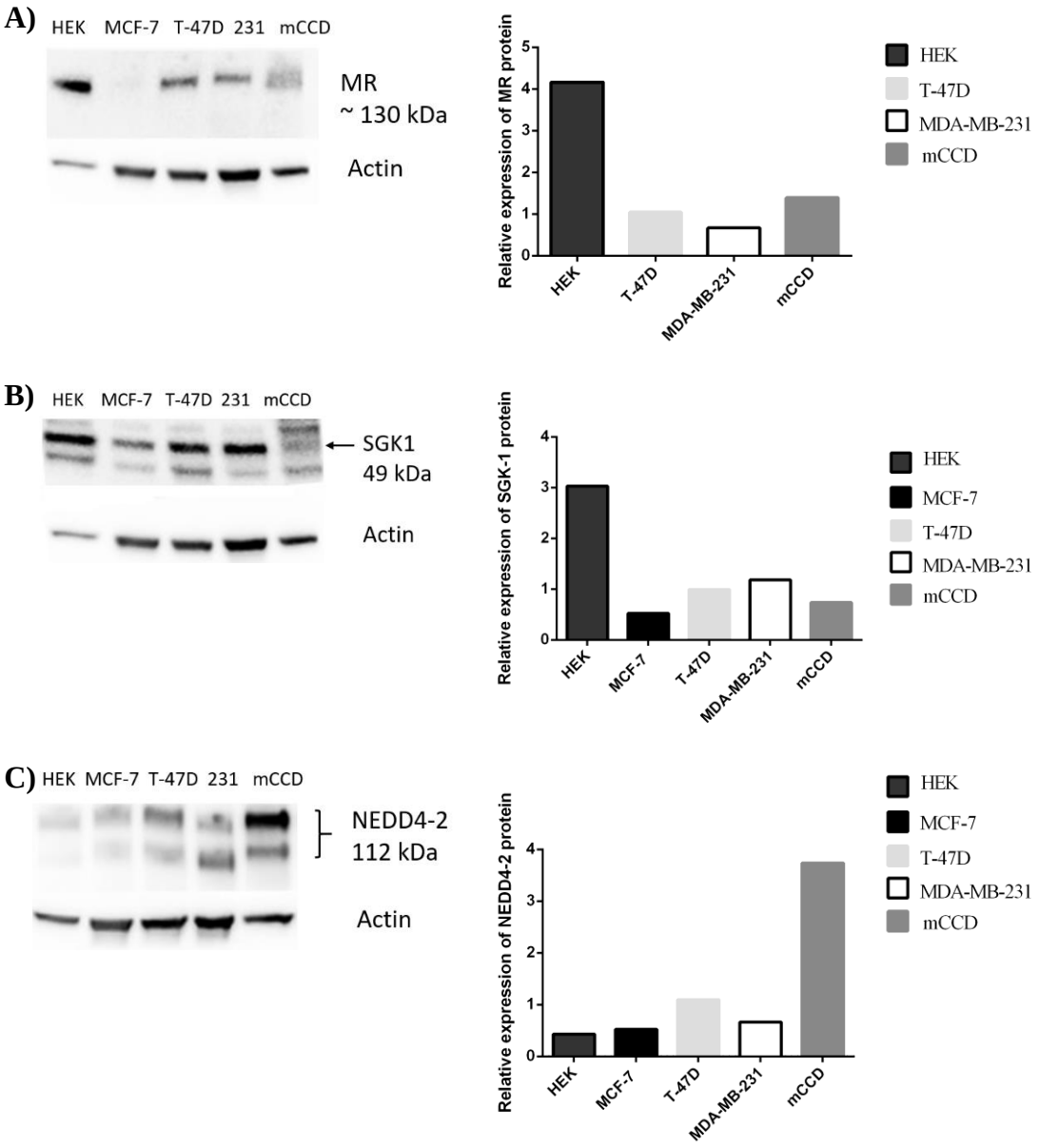

Figure 3.3: MR, SGK1 and NEDD4-2 expressions across ER (+) and ER (-) breast cancer cell lines. **A.** WB image and quantitative representation of MR expression. **B.** WB image and quantitative representation of SGK1 expression. **C.** WB image and quantitative representation of NEDD4-2 expression.

Protein expressions of α, β and γENaC also were detected in these breast cancer cell lines (Figure 3.4). Figure 3.4A shows full-length and cleaved forms of αENaC protein expression in the control cell lines and breast cancer cell lines. $MCCD_{C11}$ clearly exhibited the full length as well as the cleaved form (around 35kDa). All three breast cancer cell lines used in this study showed of the full length αENaC. Notably, a potentially cleaved form of αENaC migrated at an apparent weight close to 25 kDa in breast cancer cell lines whereas its size was almost 35 kDa in the

control cell lines (Figure 3.4B and 3.4C). βENaC expression was detected in T-47D and MCF-7 cell lines. MCF-7 cells had highest βENaC expression between all cell lines used in the study (Figure 3.4B). Furthermore, γENaC has been shown to be expressed in ER (+) and ER (-) breast cancer cell lines (Figure 3.4C). Similar expression levels of γENaC protein were detected in MCF-7 and T-47D. In contrast, MDA-MB-231 cells had higher expression of γENaC protein in comparison to other two breast cancer cells but γENaC displayed a lower expression pattern compared to control cells (i.e.; HEK and mCCDc$_{11}$) used in this study (Figure 3.4C).

A)

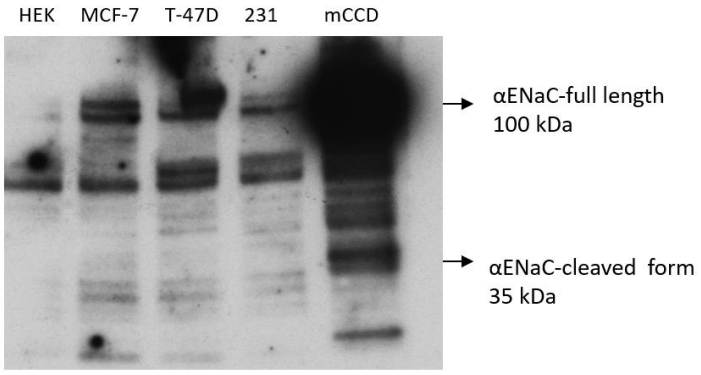

B)

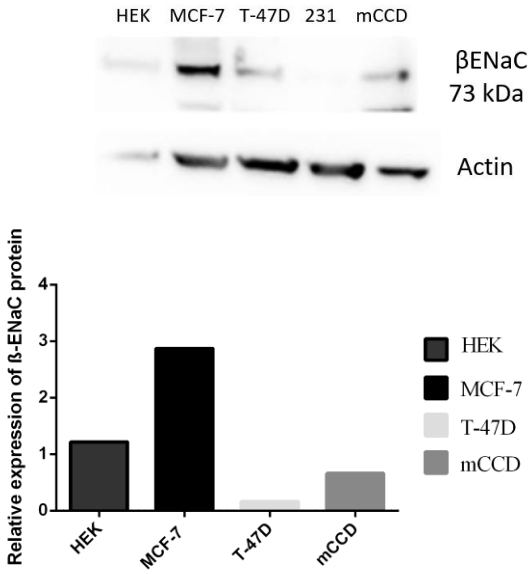

C)

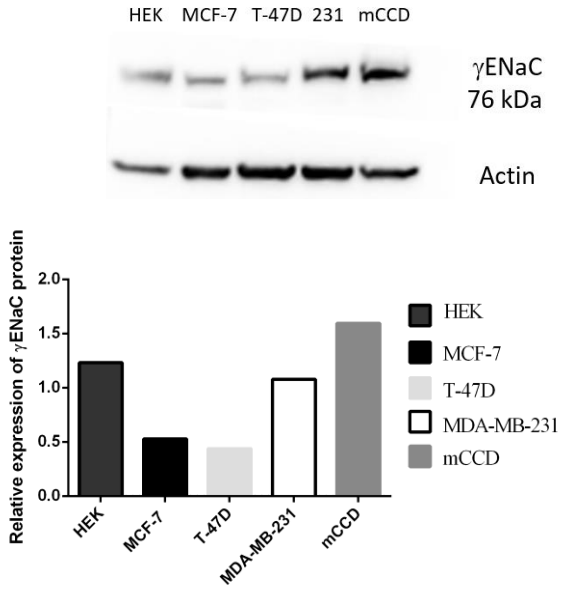

Figure 3.4: ENaC subunits expressions among ER (+) and ER (-) breast cancer cell lines. **A.** αENaC expression; WB image and its quantitative representation. **B.** βENaC expression; WB image and its quantitative representation. **C.** γENaC expression; WB image and its quantitative representation.

As a conclusion, our studies showed that MR and its downstream targets were expressed in different breast cancer cell lines at the protein level and exhibit differences in amount. This suggests that they are differentially regulated and have important functional consequences.

3.3. Effects of E2 on expression levels of MR downstream targets in breast cancer cells: *In silico* findings

As a part of our aims in this study, we would like to find out possible regulators of MR downstream targets in breast cancer. Therefore, we performed an *in silico* analysis by using publicly available breast cancer microarray datasets from GEO. *In silico* findings revealed E2 modulatory effects on expression levels of MR downstream genes: SGK1, NEDD4-2 and three subunits of ENaC (namely α, β and γ). Changes in gene expressions were shown as tables indicating logarithmic fold changes (LogFC) and significance (significant values in bold) and represented as figures in Appendix A.

3.3.1. E2-regulatory role on expressions of MR downstream target genes in ER (+) breast cancer cells

We analyzed three studies showing E2 regulatory roles in MCF-7 cells. First one was examining the changes in gene expressions in response to 100 nM E2 for 3, 6 and 12 hrs in MCF-7 cells (GSE GSE1132; Mansourian R. et. al., 2004). Another study found out E2-regulated genes by applying E2 starvation up to 2 days again in MCF-7 cells (GSE4668; Coser KR et. al., 2003). Last study on E2 regulated genes were constructed by treating three ER (+) breast cancer cell line, T-47D, MCF-7, BT-474, with 10 nM E2, each for 48hrs (GSE3529; Rae JM. et. al., 2005). Alterations in gene expressions were represented in graphs adopted from GEO profile database in the Appendix A. Microarray results were analyzed by GEO2R and gene expression changes were summarized in Table 3.1, 3.2 for MCF-7, Table 3.3 for both MCF-7 and T-47D by showing fold changes and P values (significance with bold styling) individually for each gene.

In the first E2 study, expression levels of SGK1 mRNA was significantly upregulated in response to E2 in a time-dependent manner while a significant dramatic decrease was observed in NEDD4-2 expression in late time point of E2 exposure (12 hrs) when compared to earlier time points (Table 3.1) (Appendix Figure 1A, 1B). Differential effect of E2 on expression patterns SGK1 and NEDD4-2 mRNA were also shown in the E2 starvation in MCF-7 cells. Downregulations were detected in expression level of SGK1 mRNA in absence of E2 along two days (Appendix Figure 2A). However, changes were approached significance at second day of E2 starvation. In addition, NEDD4-2 expression levels were increased in parallel to time, significantly (Appendix Figure2B) (Table 3.2). According to the last E2 study, no significant changes were noticed in expression levels of SGK1 and NEDD4-2 with regard to 10 nM E2 treatment for 48 hrs in MCF-7 cells and T-47D cells (Appendix Figure 3A, 3B) (Table 3.3). These results suggested that mRNA level of SGK1 increases and that of NEDD4-2 decreases upon E2 treatment, as expectedly in the opposite direction (Figure 1.3).

Gene expression changes in response to E2 were also examined in ENaC subunits in same platforms as SGK1 and NEDD4-2 were investigated. Time course E2 treatment

(3, 6 and 12 hrs) in MCF-7 cells showed that expression of αENaC decreased gradually and significantly in time (Appendix Figure 4A). Neither γENaC nor βENaC expression were affected from E2 treatment in MCF-7 cells; observed changes were not significant when it compared to control (Appendix Figure 4B, 4C) (Table 3.1). Significant upregulations in expression levels of αENaC mRNA also were detected after 2 days of E2 starvation complementing the E2 exposure study shown in Appendix Figure 4A. Significant decline was noticed in expression of βENaC only after 2 days E2 starvation in MCF-7 cells. Moreover, a decrease trend was observed in expression pattern of γENaC in response to E2 absence since changes were indicated as non-significant between control and E2 treatments. These results proposed that E2 might have role in regulation of αENaC and but not the beta or γENaC expression at mRNA levels (Appendix Figure 5) (Table 3.2). The direction of change is expected to be the same with SGK1 and in opposite of NEDD4-2.

In the last selected E2 experiment, three subunits of ENaC displayed non-significant changes between untreated and 10 nM E2 treated MCF-7 and T-47D cells. (Appendix Figure 6) (Table 3.3).

Table 3.1: Log fold changes observed in expressions of MR downstream targets at mRNA levels in response to MCF-7 cells treated to 0, 3, 6, 12 hrs E2 were shown with their P values.

GENES	Treatments	LogFC	P value	LogFC	P value	LogFC	P value
		0-3 h		0-6 h		0-12 h	
SGK1	100 nM E2	**2.02**	**3.04E-10**	**2.12**	**4.86E-12**	**2.55**	**3.56E-12**
NEDD4-2		**-0.39**	**3.17E-04**	**-0.54**	**3.51E-06**	**-0.59**	**6.31E-06**
αENaC		**-0.27**	**7.46E-03**	**-0.69**	**1.71E-06**	**-1.64**	**4.62E-11**
βENaC		0.07	4.04E-01	-0.07	4.43E-01	-0.08	2.80E-01
γENaC		-0.11	2.95E-01	-0.06	5.54E-01	-0.11	2.59E-01

Table 3.2: Log fold changes observed in expressions of MR downstream targets at mRNA levels in response to E2 starvation for 1 day and 2 days in MCF-7 cells were indicated with their P values.

GENES	Treatment	LogFC	P value	LogFC	P value
		0-1 day		0-2 days	
SGK1	E2 starvation	-0.75	0.35525	**-1.17**	**3.54E-02**
NEDD4-2		**0.67**	**0.028275**	**1.06**	**1.69E-03**
αENaC		**0.67**	**0.042869**	**1.20**	**3.36E-02**
βENaC		-0.89	0.058336	**-0.68**	**2.12E-02**
γENaC		-0.76	0.35525	-0.16	6.34E-01

Table 3.3: Log fold changes observed in expressions of MR downstream targets at mRNA levels in response to 10 nM E2 treatment for 48hrs in MCF-7 and T-47D cells were indicated with their P values.

GENES	Treatment	LogFC	P value
		0-48 h	
SGK1	10 nM E2 in MCF-7	-0.1	3.33E-01
NEDD4-2		**0.51**	**8.27E-04**
αENaC		**0.55**	**7.05E-04**
βENaC		**-0.50**	**1.35E-03**
γENaC		0.24	7.96E-02
SGK1	10 nM E2 in T-47D	0.11	3.26E-01
NEDD4-2		-0.19	9.85E-02
αENaC		-0.26	1.37E-01
βENaC		-0.01	9.22E-01
γENaC		-0.17	1.33E-01

3.3.2. E2-regulatory role on the expression of MR downstream target genes in an ER (-) breast cancer cell line, MDA-MB-231

We carried out another *in silico* analysis by using data from Rae et. al study, reporting gene expression changes regarding 10 nM E2 treatment for 48 hrs in MDA-

MB-231 cells (GSE2251; Moggs JG et.al., 2005). In this experiment, ERα was re-expressed in MDA-MB-231 cells by a vector transfection. We selected the empty vector transfected samples and corresponding E2 treated samples (which called as control group in the experiment). Alterations in gene expressions were represented in graphs adopted from GEO profile database as shown in the Appendix A. Microarray results were analyzed by GEO2R and gene expression changes were summarized in Table 3.3 by showing fold changes and P values (significance with bold styling) individually for each gene.

As shown in Appendix Figure 7, SGK1 and NEDD4-2 expression displayed no changes in MDA-MB-231 cells treated with E2 (Table 3.4).

Increased trend was observed in the three subunits of ENaC expression, although non-significant, in response to E2 in MDA-MB-231 cells as demonstrated in Appendix Figure 8 (Table 3.4). In addition, both β and γENaC expression values were represented as absent in Appendix Figure 8B and 8C, meaning that expressions of those genes were different than zero however level of expression was under the threshold value for detection. These findings suggested that expressions of SGK1, NEDD4-2, and ENaC subunits could be regulated in an ER status dependent manner in breast cancer cell lines.

Table 3.4: Log fold changes observed in expressions of MR downstream targets at mRNA levels in response to 10 nM E2 treatment for 48hrs in MDA-MB-231 cells were indicated with their P values.

GENES	**Treatment**	**LogFC**	**P value**
		0-48 hrs	
SGK1	10 nM E2	-0.04	8.62E-01
NEDD4-2		-0.03	9.07E-01
αENaC		0.96	2.35E-01
βENaC		0.59	3.72E-01
γENaC		1.1	1.02E-01

3.4. Effects of E2 treatments on MR and its downstream targets in breast cancer: Validation by qPCR and Western Blot

E2's regulatory role in expression levels of MR and its downstream targets, i.e., ENaC subunits, SGK1 and NEDD4-2, also were studied using two ER (+) breast cancer cell lines (MCF-7 and T-47D) and an ER (-) breast cancer cell line (MDA-MB-231) *in vitro*. E2 experiments were carried out by treating cells with 100 nM E2 for 24 hrs to examine its effect on mRNA levels or 10 nM and 100 nM E2 for 24 hrs to study its effect on protein levels (Materials and Methods, 2.2.1.8). Changes in expression were analyzed by qPCR at the mRNA level and by Western Blot at the protein level. TPT-1 and Beta-Actin were used as references in the qPCR and Western Blot studies, respectively. Gene expression changes at the mRNA level were analyzed by applying a Two-way ANOVA test. If significant changes were observed in the effect of treatment or interaction on gene expression levels as a result of two-way ANOVA, a t-test was applied to each cell line experiment, individually. Significant results were demonstrated on each figure with asterisks indicating the significance level. Due to the one biological replicate in each Western Blot study, statistical analysis could not be applied. Gene expression changes at protein levels were given as in comparison to reference gene; Actin. In addition, expressions of β and γENaC mRNA in MDA-MB-231 cells were too low to be detected by qPCR.

3.4.1. Determining the E2 response in breast cancer cell lines

Breast cancer cell lines treated with 100 nM E2 were tested to see whether E2 signaling was transcriptionally activated or not. For this purpose, two well-known downstream target genes of E2 signaling in breast cancer, the progesterone receptor gene (PGR) and the trefoil factor 1 (TFF1)/ pS2 were used as internal controls of E2 response in qPCR.

In PGR tested experiment, we found a significant interaction between cell lines and E2 treatment by applying two-way ANOVA test ($p=0.0034$). Corresponding P values either between cell lines or between estrogen treatments were found as $P_{cell\ line}=0.0034$ and $P_{treatment}=0.0030$, respectively. PGR expression was significantly upregulated in response to E2 treatment in MCF-7 and T-47D as ER (+) cell lines

(Figure 3.5A; p value, 0.0080 for MCF-7; and p value, 0.0262 for T-47D; t-test). No change in expression level of PGR was occurred in MDA-MB-231 as an ER (-) cell line (p=0.3262, t-test).

When PS2 gene expression was examined in response to E2, we found significant cell line. Treatment and interaction effects between E2 treated breast cancer cells in terms of PS2 mRNA expression ($P_{cell\ line}$=0.0012, $P_{treatment}$ < 0.0001, $P_{interaction}$=0.0012, two-way ANOVA). We found that PS2 mRNA expression significantly increased in both the MCF-7 and T-47D cells with p values 0.0211 and 0.0052, respectively (t-test) No significant increase in pS2/TFF1 was detected in MDA-MB-231 cells (p=0.2327, t-test) (Figure 3.5B).

These results indicated clearly that our experiment exhibited a reliable and expected response to E2 and only in the ER+ cells.

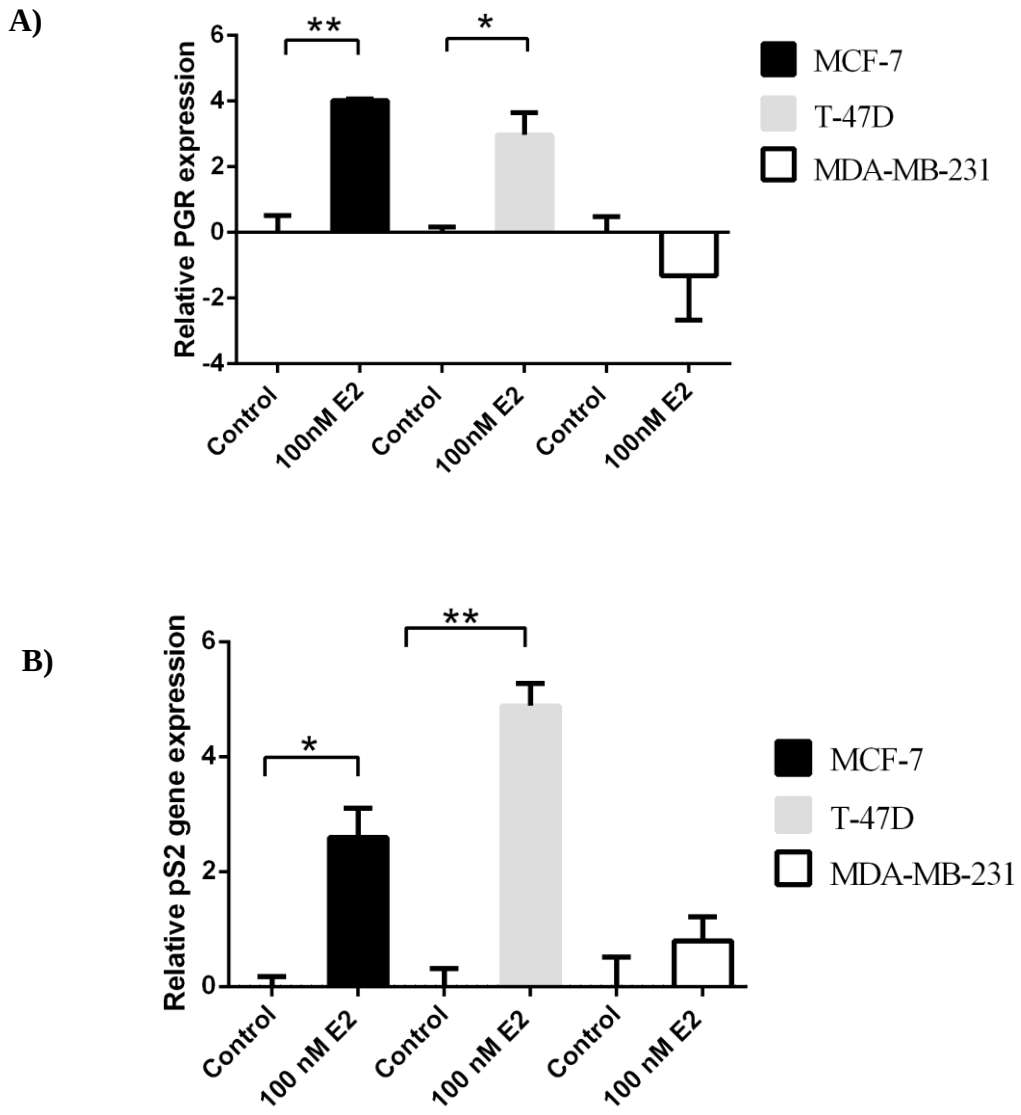

Figure 3.5: Changes in transcription levels of E2 target genes PGR and pS2 upon E2 stimulation. **A.** E2 response of PGR gene in MCF-7, T-47D and MDA-MB-231 cells. **B.** E2 response of pS2 gene in MCF-7, T-47D and MDA-MB-231 cells. (*P ≤ 0.05; ** P ≤ 0.01; *** P ≤ 0.001).

3.4.2. Alterations in MR/NR3C2 mRNA expression levels in response to E2

After demonstrating the activity of estrogen signaling via alterations in its downstream targets, E2 modulatory effect on MR expression was analyzed in breast cancer cell lines. We could not observe any significant cell line, treatment or interaction effect in E2 and vehicle treated breast cancer cells with regard to MR expression (Pcellline=0.4206; Ptreatment=0.1269.; Pinteraction=0.6541; two-way

ANOVA). It can be concluded that MR exhibited no significant response to the E2 treatment.

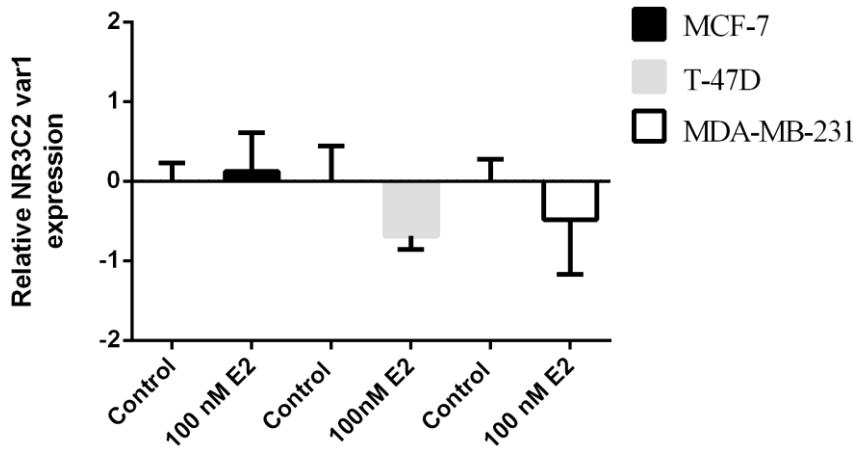

Figure 3.6: Response of NR3C2/MR var1 gene expression to E2 treatment in ER (+) and ER (-) breast cancer cell lines.

3.4.3. Alterations in SGK1 mRNA expression levels in response to E2

E2 treatment studies were continued with investigating E2 regulatory role in the downstream targets of MR. E2 effect on SGK1 whose transcription can be stimulated upon MR activation was explored within breast cancer cells. In silico analyses suggested that SGK1 mRNA levels should increase upon E2 treatment in MCF7 cells.

Figure 3.7 displays the changes in SGK1 mRNA levels among three breast cancer cell lines. We found a significant interaction between E2 treated breast cancer cell lines in terms of SGK1 expression (Pinteraction=0.0006, two-way ANOVA). In addition, cell lines exhibited differential response to E2 treatments (Ptreatment=0.0006) and there were also differences between the control and E2 treatments among breast cancer cell lines with regard to SGK1 expression (Pcellline= 0.0179) (Two-way ANOVA result)

SGK1 expression tended to increase in MCF-7 cells exposed to E2 although without showing any statistical significance at the $p<0.05$ ($p= 0.0955$, t-test). E2 did not

affect mRNA levels of SGK1 in MDA-MB-231 (p=0.1988, t-test), as we expected from the in silico analyses; and T-47D cells exhibited a decreased pattern of expression when compared to the control cells (p=0.0075, t-test). The expression of SGK1 in the two ER (+) cell lines displayed different responses to the E2 (Figure 3.7).

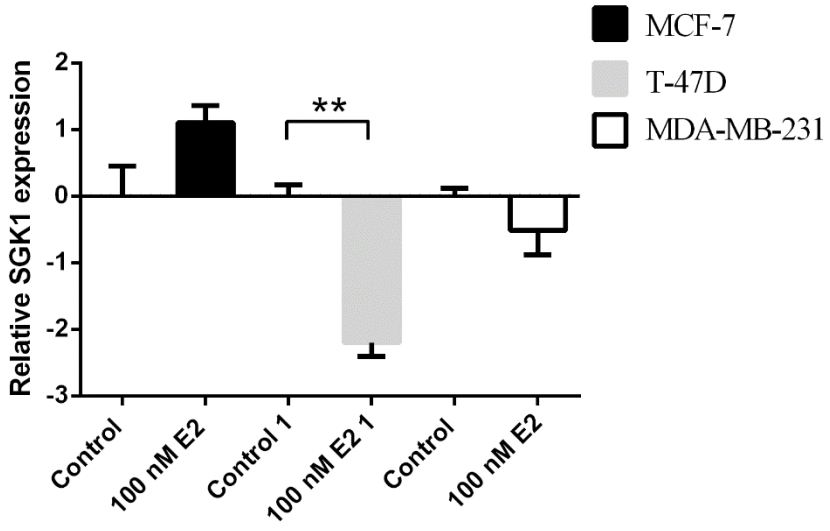

Figure 3.7: Alterations in expression levels of SGK1 mRNA across ER (+) and ER (-) breast cancer cell lines (*P ≤ 0.05; ** P ≤ 0.01; *** P ≤ 0.001).

No protein study for the SGK1 was performed in this thesis.

3.4.4. Alterations in NEDD4-2 mRNA and protein expression levels in response to E2

E2 treatment resulted in significant decreases in NEDD4-2 expression in both the ER (+) cell lines and ER (-) cell lines (Figure 3.8). However, we could not observe any interaction between the cell lines and E2 treatment (Pinteraction=0.1170) suggesting that all cell lines exhibited a similar behavior in response to E2. Accordingly, effect of E2 on NEDD4-2 were significant in at least one of the cell lines (Ptreatment=0.0006) and cell lines were behaving exhibited differences in expression (Pcellline=0.1170; Two-way ANOVA results). Reduced pattern in NEDD4-2 mRNA levels were significant only in the T-47D cell line (p=0.0235, t-test). NEDD4-2 expression although approaching significance exhibited no significant difference in

expression when compared with own controls in the MCF-7 and MDA-MB-231 cells with p values 0.1007 and 0.0640, respectively (T-test results).

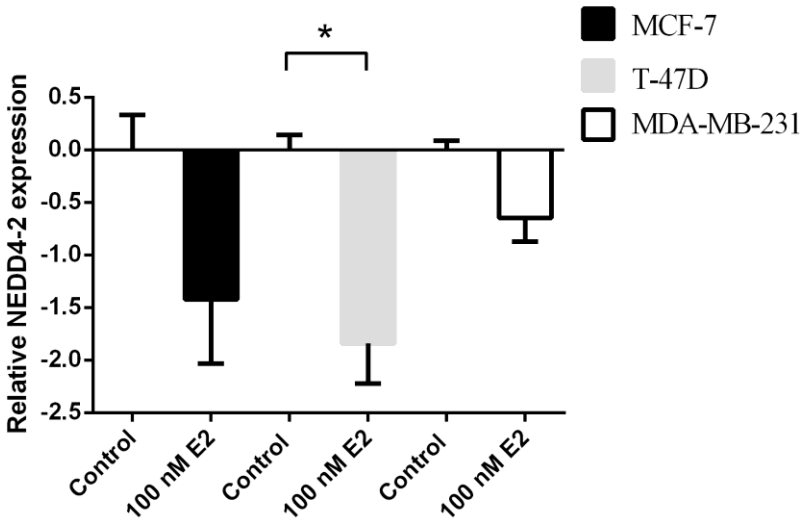

Figure 3.8: Alterations in expression levels of NEDD4-2 mRNA across ER (+) and ER (-) breast cancer cell lines in response to E2 (*P ≤ 0.05; ** P ≤ 0.01; *** P ≤ 0.001).

Alterations in the expression of NEDD4-2 protein were represented in Figure 3.9A. NEDD4-2 expression levels was downregulated with respect to ACTIN in particularly the MCF7 cells treated with E2 (Figure 3.9B) while no change was observed in NEDD4-2 protein expression with regard to E2 in MDMB-231 and T-47D cells. 100 nM doses showed almost similar amount of changes across ER (+) and ER (-) cell lines. We could conclude that E2 affected expression levels of NEDD4-2 in the same direction at both mRNA and protein in MCF7 cell lines. The downregulation detected at the mRNA levels of T47D cells in response to E2 could not be observed for the protein levels in T47D cells. MDA-MB-231 NEDD4-2 expression on the other hand was not responsive to E2 at both the mRNA and protein levels.

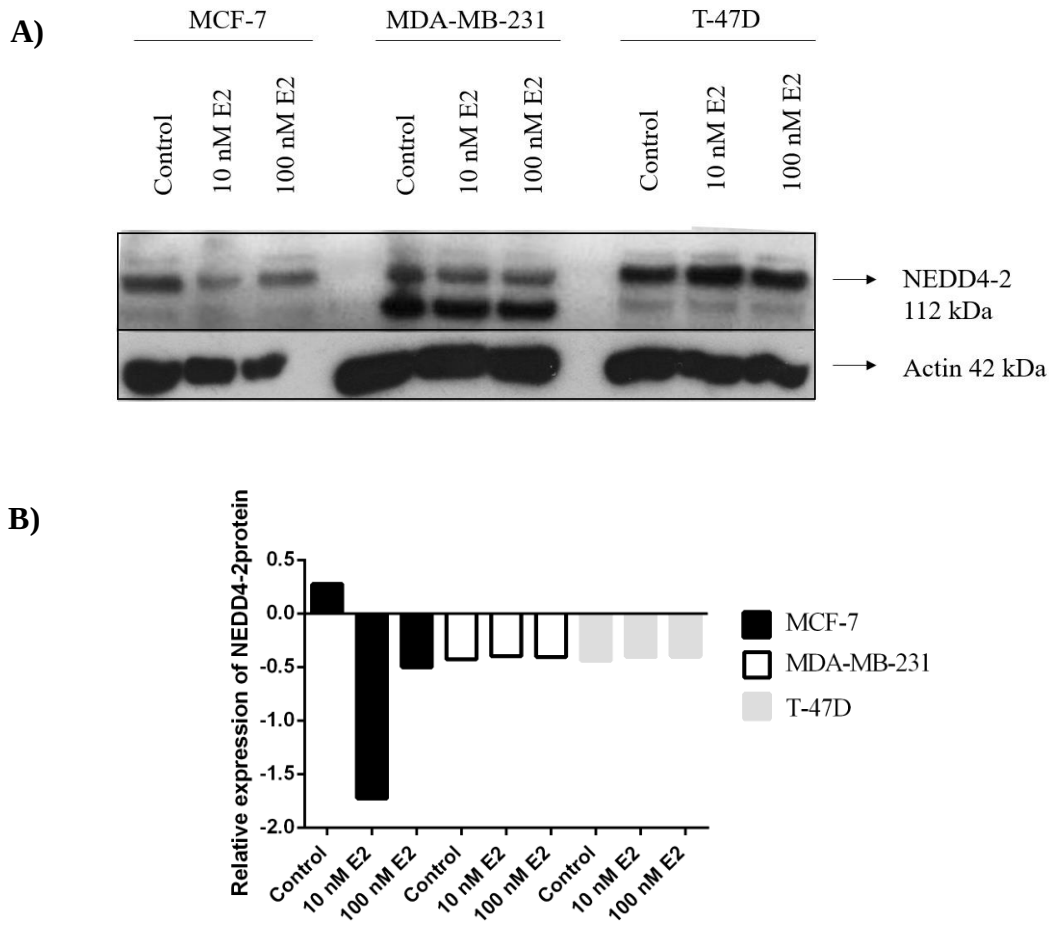

Figure 3.9: E2 effect on NEDD4-2 protein levels detected by Western blot in ER (+) and ER (-) breast cancer cell lines. **A.** Western Blot image of changes in NEDD4-2 protein in response to E2. **B.** Graphic showing analysis of changes in NEDD4-2 protein in response to E2, normalized to ß-Actin.

3.4.5. Alterations in ENaC subunits expression levels in response to E2

It has been found in microarray studies done in breast cancer by other groups that three subunits of ENaC, namely α, β and γ, were responsive to the E2. Since ENaC is one of the downstream gene regulated by MR signaling, we would like to further find out E2 activity on ENaC expression. Thus, we performed E2 experiments as explained in Results section, 3.3. Then, we tested modulations in expression of ENaC subunits with respect to E2 in both mRNA and protein levels.

3.4.5.1. Alterations in αENaC expression levels in response to E2

As it can be seen in Figure 3.10, E2 response was observed as downregulation in αENaC mRNA expressions in all three breast cancer cell lines. Two-way ANOVA test did not point out any significant differences in terms of interaction or variation between cell lines in expression levels of αENaC mRNA between E2 treated breast cancer cells (Pinteraction=0.6492, Pcell line=0.6492). However, we found that a significant treatment effect in breast cancer cell lines in terms of αENaC expression (Ptreatment=0.0125) suggesting that E2 overall reduces αENaC expression overall across cell lines. In addition, due to small sample sizes no significant change in expression of αENaC in each cell lines treated with E2 was observed when compared to control (MCF-7; p=0.2448, T-47D; p=0.0859, MDA-MB-231; p=0.2528, t-test).

Many efforts attributed to optimize antibody recognizing the full and cleaved form of αENaC, however we could not finalize the optimizations successfully so that E2 modulatory role could not be studied at protein level.

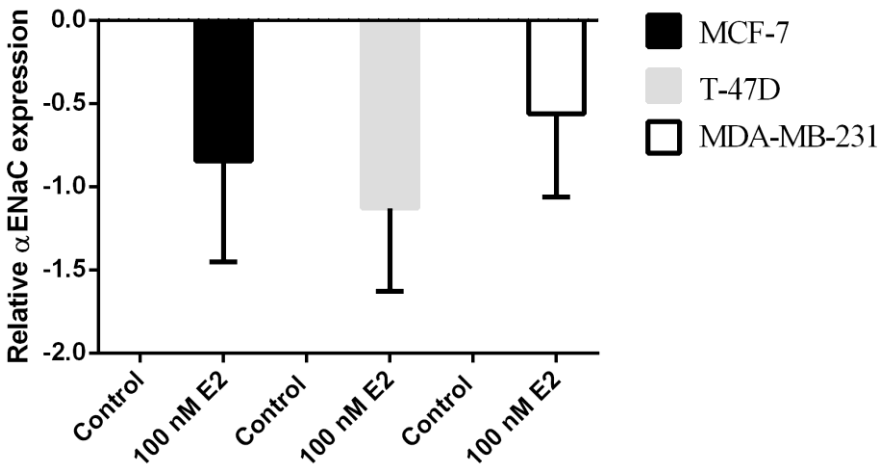

Figure 3.10: aENaC response to E2 at mRNA level in ER (+) and ER (-) breast cancer cell lines.

3.4.5.1. Alterations in βENaC mRNA and protein expression levels in response to E2

Modulations in expression of βENaC with regard to E2 response were also examined. We found a significant change in expression levels of βENaC mRNA between E2 treated breast cancer cells (Pinteraction=0.0078, Pcell line=0.0078; two-way ANOVA) but, E2 treatments did not show any effect between cell lines (Ptreatment=0.6336).

βENaC expression increased significantly in MCF-7 cells while it tended to decrease in T-47D cells (p=0.0448 for MCF-7, p=0.1117 for T-47D, t-test) (Figure 3.11).

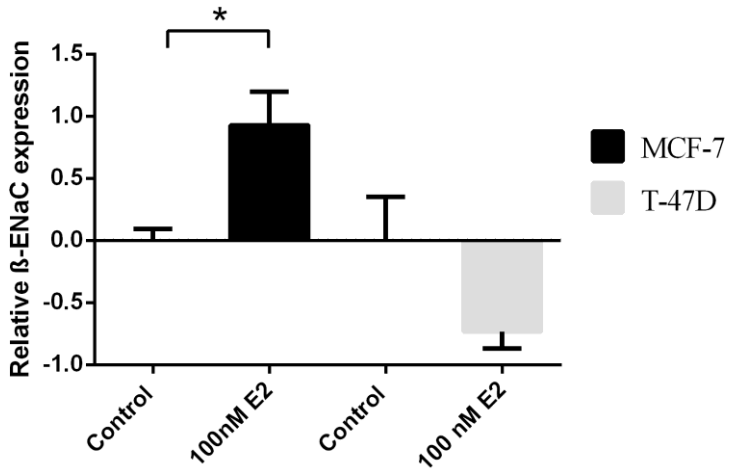

Figure 3.11: βENaC response to E2 at mRNA level in ER (+) breast cancer cell lines (*P ≤ 0.05; ** P ≤ 0.01; *** P ≤ 0.001).

Studies continued with investigating the alterations at protein level (Figure 3.12). βENaC protein expression increased in parallel to change at mRNA level in MCF-7 cells. 100 nM E2 dose resulted in slight increase in expression of βENaC protein in contrast to the results obtained for mRNA in T-47D cells. Furthermore, MDA-MB-231 cells showed decreased pattern with regard to E2 at protein level. Overall response to E2 in terms of βENaC protein expression among breast cancer cells were indicated as decrease compared to Actin.

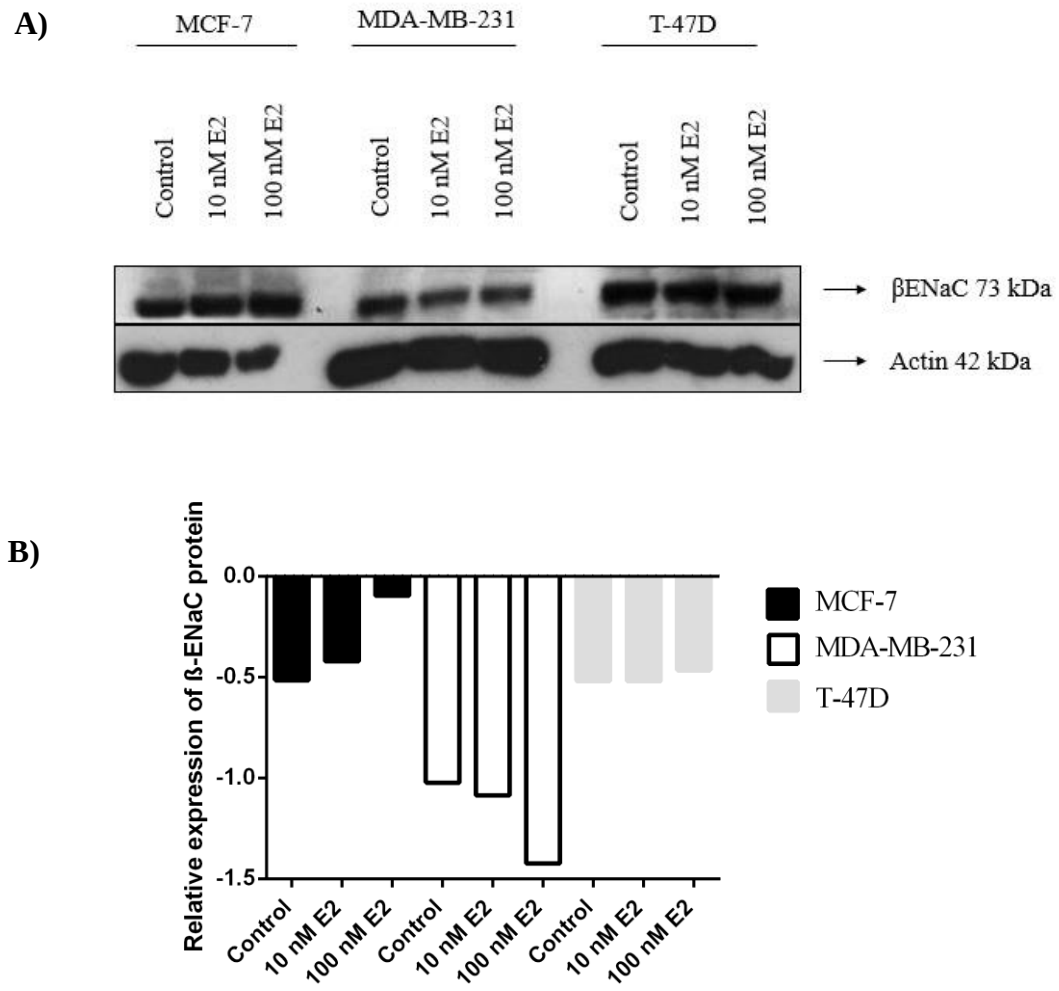

Figure 3.12: βENaC response to E2 at protein level in ER (+) and ER (-) breast cancer cell lines. **A.** Western Blot image of changes in βENaC protein in response to E2. **B.** Graphic showing analysis of changes in βENaC protein in response to E2.

3.4.5.2. Alterations in γENaC mRNA and protein expression levels in response to E2

E2 response was evaluated in γENaC as the third constituent of heterotrimeric structure of ENaC. We noticed a significant interaction between E2 treated breast cancer cells in terms of γENaC expression due to differences in behavior of cell lines in response to E2 ($P_{interaction}=0.0037$). A remarkable difference was also observed in response to 100 nM E2 between MCF-7 and T-47D cells ($P_{cell\ line}=0.0037$, two-way ANOVA). However, there was not any significant change between estrogen treatments and control groups among breast cancer cell lines ($P_{treatment}=0.6049$) (Figure 3.13).

There was an increasing trend in γENaC expression in MCF-7 cellstreated with 100 nM E2 (p=0.0746, t-test) while we detected a significant decrease in the γENaC expression in T-47D cells treated with E2 (p=0.0102, t-test)

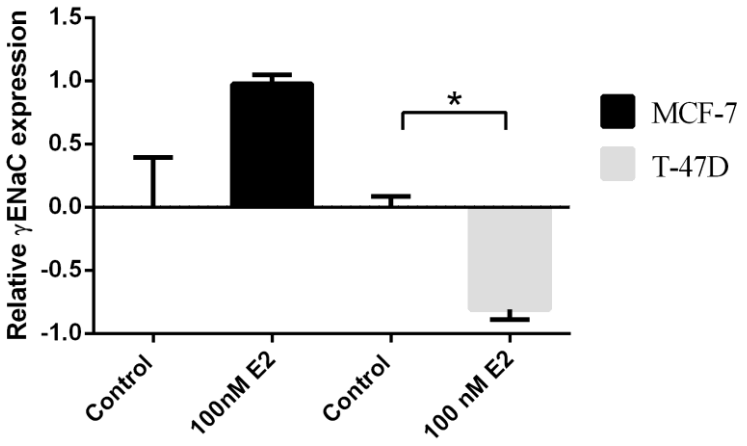

Figure 3.13: γENaC response to E2 at mRNA level in ER (+) and ER (-) breast cancer cell lines (*P ≤ 0.05; ** P ≤ 0.01; *** P ≤ 0.001).

When the response of E2 was investigated at the protein level, MCF-7 cells exhibited an increase trend to 10 nM E2 and a decrease trend to 100 nM E2 in terms of γENaC protein levels. Response to 100 nM E2 was found to be different between mRNA and protein levels of γENaC in MCF-7 cells. A contrary pattern was also observed in response to 100 nM E2 as displaying remarkable increase in γENaC protein expression in T-47D cells when it compared to mRNA result. Moreover, we could detect a noticeable change in γENaC protein expression in only MDA-MB-231 cells treated with 100 nM E2 (Figure 3.14). Increase trend (relative to Actin) in terms of γENaC protein expressions were observed across breast cancer cells.

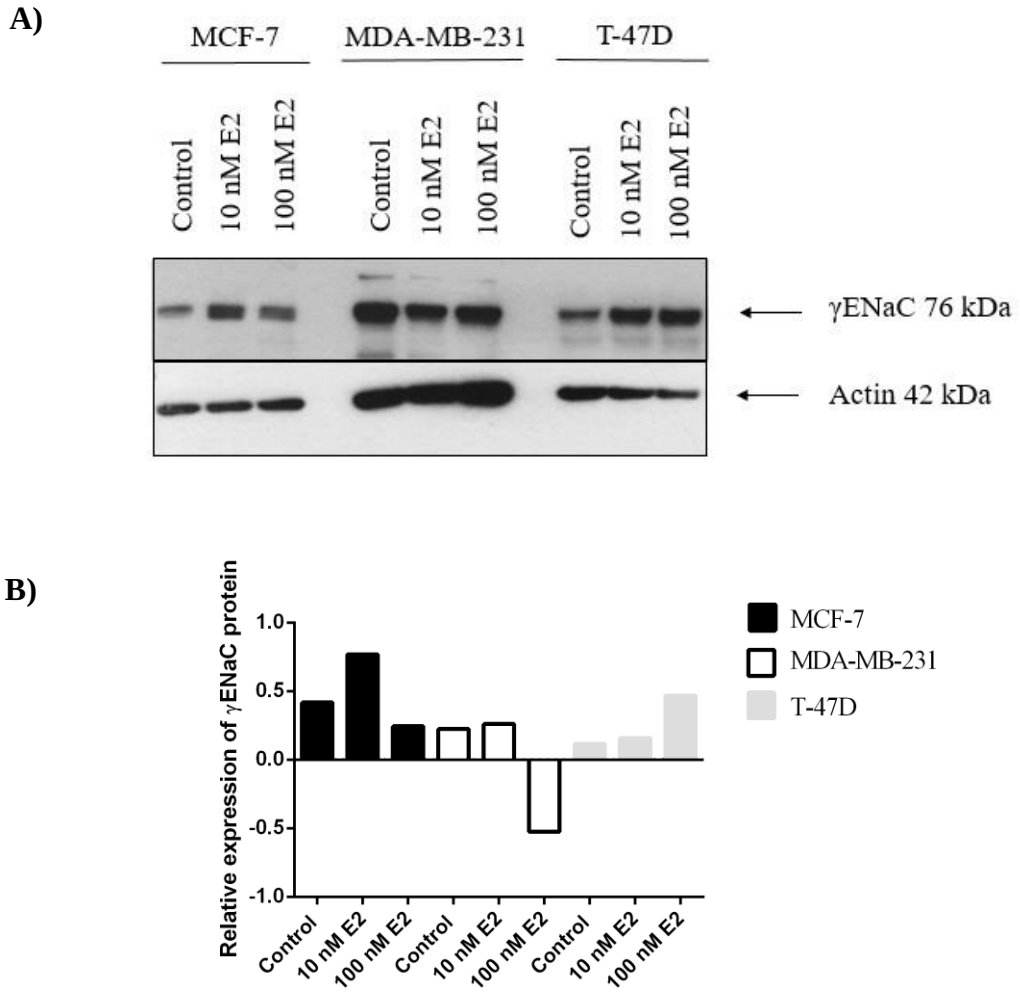

Figure 3.14: γENaC response to E2 at protein level in ER (+) and ER (-) breast cancer cell lines. **A.** Western Blot image of changes in γENaC protein in response to E2. **B.** Graphic showing analysis of changes in γENaC protein in response to E2.

3.5. Effects of ALDO on MR and its downstream targets in breast cancer

ALDO stimulated MR signaling play a pivotal role in controlling the expression patterns of ENaC and its regulators in epithelial tissues and its effect on ENaC subunits, SGK1 and NEDD4-2 that are mostly studied in kidney and cardiovascular system. Thus, we designed experiments to decipher the modulatory role of ALDO on ENaC and its regulators within MR signaling in breast cancer. Two breast cancer cell lines showing different MR expression patterns at both mRNA and protein levels (MCF-7 low, MDA-MB-231 high) were selected for mRNA studies. Since difficulties to detect low MR expressing MCF-7 protein occur in some Western Blot

studies, T-47D cells were added to the experimental design for protein studies in aldosterone experiments.

Aldosterone experiments were conducted by treating cells with 100 nM Aldosterone for 24 hrs to evaluate changes in mRNA levels and 10 nM and 100 nM Aldosterone for 24 hrs for protein levels as detailed in Materials and Methods, 2.2.1.9. Gene expression changes at the mRNA level were analyzed by applying two-way ANOVA test. If significant changes were observed in the effect of treatment or interaction on gene expression levels as a result of two-way ANOVA, a t-test was applied to each experiment, individually. Significant results were demonstrated on each figure with asterisks indicating significance levelDue to the one biological replicate in each Western Blot study, statistical analysis could not be applied. In addition, expressions of B and γENaC mRNA could not be detected in MDA-MB-231 cells.

3.5.1. Determining the effect of ALDO in breast cancer cell lines

As an initial step, ALDO effect was tested upon its two well-known downstream targets; αENaC and SGK1 which have been reported as transcriptionally induced by ALDO in epithelial tissues such as kidney and colon.

Figure 3.15 shows the changes observed in expressions of αENaC and SGK1 mRNA in response to ALDO in MCF-7 and MDA-MB-231 cells. No interaction, cell line or treatment effects were found between ALDO treated breast cancer cells with regard to αENaC expression (Pinteraction=0.0735, Pcell line=0.0735, Ptreatment=0.1124, two-way ANOVA).

Changes in expression levels of SGK1 significantly varied depending on the interaction and type of cell line (P interaction=0.0461, Pcell line=0.0461). In contrast, no significant treatment effect on SGK-1 mRNA expression was found in breast cancer cells (Ptreatment=0.3014, two-way ANOVA).

αENaC and SGK1 expressions showed increase patterns upon ALDO induction in MCF-7 cells while their expressions tent to decrease in MDA-MB-231 cells (For SGK-1 p_{MCF-7}=0.1609 $p_{MDA-MB-231}$=0.1562, t-test). An inverse regulation pattern

with respect to ALDO stimulated SGK1 and αENaC expressions was found between MCF-7 and MDA-MB-231 cells.

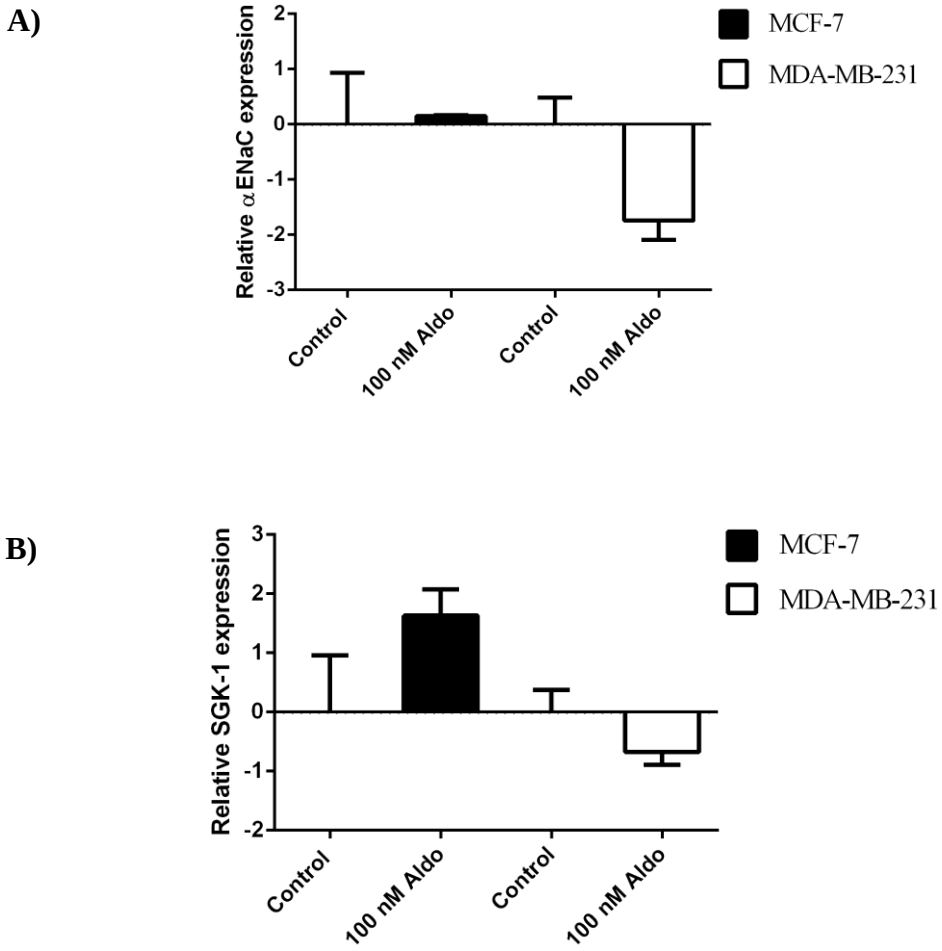

Figure 3.15: Changes in transcription levels of ALDO target genes αENaC and SGK1 upon ALDO stimulation. **A.** ALDO response of αENaC in MCF-7 and MDA-MB-231 cells. **B.** ALDO response of SGK1 in MCF-7 and MDA-MB-231 cells.

3.5.2. Detection of changes in MR expression levels

MR signaling is activated upon ALDO induction in epithelial tissues. To show this phenomenon also in breast cancer, we performed qPCR experiments in ALDO exposed MCF-7 and MDA-MB-231 cells. Figure 3.16 represents the results of these experiments. Interaction term and cell line effect between cell lines and E2 treatment were found significant (Pinteraction= 0.0355, Pcell line=0.0355). However,

treatment effect on MR mRNA expression was not significant in breast cancer cells (Ptreatment=0.3379) (Two-way ANOVA results).

Expression of MR mRNA in MCF-7 cells showed a significant upregulation (p= 0.0501) whereas it exhibited a downregulation trend in MDA-MB-231 cells in response to ALDO. ALDO could not be effective to change expression patterns in a significant manner in MDA-MB-231 cells (p=0.3638) (T-test results). The inverse regulation patterns among breast cancer cell lines were also observed for MR expression. MR protein could not be detected in Western Blot studies due to antibody related problems.

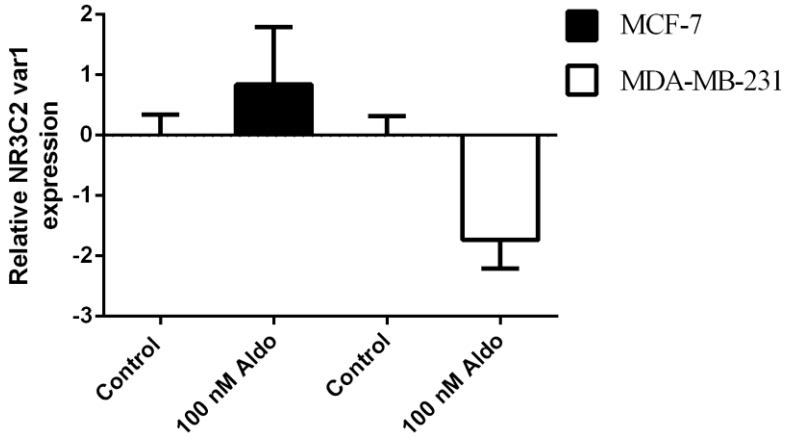

Figure 3.16: Changes in the expressions of MR mRNA in MCF-7 and MDA-MB-231 cells.

3.5.3. Detection of changes in NEDD4-2 expression levels in response to ALDO

Alterations in response to ALDO were studied in NEDD4-2 gene since the function of NEDD4-2 was controlled by ALDO in epithelial cells. NEDD4-2 response to ALDO in breast cancer cells was found to be affected by interaction and cell lines effects (Pinteraction=0.0107, Pcell line=0.0107, two-way ANOVA) while treatment did not lead to any effect on NEDD4-2 mRNA expression levels in breast cancer cells treated with ALDO (Ptreatment=0.8095).

An upregulation trend in NEDD4-2 mRNA expression was seen in MCF-7 cells stimulated by ALDO (p=0.1315, t-test). In contrast a significant decrease in NEDD4-

2 mRNA expression was observed in MDA-MB-231 cells (p=0.0428, t-test) (Figure 3.17).

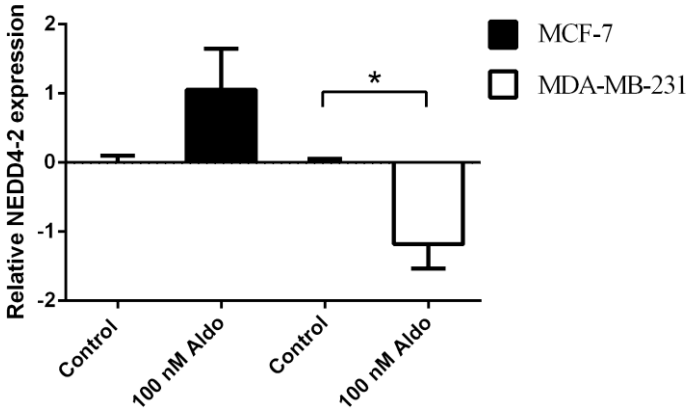

Figure 3.17: Changes in the expressions of NEDD4-2 mRNA in MCF-7 and MDA-MB-231 cells (*P ≤ 0.05; ** P ≤ 0.01; *** P ≤ 0.001).

ALDO effect was also studied at protein level of NEDD4-2 in breast cancer cells. Western Blot image of the results can be seen in Figure 3.18A. A controversial response was seen between mRNA and protein changes in terms of NEDD4-2 expression in MCF-7 cells treated with 100 nM ALDO since NEDD4-2 protein expression showed slight decreases at protein level. No changes were obtained in T-47D and MDA-MB-231 cells in response to ALDO (Figure 3.18B).

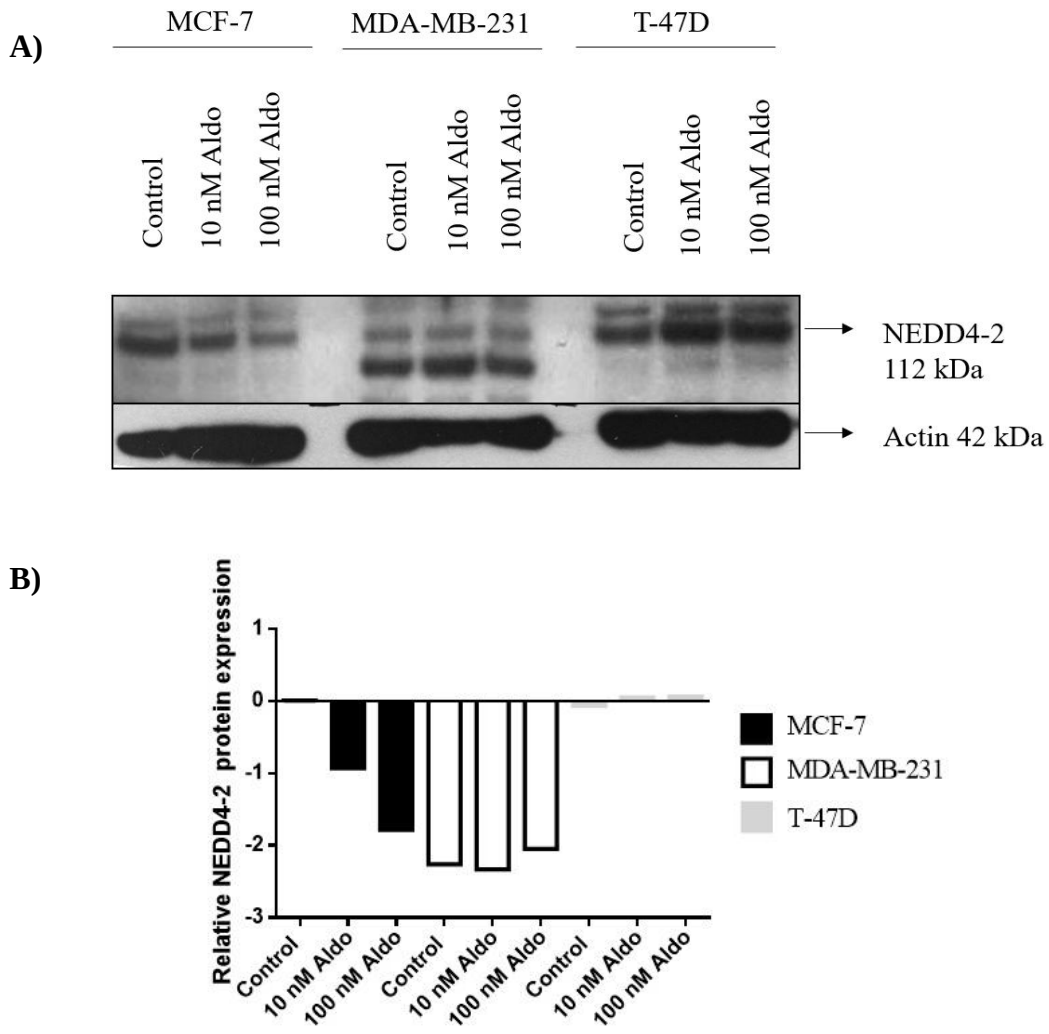

Figure 3.18: ALDO effect on NEDD4-2 protein levels detected by Western blot in ER (+) and ER (-) breast cancer cell lines. **A.** Western Blot image of changes in NEDD4-2 protein in response to ALDO. **B.** Graphic showing analysis of changes in NEDD4-2 protein in response to ALDO.

3.5.4. Detection of changes in expression of ENaC subunits in response to ALDO

ALDO induced mechanisms regulating ENaC expression at cell surface was delineated in epithelial tissues. As a part of our aims, we would like to further investigate this modulation of ENaC in breast cancer. Thus, we performed ALDO treatments and evaluated ALDO role in expression patterns of ENaC subunits.

3.5.4.1. Alterations in βENaC expression levels in response to ALDO

Expression changes in βENaC gene in response to ALDO were tested with both qPCR and ALDO experiments in order to reveal ALDO regulatory role in this subunit of ENaC.

βENaC expression was decreased upon ALDO induction without showing any statistical significance (p=0.3026) (Figure 3.19).

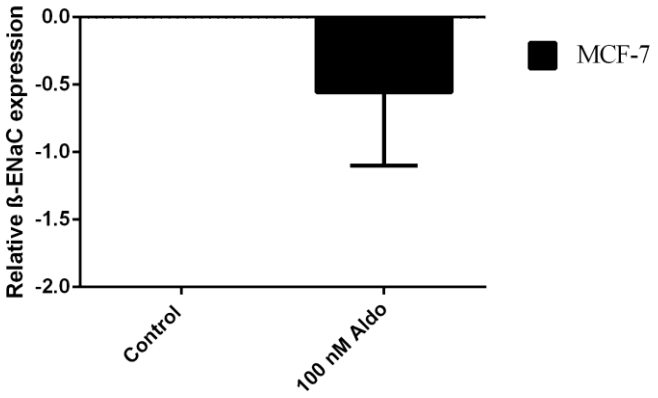

Figure 3.19: Changes in the expressions of βENaC mRNA in MCF-7 and MDA-MB-231 cells.

Figure 3.20 demonstrates expression changes of βENaC protein in response to ALDO across breast cancer cell lines. βENaC expression was increased in MCF-7 and T-47D cells treated with different dose of ALDO (10 nM and 100 nM). Change in βENaC expression with regard to 100 nM ALDO exposure was different between mRNA and protein in MCF-7 cells. Decreased expression pattern were observed in MDA-MB-231 cells treated with 100 nM ALDO (Figure 3.20B).

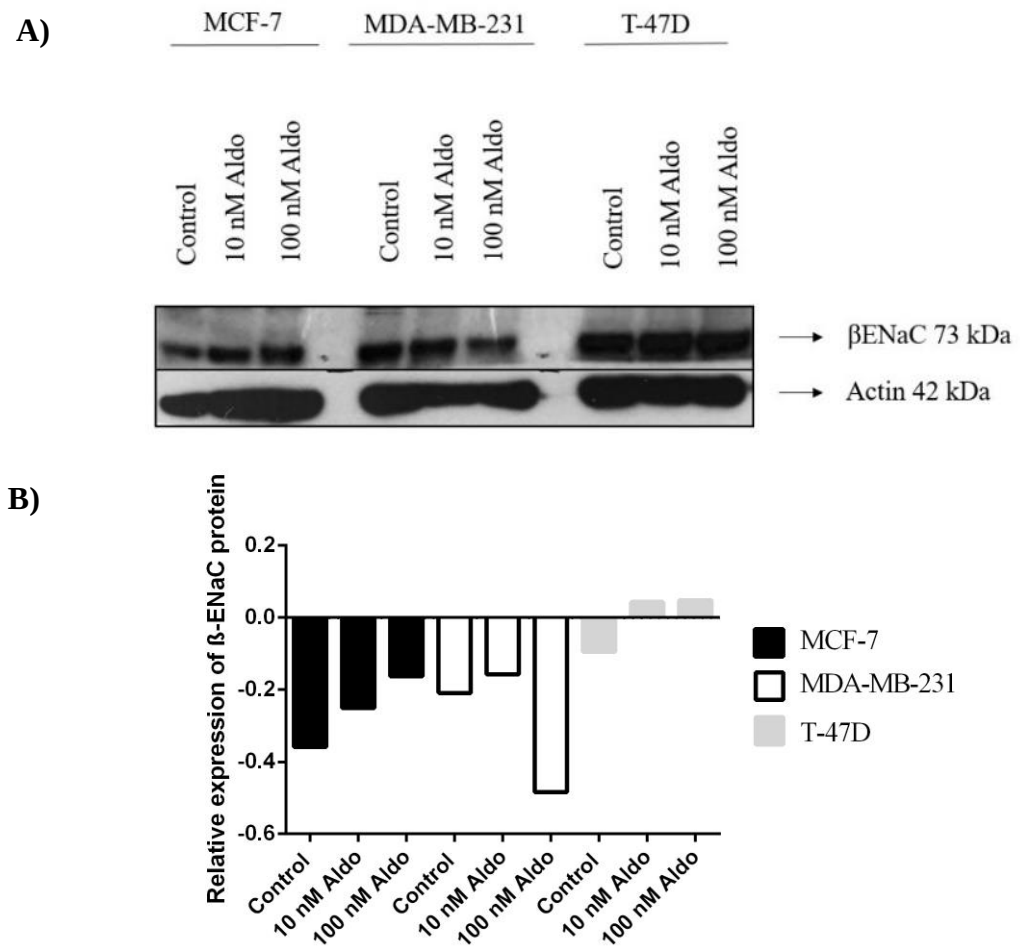

Figure 3.20: ALDO effect on βENaC protein levels detected by Western blot in ER (+) and ER (-) breast cancer cell lines. **A.** Western Blot image of changes in βENaC protein in response to ALDO. **B.** Graphic showing analysis of changes in βENaC protein in response to ALDO.

3.5.4.2. Alterations in γENaC expression levels

In the last step of our ALDO study, we investigated changes in γENaC expression. γENaC response to the ALDO treatment was a downward in its mRNA expression compared to the control in MCF-7 cells but, this was not a statistically significant change (p=0.4205) (Figure 3.21)

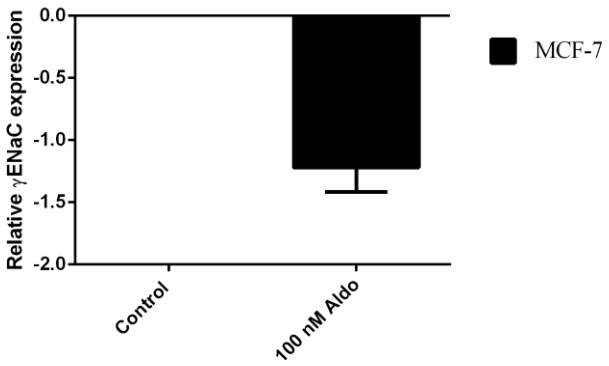

Figure 3.21: Changes in the expressions of γENaC mRNA in MCF-7 and MDA-MB-231 cells.

When we examined the ALDO effect at γENaC protein levels, we observed decrease in protein levels of MCF-7 cells treated with 100 nM ALDO in paralel to alteration at mRNA level in MCF-7 cells. However, we could observe no remarkable changes in expression of γENaC protein with regard to ALDO in T-47D and MDA-MB-231 cells. (Figure 3.22A, 3.22B).

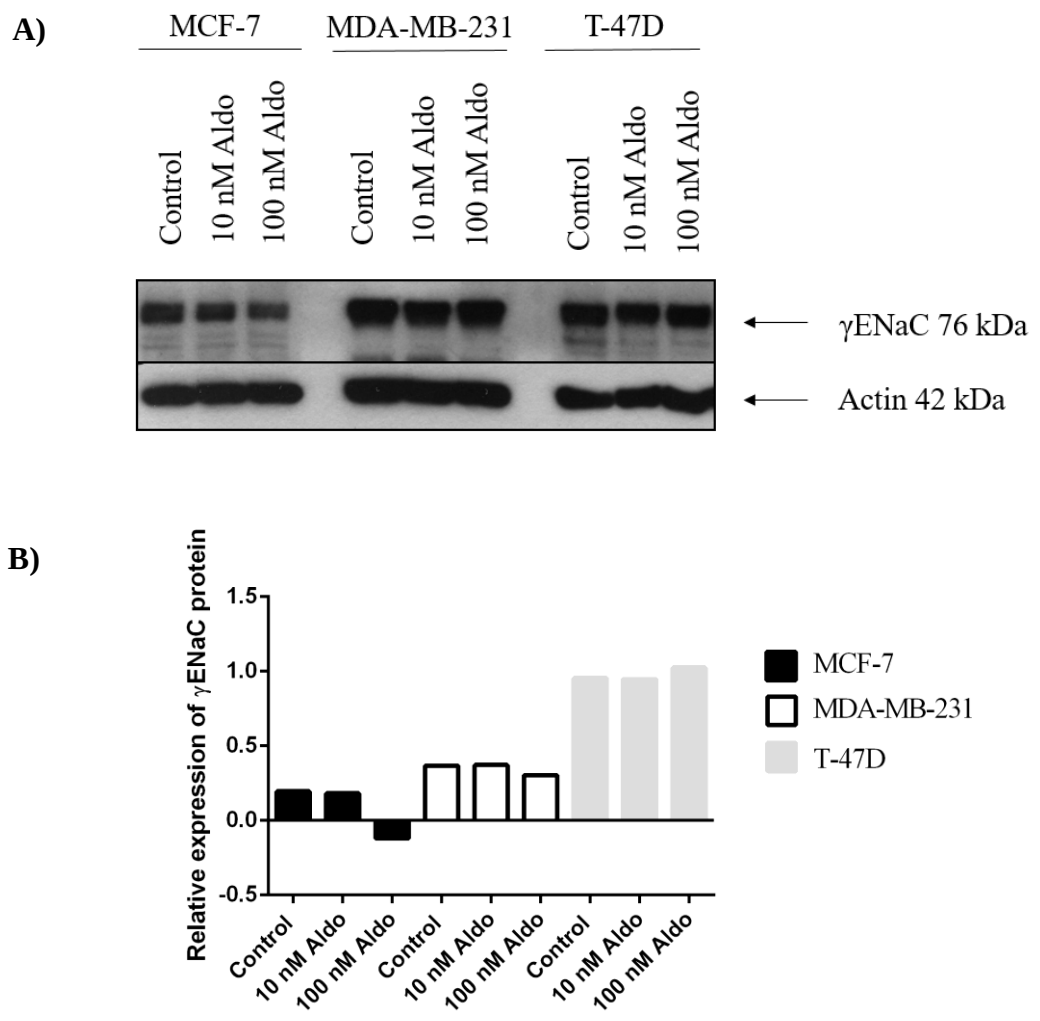

Figure 3.22: ALDO effect on γENaC protein levels detected by Western blot in ER (+) and ER (-) breast cancer cell lines. **A.** Western Blot image of changes in γENaC protein in response to ALDO. **B.** Graphic showing analysis of changes in γENaC protein in response to ALDO.

3.6. Heat map analyses of E2 and ALDO response in ER (+) and ER (-) breast cancer cell lines

Heat map analyses were performed in order to better visualize changes in gene expressions observed in response to E2 and ALDO exposures in MCF-7, T-47D and MDA-MB-231 cell lines. Heat maps were constructed by a web-based tool called as Morpheus, detailed in Materials and Methods section. Expression changes were adjusted to log fold changes with regard to control/untreated cells for mRNA and relative changes to reference gene (β-Actin) for protein. Changes were shown in a

colorimetric scale as higher expression, red color while lower expression, blue color. White color indicated no change in expression pattern.

MR and SGK1 displayed changes in similar directions in response to E2 by increasing their expressions at mRNA levels. In contrast to MR and SGK1, expression of NEDD4-2 decreased with regard to E2 treatments in ER (+) and ER (-) cell lines. β and γENaC were affected in same manner from E2 exposure in ER (+) cell lines. In contrast, there were differential responses in expression levels of αENaC mRNA with regard to E2 in ER (+) and ER (-) cell lines.

All genes tested for ALDO response exhibited totally different changes in their mRNA levels between MCF-7 and MDA-MB-231 cells with an exception of SGK1, since its expression levels were increased in response to ALDO in both MCF-7 and MDA-MB-231 cells. Furthermore, there were two genes; αENaC and NEDD4-2 that their expressions were not modulated by ALDO in MCF-7 and MDA-MB-231 cells, respectively (Figure 3.23).

We observed similar changes in expressions of MR and SGK1 between E2 and ALDO treatments in MCF-7 cells. Alterations seen in expression of αENaC mRNA in response to either E2 or ALDO were always different than other two subunits of ENaC, β and γENaC. Opposite regulatory patterns of E2 and ALDO were shown between expression of NEDD4-2 and β, γENaC with an exception in T-47D cells for γENaC.

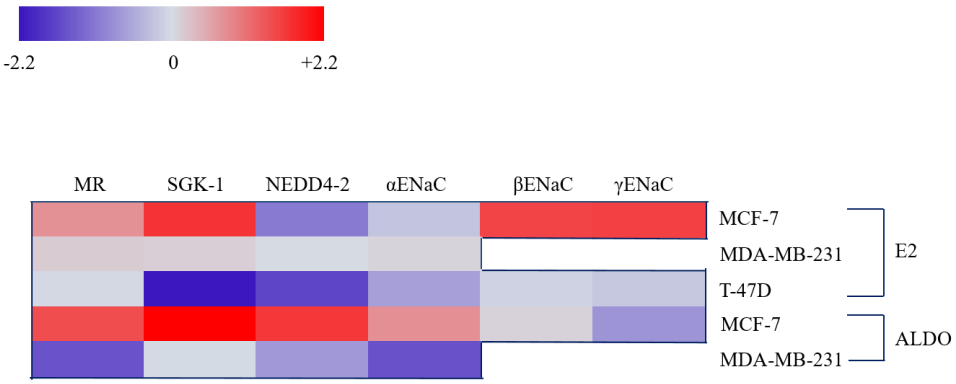

Figure 3.23: Heat map analysis of MR and its downstream targets genes in response to E2 or ALDO at mRNA level.

Figure 3.24 represents visual summary of changes detected at protein levels with regard to E2 or ALDO exposure. NEDD4-2 and γENaC displayed reverse changes in their protein expression levels in either E2 or ALDO treated breast cancer cells. The reverse pattern was disrupted in MDA-MB-231 cells treated with either 100 nM E2. Reverse regulation pattern was also observed in βENaC and γENaC expressions in breast cancer cells exposed to E2 or ALDO. Only 10 nM ALDO induction in MDA-MB-231 cells and 100 nM ALDO stimulation in MCF-7 cells regulated both ENaC subunits in a same manner as appearance of upregulations.

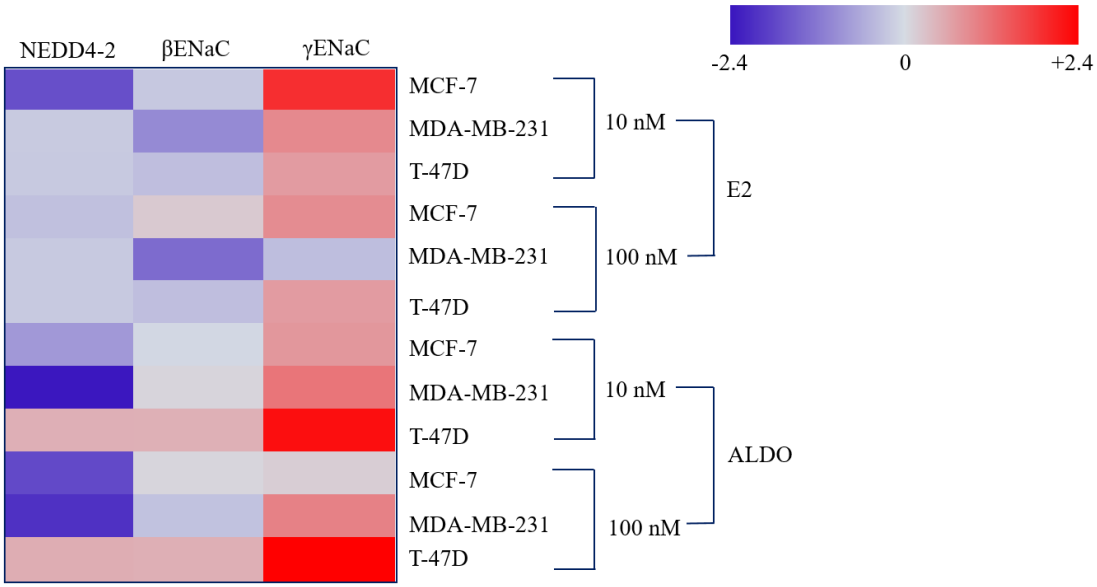

3.24: Heat map analysis of MR and its downstream targets genes in response to E2 or ALDO at protein level.

3.7. Summary tables for observed changes in response to either E2 or ALDO treatments

Visually represented data in 3.6 were summarized numerically in two tables according to changes detected in mRNA or protein levels in E2 or ALDO exposed breast cancer cell lines. Alterations in mRNA expression levels were given as log fold changes calculated by comparison to control/untreated cells while differences between protein expressions were compared to reference gene (β-Actin) expression. Significant changes in gene expression levels were shown by bold stylings.

As shown in Table 3.5, the most significant change was found in expression of SGK1 mRNA in E2 treated T-47D cells. Alterations in NEDD4-2 mRNA expression approached significance with regard to E2 exposure in ER (+) breast cancer cells. No significant changes were observed in expression levels in responses given to ALDO stimulation in breast cancer cell lines used in this study.

According to Table 3.6, MR is the most negatively affected gene by both E2 and ALDO treatments. E2 generally affected protein levels negatively whereas ALDO showed same number of positive and negative effects on MR and its downstream targets genes at protein levels.

Table 3.5: Log fold changes in mRNA expression levels of MR and its downstream targets in response to either 100 nM E2 or 100 nM ALDO with their significance values.

GENES	**CELL LINES**	MCF-7	MDA-MB-231	T-47D	MCF-7	MDA-MB-231
	TREATMENT	E2			ALDO	
MR	100 nM dose	0.125 (p=0.9995)	-0.48 (p=0.8496)	-0.6875 (p=0.6097)	0.838333 (p=0.5416)	-1.735 (p=0.1271)
SGK1		1.1075 (p=0.0568)	-0.515 (p=0.5284)	-2.1975 **(p=0.0020)**	1.6325 (p=0.1417)	-0.675 (p=0.6672)
NEDD4-2		-1.425 **(p=0.0414)**	-0.64722 (p=0.4841)	-1.8425 **(p=0.0126)**	1.055 (p=0.1230)	-1.1825 (p=0.0889)
αENaC		-0.845 (p=0.4215)	-0.5625 (p=0.7253)	-1.13 (p=0.2018)	0.15 (p=0.9921)	-1.7425 (p=0.1097)
βENaC		0.9275 (p=0.0572)	-	-0.7325 (p=0.1155)	-0.555 (p=0.3026)	-
γENaC		0.975 **(p=0.0314)**	-	-0.81 (p=0.0576)	-1.22 (p=0.4205)	-

Table 3.6: Log fold changes (relative to Actin) in protein expression levels of MR and its downstream targets in response to either 10, 100 nM E2 or 10, 100 nM ALDO.

GENES	CELL LINES	MCF-7	MDA-MB-231	T-47D	MCF-7	MDA-MB-231	T-47D
	TREATMENT	**E2**			**ALDO**		
NEDD4-2	10 nM dose	-1.72563	-0.3983	-0.40595	-0.93127	-2.33094	0.046667
βENaC		-0.42188	-1.08729	-0.52041	-0.25071	-0.15753	0.043339
γENaC		0.769167	0.261157	0.15752	0.182803	0.372227	0.947759
NEDD4-2	100 nM dose	-0.5016	-0.40467	-0.40595	-1.78666	-2.04843	0.061088
βENaC		-0.09654	-1.42457	-0.52041	-0.16234	-0.48397	0.048177
γENaC		0.243394	-0.52626	0.15752	-0.11888	0.303713	1.025494

3.8. Overexpression of Mineralocorticoid Receptor/MR

3.8.1. Optimization studies of MR overexpression in breast cancer cell lines

Expression of MR is often downregulated in breast cancer and this finding prompted us to perform MR overexpression studies in order to reveal novel signaling pathways counteracting with MR signaling and later define transcriptomic changes taking place when MR is overexpressed in breast cancer.

3.8.1.1. Testing transfection efficiencies of breast cancer cell lines by using the pEGFP vector

Breast cancer cell lines planned to use in overexpression studies of MR were tested to determine transfection capabilities. For this purpose, MCF-7, T-47D and MDA-MB-231 cell lines were transfected with pEGFP vector as explained in Materials and Methods section (2.2.1.10). After 48 hrs transfection, images were taken under the light microscope and fluorescent microscope for control/non-GFP transfected cells and GFP transfected cells as shown in Figure 3.25 and 3.26. Two images in upper sides represented the control cells while remaining images in below were GFP-transfected cells (Figure 3.25 and 3.26). There are many cells successfully transfected with pEGFP vector compared to control cells in MCF-7 as shown in Figure 3.25.

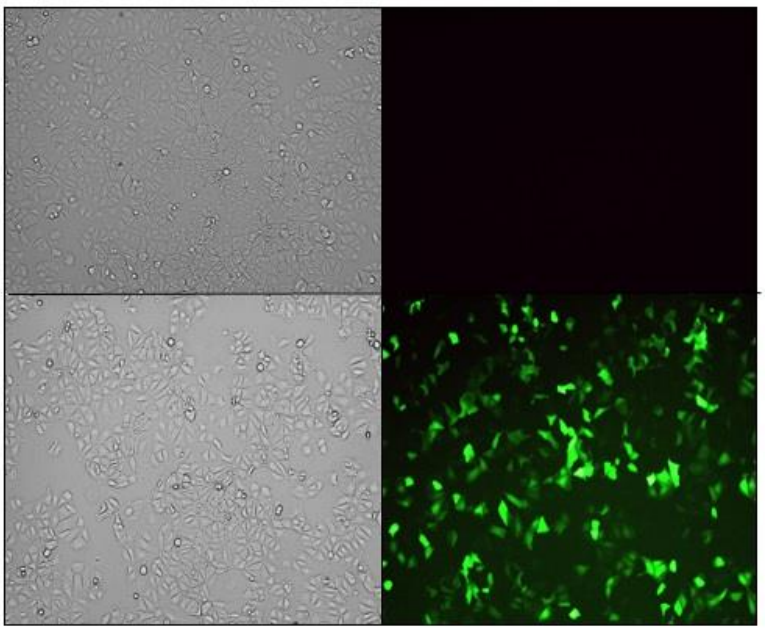

Figure 3.25: Image representing GFP transfected MCF-7 cells.

No GFP signal were obtained from the GFP transfected T-47D cells while only one cell could be transfected in MDA-MB-231 cells (Figure 3.26).

A)

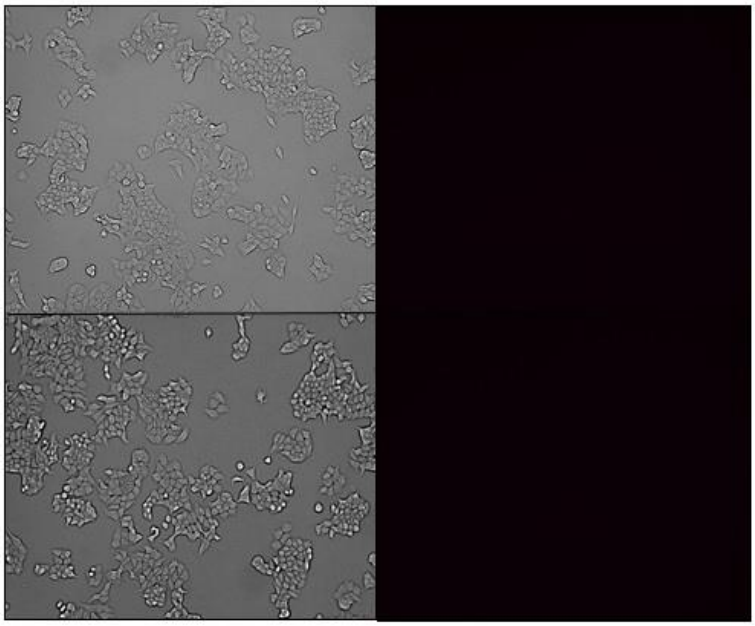

B)

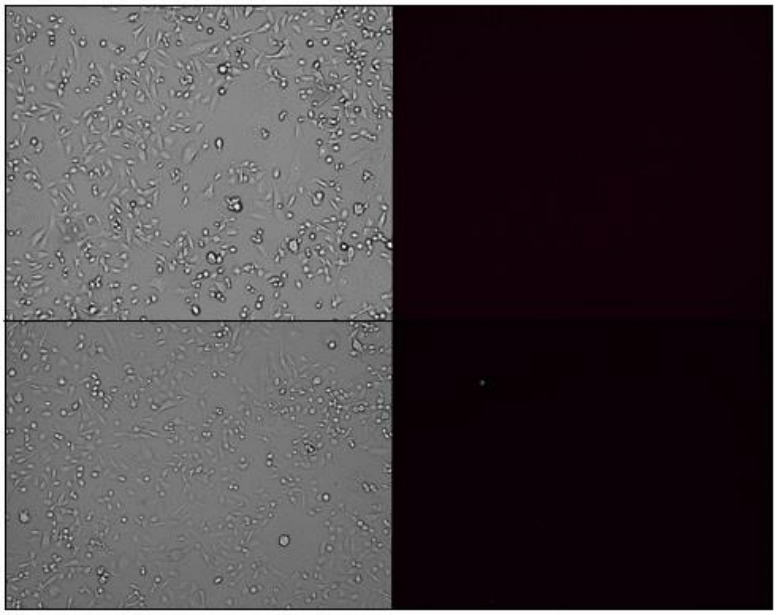

Figure 3.26: Images showing control (upper) and pEGFP transfected (below) breast cancer cell lines. **A.**T-47D cell line; control and GFP transfected cell images. **B.** MDA-MB-231 cell line; control and GFP transfected cell images.

3.8.1.2. MR overexpression in various breast cancer cell lines

First trial of MR overexpression was performed with the MCF-7 and T-47D cell lines as they were relatively easier to transfect and study in the cell culture. MCF-7, T-47D and HEK cells (as positive control of the study) were transfected with vectors overexpressing MR (pcDNA3.1 S-tag MR/S-tag MR) for 48 hrs as described in Materials and Methods, 2.2.1.11. Overexpression of MR was determined by using S-

tag antibody recognizing the S-tagged MR in overexpression vector by using Western Blot (Materials and Methods, 2.2.2.9).

Figure 3.27 represents the S-tag expression across cell lines used for MR overexpression. MR could not be overexpressed in MCF-7 and T-47D cells. However, overexpression was achieved in HEK cells transfected as evidenced by WB using S-tag MR.

Ponceau red staining of the blot indicating the presence of proteins on membrane after transfer step in Western Blot was used as reference (Figure 3.27). As seen in the image, proteins were successfully transferred to the membrane in this experiment.

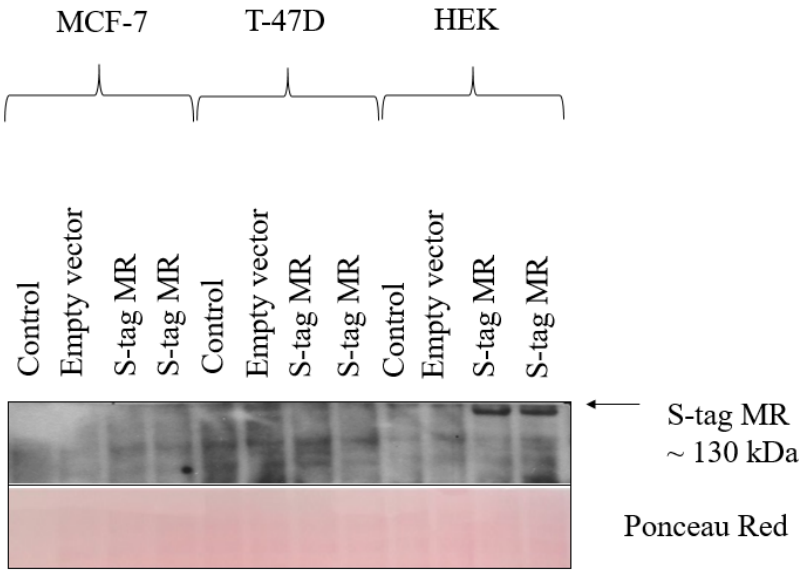

Figure 3.27: Western blot image and Ponceau Red staining of MR overexpression in MCF-7, T-47D and HEK cell lines.

3.8.2. q-PCR Analyses of MR overexpression in MCF-7 cells

Overexpression studies performed with HiPerFect transfection reagent at the protein level could not be finalized successfully. We also tested overexpression at the mRNA level in MCF-7 cells. Transfection of S-tag MR to MCF-7 cells was performed by following the same procedure as in the protein study.

In addition to using the HiPerFect transfection reagent in transfection studies, we also utilized Lipofectamine® 2000 transfection to test if any difference between HiPerFect and Lipofectamine® existed. Overexpression of MR studies conducted by Lipofectamine® as explained in Materials and Methods 2.2.1.10. MCF-7 cells also were transfected with S-tag MR for 48 hrs and total RNA isolation, qPCR experiment was performed.

Figure 3.28 shows mRNA expressions of MR across control cells (dmem, mock), cells transfected with either S-tag MR or empty vector by using either HiPerFect or Lipofectamine®. We found significant relationship between cell lines and overexpression of MR with regard to MR expression in this study ($p=0.0235$, two-way ANOVA). Overexpression of MR was observed higher in Lipofectamine® used cells than those transfected by HiPerFect used cells ($p=0.0171$, two-way ANOVA). Moreover, Overexpressed cells displayed sharp increase in expression of MR when they compared to control cells ($p < 0.0001$, two-way ANOVA). Expression of MR was increased in MR overexpressing cells in both HiPerFect and Lipofectamine® treatments, significantly with p values 0.0003 and 0.0004, respectively.

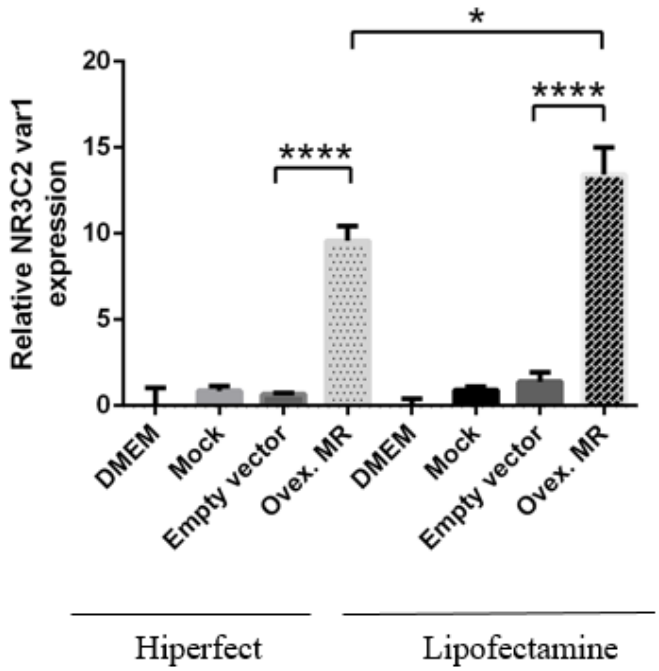

Figure 3.28: Overexpression of MR at mRNA level by using HiPerFect or Lipofectamine® transfection reagents.

3.8.3. Western Blot analysis of MR overexpression in MCF-7 cell line

According to the result demonstrated in Figure 3.29, MR mRNA was significantly upregulated in MCF-7 cells when Lipofectamine® was used in the experiment. Therefore, we performed overexpression study at the protein level by using Lipofectamine®. MCF-7 cells were transfected with different concentrations of S-tag MR construct and empty vector for 48 hrs. HEK cells were used as positive control for transfection experiments (1 µg/µl vectors were transfected) and Western Blot studies.

MR protein was upregulated in 200ng/µl, 1 µg/µl and 2 µg/µl S-tag MR vector transfected MCF-7 cells and HEK cells. However, S-tag antibody could not detect the overexpression in 200 ng/µl vector used cells in MCF-7. Stripping protocol was carried out in order to re-blot the same membrane with MR antibody. Overexpression was confirmed with antibody against MR across all concentrations of MR overexpressing vector in MCF-7 cells in Western Blot (Figure 3.29). For better images, brightness and contrast were adjusted to +20.

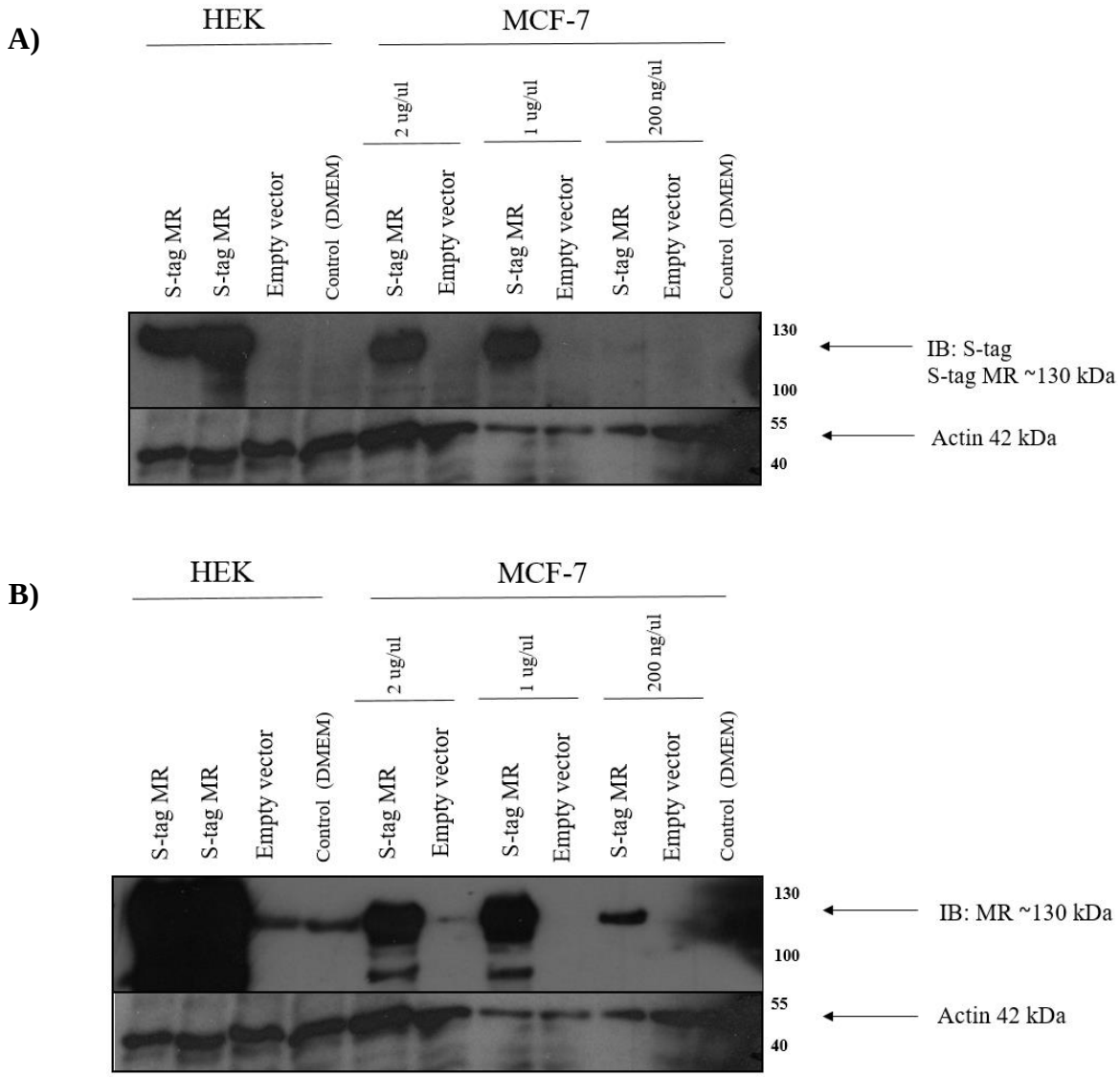

Figure 3.29: Western Blot analysis of MR overexpression. **A.** Detection of MR overexpression using S-tag antibody. **B.** Detection of MR overexpression using MR antibody.

3.8.4. Effects of MR overexpression and activation on MR and its downstream targets

MR and its relation with its downstream targets were investigated upon overexpression by S-tag MR construct and activation by ALDO. MR was overexpressed in MCF-7 cells, and later MR activity was induced by ALDO upon overexpression.

As represented in Figure 3.30, expressions of MR, SGK1 and NEDD4-2 mRNA increased in parallel with MR overexpression in MCF-7 cells. Changes in MR and SGK1 levels (Figure 3.30A and 3.30B) were statistically significant with p values 0.0001 and 0.0162, respectively while the change in NEDD4-2 was not significant (p=0.4984) (One-way ANOVA) (Figure 3.30C). There were also significant difference with regard to SGK1 and MR expressions between empty vector and S-tag MR transfected cells (p=0.0283, p=0.0004). Overexpression of MR and ALDO stimulation in MCF-7 cells did not result in significant change of expression in MR, SGK1 and NEDD4-2 mRNA levels.

A)

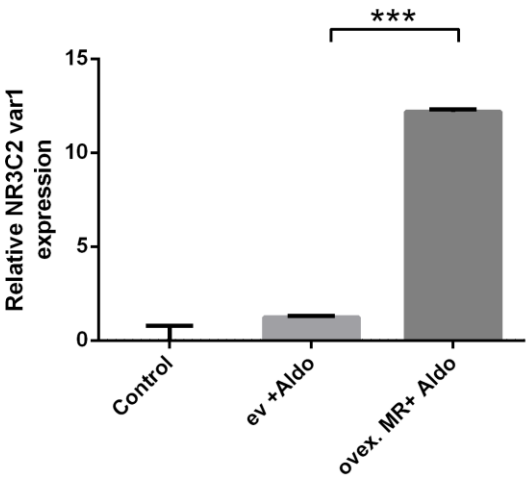

B)

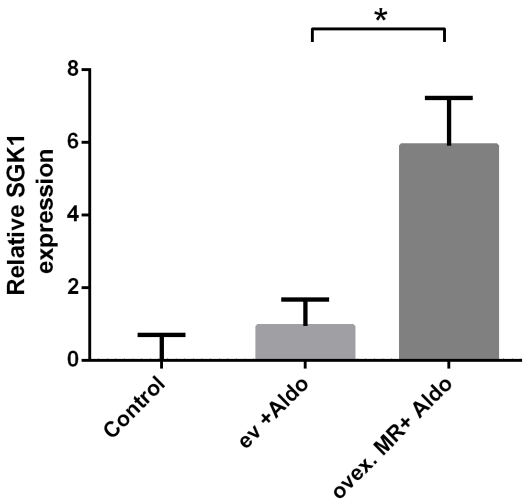

C)

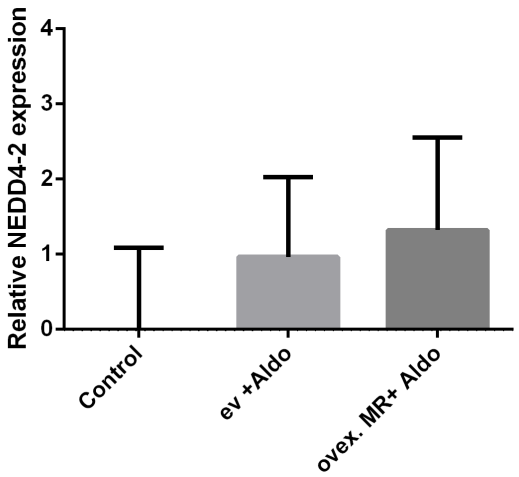

Figure 3.30: Effects of overexpression and activation of MR on MR, SGK1 and NEDD42 mRNA expression levels.

ENaC subunits were also affected by upregulated and induced activity of MR. The effects of both ALDO and MR overexpression on expression level of αENaC as a well-known downstream target of MR in response to ALDO was similar however, observed increases in mRNA expression levels only approached significance ($p=0.1072$) (Figure 3.31A). The two other subunits of ENaC, β and γ exerted a similar change patterns in terms of expression in response to overexpression and activation of MR (Figure 3.31B, 3.31C). Expressions of both subunits were upregulated in ALDO induced MR overexpression significantly ($p=0.0410$ for βENaC, $p=0.0263$ for γENaC). In addition, changes observed in MR overexpressing cells were significantly higher than empty vector transfected cells in β and γENaC.

A)

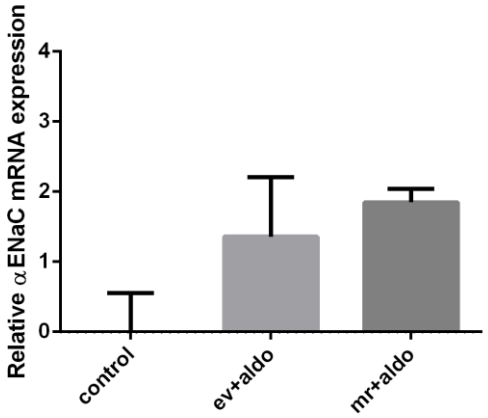

B)

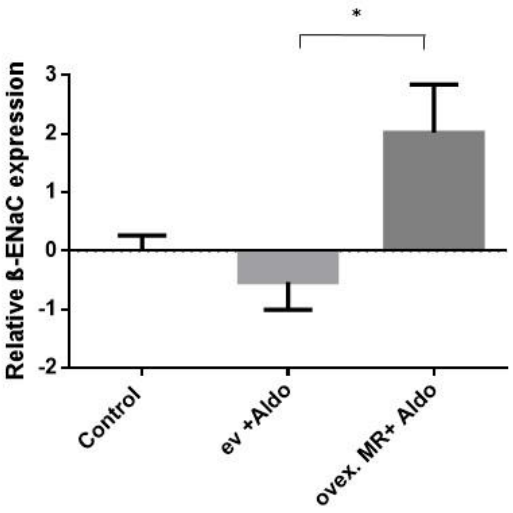

C)

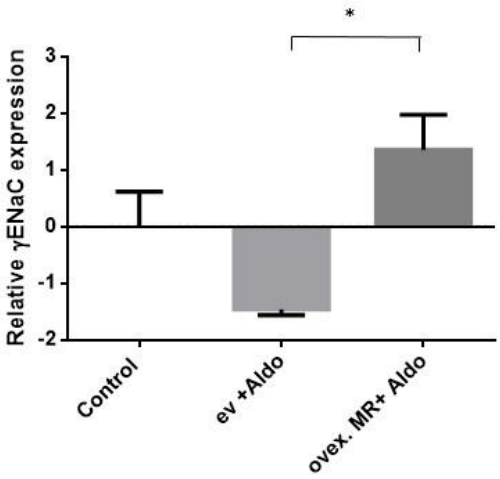

Figure 3.31: Effects of overexpression and activation of MR on subunits of ENaC mRNA expression levels. **A.** Expression levels of αENaC. **B.** Expression levels of βENaC. **C.** Expression levels of γENaC.

Chapter 4

Discussion

Mineralocorticoid receptor is expressed in many epithelial tissues and diverse action of MR is regulated by its tissue specific expression status. Dysregulation in MR signaling was reported in the studies involving lung cancer[45], hepatocellular carnicoma[46] and colon cancer[47-48]. We also showed similar dysregulation of MR in breast cancer by analyzing breast cancer microarray data sets *in silico*. In this study, we moved our direction into another member of steroid hormone receptors, GR since it shares structural and ligand similarities with MR and diverse actions of GR have been indicated in breast cancer. In the light of these similarities and lack of any study interrogating association between GR and MR expression related with breast cancer in the literature, we aimed to find out a) possible coregulation of MR and GR expression which might contribute to subtyping of breast cancer as possible new biomarkers thereby affecting disease diagnosis and prognosis and b) regulation of MR signaling in breast cancer cells in response to Estrogen (E2) and aldosterone (ALDO).

We delineated the modulation of MR and GR in breast cancer for the first time in the literature. Our study revealed that MR and GR displayed correlative expression pattern (with an exception of two cell lines; MCF-7 and CAL-51) across breast cancer cells. Both receptor expressions were found to be higher in triple negative breast cancer cell lines which don't express ER and PR and belong to basal subtype, than other breast cancer cells. We hypothesized that either E2 or Progesterone might make an inhibitory crosstalk/interaction with MR and/or GR when there is not enough ESR1 thereby decrease transcriptional activity of MR or GR in breast cancer cells. The higher expression of MR and GR could be a positive feedback to increase

the amount of receptor in response to potential crosstalk and inhibition by E2 or Progesterone. Since, it has been previously shown that E2-stimulated ER makes an inhibitory complex with MR in nucleus, this interaction can block transcriptional activity of MR in kidney and vascular endothelial cells[117]. Furthermore, it can feedback the expression of receptors.

In the second part of this study, we demonstrated that ER (+) (MCF-7 and T-47D) and ER (-) (MDA-MB-231) breast cancer cells expressed MR and its downstream targets, namely, SGK1, NEDD4-2 and three subunits of ENaC at the protein level. MR normally expresses a 107 kDa protein however we observed a shift in its molecular weight. MR activity has been modulated by many posttranslational modifications (i.e.; phosphorylation, ubiquitination) so that observed shift might be as a result of these kind of modifications. It has been also shown that MR phosphorylation leads to rise in the molecular weight of MR in kidney cells[43]. We also detected different regulations and expression patterns in terms of MR downstream targets across breast cancer cells. Two closed bands representing NEDD4-2 expression across breast cancer cells were identified previously as possible NEDD4-2 alternative splice forms in kidney and adrenal[127]. Moreover, cleaved forms of αENaC were observed in breast cancer cells possibly as a result of cleavage of full form by proteases which is a necessary process for its activation[101]. However, we could observe the cleaved form of αENaC migrating 10 kDa compared to control cell lines[101]. This indicates that there could be different tissue specific proteases regulating αENaC cleavage in breast cancer cells.

Following our initial study on expression levels of MR and its downstream targets, we performed an *in silico* analysis regarding investigating a possible regulator of these genes in breast cancer. We found out that E2 has role in regulation of MR downstream targets in breast cancer and aimed to validate our *in silico* findings with *in vitro* experiments, thereafter. Since we carried out in silico study by using only one probeset for each gene in our GEO2R analyses, thus this might have caused inconsistencies; the findings might improve if more than one-probe set were used and as well as other potential datasets were analyzed. However, in silico analyses for SGK1, NEDD4-2 and αENaC E2 induction/repression were strongly validated in vitro in MCF7 cells. This suggests that there is an inverse association between SGK1

and NEDD4-2 at the mRNA and possibly protein levels in the breast cancer cell MCF7. This is the first time validation and it was as expected from their functional inverse associations in regulating ENaC expression[133]. Future studies should focus on the mechanisms mediated by E2/ESR1 signaling and how it crosstalks with MR/GR signaling.

We used MDA-MB-231 cells as negative control in our E2 studies since this cell line does not express ER. Thus, we could not detect any alterations in MR downstream target genes with regard to E2 in MDA-MB-231 cells in line to our *in silico* results.

SGK1 has been shown previously with its anti-apoptotic role in breast cancer and expression levels of SGK1 indicated as an important parameter in Akt inhibitor resistant breast cancer therapies[84]. Our study demonstrated that E2 regulates the expression patterns of this gene in ER (+) breast cancer cell MCF7 but not in T47D thus E2-regulated SGK1 expression patterns might become an important parameter in diversified therapies against ER (+) breast cancer cells.

As another downstream target of MR, NEDD4-2 was also found to be downregulated by E2 across ER (+) cells both *in silico* and *in vitro* (at both mRNA and protein levels), *c*onsistently. NEDD4-2 has an important role in cancer progression since copy number loss of NEDD4-2 result in decreased expression of NEDD4-2 which further contributes to tumor growth and invasiveness in glioma, melanoma[91]. It has been also suggested that the same role of NEDD4-2 could be observed in breast cancer as another cancer type had copy number loss in NEDD4-2[91]. We showed that expression of NEDD4-2 at mRNA and protein levels were decreased in response to E2. We concluded that NEDD4-2 is ER responsive in breast cancer. Strategies against increasing NEDD4-2 expression levels might disrupt cancer progression in these cancer cells. Regulation of NEDD4-2 by E2 highlights a possible modulatory mechanism to alter cancer progression in ER (+) breast cancer cells.

ENaC has been well-known for its regulatory role in ion homeostasis in epithelial tissues. Na^+ and Cl^- exchange with extracellular compartments by ENaC activities contributes cell-volume and shape changes which is required for cell invasion[104]. There are many recent studies indicating that ENaC could be a possible target for invasive, metastatic cancer types due to its role in modulating cell shape and

volume[131-132]. Moreover, altered expression patterns of αENaC and γENaC have been previously shown to be associated with tumor invasion in melanoma and glioma[103-104]. As we demonstrated that expression patterns of ENaC subunits tend to be regulated by E2 in ER (+) breast cancer cells. We proposed that E2 actions on ENaC might be a possible regulatory mechanism of tumor invasion in breast cancer and ENaC could serve as new target in breast cancer. A recent study showed that E2 regulates ENaC expression in kidney ductal cells[134] An increase in cell volume is characteristic of high estrogen states, which might be explained by increased Na^+ absorption[134]. However, we did not examine any contribution of these changes to tumor invasion in these breast cancer cells. However, cell size changes can also affect migration and invation of cancer cell lines and sodium influx could be an important factor herein too[132]. Moreover, we observed differential regulation of βENaC and γENaC expression between mRNA and protein in E2 treated ER (+) breast cancer cells. It is possible that posttranscriptional mechanisms could lead to inconsistent results between mRNA and protein levels in ENaC subunits expressions in response to E2. A study performed with kidney cells showed that transcriptional activity of γENaC was downregulated by a transcription repressor protein, an RNA binding protein regulating post-transcriptional mechanisms[128]. Expression of this negative regulator protein is upregulated upon ALDO stimulation and causes constitutively active MR which result in decrease in expression of βENaC and γENaC mRNA. Negative regulator exerts its function rapidly and de novo protein synthesis is not involved so that only the mRNA levels were affected through actions of negative regulatory protein.

As a part of our second aim, we further investigated ALDO actions on MR and its downstream targets in same set of ER (+) and ER (-) breast cancer cells used in E2 study. Our data demonstrated that there were an inverse expression pattern in MR and its downstream targets with regard to ALDO response between MCF-7 and MDA-MB-231 cells. The reason behind this opposite regulation might arise from difference in basal MR expression in MCF-7 and MDA-MB-231 cells (Figure 3.1 and 3.2) as well as molecular differences between these two cell lines with respect to ER and PR status. However, observed changes could not reach any statistical significance possibly due to either sample size or variations between Ct values of biological replicates in response to ALDO; thus, should be repeated.

Main function of ALDO in body is to regulate Na^+ reabsorption and K^+ excretion in kidney thereby controlling the fluid balance and blood pressure of the body. ALDO have been already demonstrated as regulator of MR and its downstream targets in epithelial tissues involving kidney[80-98-107]. ALDO exerts its functions through binding to MR in its target tissues[133].

We found that in MCF7 cells SGK1 mRNA increased in response to ALDO, as expectedly but this did not reflect on ENaC mRNA levels since NEDD4-2 was also induced. On the other hand, we saw that E2 resulted in the expected direction of changes. On the other hand, there was a reduction in NEDD4-2 protein level upon ALSO exposure. These results suggested that ALDO affects MCF7 cells that contain low levels of MR yet since it has low levels it may not be as significantly effective as it could be as suggested by the MR overexpression studies. This means that we could manage SGK1 specific actions in breast cancer by controlling it through actions of ALDO-stimulated MR. Moreover, it has been previously indicated that ALDO-stimulated SGK1 blocks NEDD4-2 inhibitory action on ENaC expression in kidney and cardiovascular system[133].

We also found that higher MR expression stimulated with ALDO leads to low ENaC expression in ER (-) breast cancer cell; MDA-MB-231. As explained in Introduction part, expression patterns of ENaC was associated with tumor progression and invasiveness in many cancer types. We suggested that ALDO regulated ENaC might be a possible target mechanism for tumor progression and invasiveness in ER (+) breast cancer cells.

Two subunits of ENaC; β and γENaC were differentially regulated by ALDO in ER (+) and ER (-) breast cancer cells. Posttranslational mechanisms controlling ENaC expression might have role in regulation of ENaC subunits at protein level[97]. Genes involved in ENaC regulatory complex such as SGK1 might have modulatory effects on expression patterns of ENaC subunits in breast cancer as it has been shown in kidney[129]. Expressions of NEDD4-2 and γENaC were effected in opposite manner from ALDO stimulation thus there is likely an inhibitory effect of NEDD4-2 on γENaC expression as stated previously by Synder et. al[129]. One of the most

interesting observations was that there was differential splicing patterns between the two ER (+) and the one ER (-) breast cancer cell line. Future studies should be performed to establish whether the differential banding pattern we observed could separate ER status and has a potential meaning[135]. There are different isoforms of NEDD4-2 shown to be involved in differential functions[136-137].

In our final aim in this study, we investigated effect of MR overexpression on MR downstream targets studied in the context of this thesis. We managed to demonstrate overexpression of MR at both the mRNA and protein levels in MCF-7 cells. When we perform overexpression study with different vector concentrations, we could not detect overexpression of MR in 200 ng/µl vector transfected MCF-7 cells by using S-tag antibody. S-tag antibody might not be capable of detecting low levels of vector overexpression. Furthermore, one additional band closed to 100 kDa was appeared in higher concentrations of MR overexpression. Possibly, this band was a result of posttranslational mechanisms (i.e.; ubiquitination) acted on MR[43]. To our knowledge overexpression of MR in MCF7 cells is the first in the literature. Hence it provides a system to test whether ligands of steroid receptors could interact with MR differentially. It also allows for testing simultaneous activation of different nuclear receptors at the same time ligand-dependent and independently as shown in other studies in the field.

After setting down the overexpression system, we concentrated our efforts on regulation of MR and its downstream targets by ALDO in MR overexpressed MCF-7 cells. We demonstrated that expressions of MR, SGK1, βENaC and γENaC displayed changes in similar directions in response to ALDO in MR-overexpressing MCF-7 cells., i.e., they all increase in expression. Previously, ALDO actions have been delineated in kidney and cardiovascular diseases. Actions of SGK1, NEDD4-2 and ENaC subunits were relied on MR activities stimulated by ALDO[130]. Result of this study indicated similar regulatory actions of ALDO via MR signaling in downstream targets of MR in breast cancer. It also showed that increased MR expression coupled with ligand stimulation led to higher MR activity. What remains to be tested is whether this increased activity results in any changes in terms of cell proliferation, apoptosis, and migration in breast cells.

We proposed regulatory mechanism for E2 and ALDO in ER (+) and ER (-) breast cancer cells. As demonstrated previously by Mueller et. al.[117] study that E2 activates ER which further can make a complex with MR in the nucleus. This complex could be suggested as activatory in MCF-7 cells since E2 actions resulted in increased trend in SGK-1 mRNA levels which is the one of the downstream targets of MR. However, an inhibitory action of this complex was observed in T-47D and MDA-MB-231 cells. We proposed that E2 stimulated actions were distributed to ENaC possibly through an MR regulated mechanism in ER (+) breast cancer cells. But the MR is not stimulated thus the actions could be ligand-independent or just depend on the ER. For ER (-) breast cancer cells, we could not detect any changes suggesting that ER was need for seing the effect on MR downstream targets with or without the effect on MR (Figure 4.1). Future studies will focus on fine-tuning the expression changes in the suggested model by using MR overexpressing cells as well as use of E2 together with ALDO to test the synergistic and/or antagonistic effects of ligands on the crosstalk of nuclear receptors.

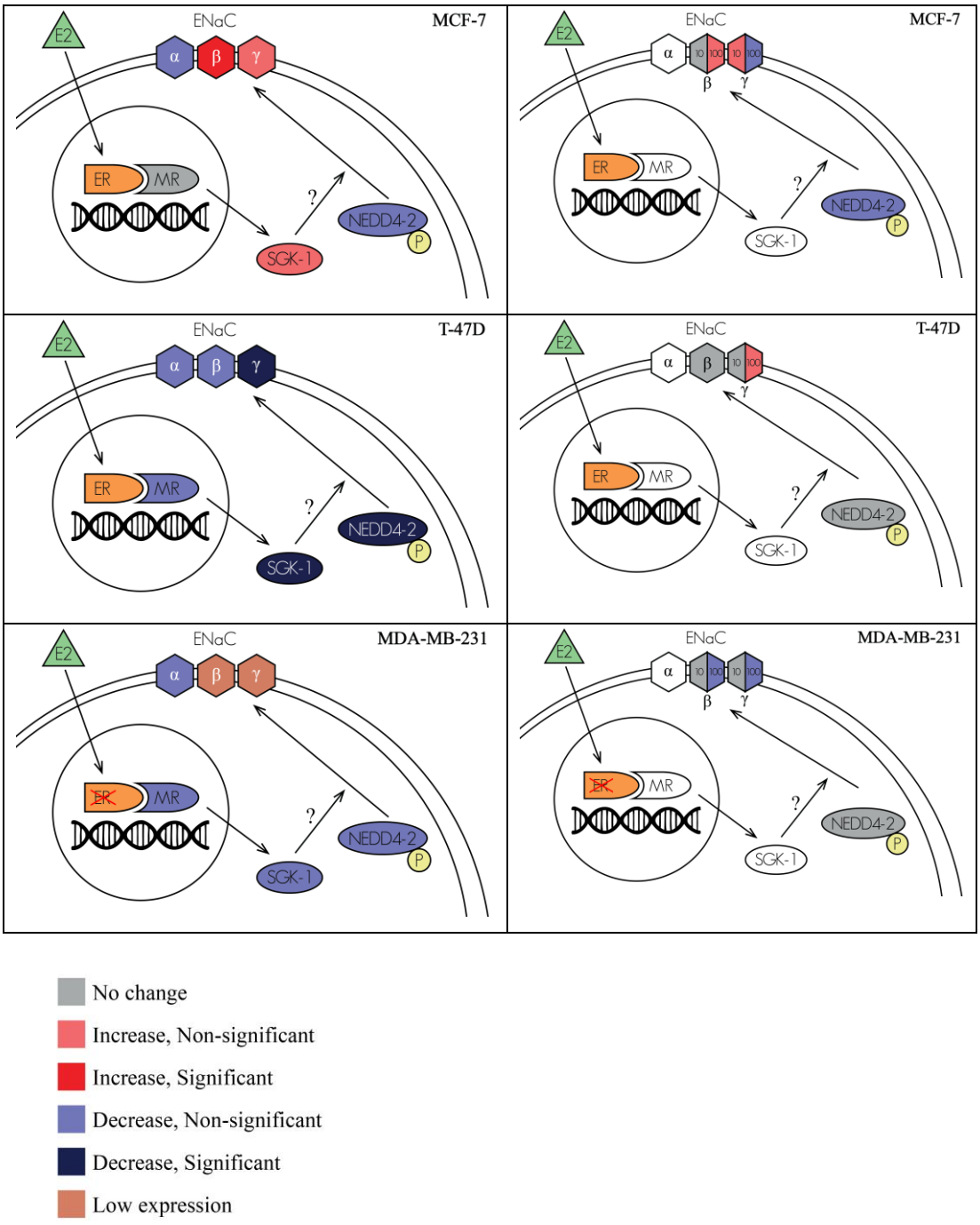

No change
Increase, Non-significant
Increase, Significant
Decrease, Non-significant
Decrease, Significant
Low expression

Figure 4.1: Alterations in expression levels of MR and its downstream targets in response to E2 across ER (+) (MCF-7, T-47D) and ER (-) (MDA-MB-231) breast cancer cells. Left panel shows gene expression changes at mRNA levels. Right panel shows gene expression changes at protein level.

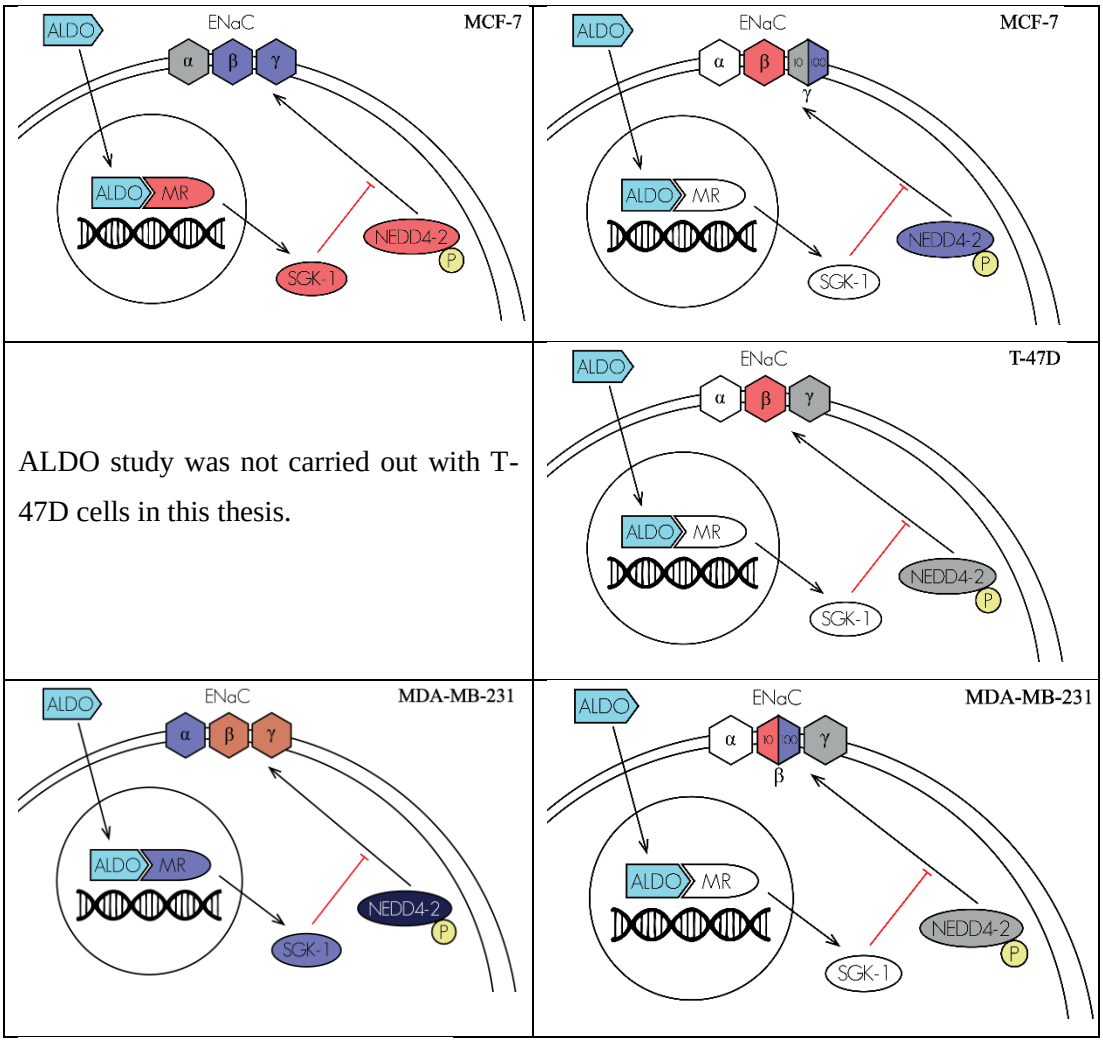

Figure 4.2: Alterations in expression levels of MR and its downstream targets in response to ALDO across ER (+) (MCF-7, T-47D) and ER (-) (MDA-MB-231) breast cancer cells. Left panel shows gene expression changes at mRNA levels. Right panel shows gene expression changes at protein level.

Chapter 5

Future Perspectives

In line with our first aim, we demonstrated MR and GR expression at the protein level was differential across multiple breast cancer subtypes. Inclusion of protein samples from normal mammary epithelial cells might help also assess whether there is relatively lower expression of MR and/or GR in tumors when compared with tumors.

When we detect expression patterns of MR and its downstream targets, we had not validated the presence of two bands representing two splice variant of NEDD4-2 with additional experiments. Since the proposed NEDD4-2 isoforms exhibit relatively distinct patterns based on ER status a larger panel of cell lines should be analyzed in the presence of NEDD4-2 RNAi or overexpression systems.

In this study, we showed that E2 serves as a possible modulator of some downstream targets of MR signaling though its downstream targets in breast cancer. We proposed an interaction mechanism of ER and MR in nucleus depending on previous findings about E2 and MR[117] in breast cancer as well. However, this requires further study and validation at different terms. Previous findings in kidney cells demonstrated that ER and MR are a part of protein complex and ER either directly binds to MR or indirectly effects its transcription. Thus, it is important to show specific interaction sites required for ER inhibitory action on MR in our study. For this purpose, mutations in functional domains of ER could be generated by site-directed mutagenesis in breast cancer cells as similar has been performed in kidney study[117]. On the other hand, we might perform a ChiP experiment to find out whether ER bind

any specific region on MR DNA or not. Furthermore, there could be other possibilities that explain the effect of E2 on MR downstream targets. E2 binds to ESR1 and this complex induces transcription of primary and secondary targets independent of other nuclear receptors. Thus SGK1, NEDD4-2 and ENaC subunits might have ERE in addition to mineralocorticoid binding sites or might interact with other targets of ESR1. Other possibilities include non-genomic actions of E2 as it is possible with MR (REF). Future studies should focus on E2 and ALDO exposure simultaneously to decipher the mechanism behind the crosstalk between ESR1 and MR and in addition to GR, thus cortisol can be a player in this as well.

Both for E2 and ALDO studies, we proposed a regulation model for MR and its downstream targets. Although it has been sown in other epithelial tissues that SGK1 disrupts inhibitory actions of NEDD4-2 on ENaC, we do not know whether this regulation between SGK1 and NEDD4-2 occur in breast cancer or not. This could be also important for ENaC regulation and ENaC mediated mechanisms that contributes tumor progression in breast cancer. Moreover, ENaC represented as an emerging target for cancer therapy and there are many studies indicating its role in invasion and metastasis. Since ENaC has been regulated by MR mediated ALDO/E2 mechanisms, future studies could reveal ENaC role in the context of breast cancer invasion and metastasis.

MR has been successfully overexpressed in MCF-7 cells by the present study. As we hypothesized that MR regulation has crucial role in breast cancer prognosis and diagnosis, MR-regulated downstream cellular processes in breast cancer could be investigated using highthroughput expression studies, e.g., a microarray study. In addition, as we detected a second band in higher concentrations of MR overexpression, posttranslational mechanisms leading to this appearance could be investigated in order to better understand MR regulatory mechanisms in breast cancer. Finally, ChIPSeq studies might help better quantify the association of E2 and ALDO alone or simultaneously in breast cancer cells overexpressing MR in the presence or absence of GR.

References

1. Caffarel, M. M., Pensa, S., Wickenden, J. A., & Watson, C. J. Molecular Biology of Breast Cancer (2011). In: eLS. John Wiley & Sons Ltd, Chichester.
2. Sting, J., Caldas, C. Molecular heterogeneity of breast carcinomas and the cancer stem cell hypothesis. Nature Reviews Cancer (2007), 7(10), 791-799.
3. Malhotra, G. K., Zhao, X., Band, H., Band, & V. Histological, molecular, and functional subtypes of breast cancers. Cancer Biology & Therapy (2010); 10(10), 955-960.
4. Weigelt, B., Horlings, H. M., Kreike, B., Hayes, M. M., Hauptmann, M., Wessels, L. F., de Jong, D., Van de Vijver, M.J., Van't Veer, L. J., & Peterse, J.L. Refinement of breast cancer classification by molecular characterization of histological special types. The Journal of Pathology (2008); 216:141-50.
5. Elston, C. W., & Ellis, I. O. Pathological prognostic factors in breast cancer. I. The value of histological grade in breast cancer: experience from a large study with long-term follow-up. Histopathology (1991); 19:403-10.
6. Ignatiadis, M., & Sotiriou, C. Understanding the molecular basis of histologic grade. Pathobiology (2008); 75:104-11.
7. Perou, C. M., Sorlie, T., Eisen, M. B., van de Rijn, M., Jeffrey, S. S., Rees, C. A., Pollack, J. R., Ross, D. T., Johnsen, H., Akslen, L. A., et al. Molecular portraits of human breast tumours. Nature (2000); 406, 747-52.
8. Stanišić V., Lonard D. M., O'Malley B. W., Chapter 9 - Modulation of Steroid Hormone Receptor Activity. Progress in Brain Research (2010); 181: 153-176.
9. Mangelsdorf, D. J., Thummel, C., Beato, M., Herrlich, P., Schutz, G., & et al. The nuclear receptor superfamily: the second decade. Cell (1995); 83:835–39
10. Kumar, R., & Thompson, E.B., Structure and functions of the nuclear hormone receptors. Steroids 64 (1999); 310–319.

11. Gronemeyer, H., Gustafsson, J. A., & Laudet, V. Principles for modulation of the nuclear receptor superfamily. Nature Reviews Drug Discovery 3 (2004); 950-964.
12. Lamers, C., Schubert-Zsilavecz, M., & Merk, D. Therapeutic modulators of peroxisome proliferator-activated receptors (PPAR); a patent review (2008-present). Expert Opinion on Therapeutic Patients (2012); 22:803–841.
13. Pascual-Garcia, M., & Valledor, A.F. Biological roles of liver X receptors in immune cells. Archivum Immunoliae et Therapiae Experimentalis (2012), 60, 235–249.
14. Verhoeven, G., Willems, A., Denolet, E., Swinnen, J. V., & De Gendt, K. Androgens and spermatogenesis: lessons from transgenic mouse models. Philosophical Transactions of the Royal Society B: Biological Sciences (2010); 365, 1537–1556
15. Beato, M., Herrlich, P., & Schütz, G. Steroid hormone receptors: Many Actors in search of a plot. Cell (1995); 83(6), 851-857.
16. Helsen, C. & Claessens, F. Looking at nuclear receptors from a new angle. Molecular and Cellular Endocrinology (2014); 382(1), 97-106.
17. Beato, M., Chávez, S., & Truss, M. Transcriptional regulation by steroid hormones. Steroids (1996) 61(4), 240-251.
18. Miller W. R., & Langdon S.P.. Steroid hormones and cancer: (III) Observations from human subjects, European Journal of Surgical Oncology (EJSO) (1997); 23(2), 163-177.
19. Schwartz, N., Verma, A., Bivens, C. B., Schwartz, Z., Boyan, B. D. Rapid steroid hormone actions via membrane receptors, Biochimica et Biophysica Acta (BBA) - Molecular Cell Research (2016), 1863(9), 2289-2298.
20. Distelhorst, C. W. Recent insights into the mechanism of glucocorticosteroid-induced apoptosis. Cell Death and Differentiation (2002); 9, 6-19.
21. Dehm, S. M., & Tindall, D. J. Molecular regulation of androgen action in prostate cancer. Journal of Cellular Biochemistry (2006); 99(2), 333-44.
22. Ahmad, N., & Kumar, R. Steroid hormone receptors in cancer development: A target for cancer therapeutics. Cancer Letters (2011); 300(1), 1-9.
23. Morrison, N., Harrap, S. B., Arriza, J. L., Boyd, E., & Connor, J. M. Regional chromosomal assignment of the human mineralocorticoid receptor gene to 4q31.1. Human Genetics (1990); 85, 130–132.

24. Zennaro, M.-C., Keightley, M.-C., Kotelevtsev, Y., Conway, G. S., Soubrier, F., & Fuller, P. J. Human Mineralocorticoid Receptor Genomic Structure and Identification of Expressed Isoforms. Journal of Biological Chemistry (1995); 270(36), 21016–21020.
25. Pascual-Le Tallec, L., & Lombes M. The Mineralocorticoid Receptor: A Journey Exploring Its Diversity and Specificity of Action. Molecular Endocrinology (2005); 19(9): 2211–2221.
26. Rossier, B. C., Pradervand, S., Schild, L., & Hummler, E. Epithelial sodium channel and the control of sodium balance: interaction between genetic and environmental factors. Annual Review of Physiology (2002); 64:877–97.
27. Sasano, H., Fukushima, K., Sasaki, I., Matsuno, S., Nagura, H., & Krozowski, Z. S. Immunolocalization of mineralocorticoid receptor in human kidney, pancreas, salivary, mammary and sweat glands: light and electron microscopic immunohistochemical study. Journal of Endocrinology (1992); 132, 305-310.
28. Caprio, M., Feve, B., Claes, A., Viengchareun, S., Lombes, M. & Zennaro, M. C. Pivotal role of the mineralocorticoid receptor in corticosteroid-induced adipogenesis. The FASEB Journal (2007); 21, 2185–2194.
29. Marzolla, V., Armani, A., Zennaro, M.-C., Cinti, F., Mammi, C., Fabbri, A., Rosano, G. M.C., & Caprio, M. The role of the mineralocorticoid receptor in adipocyte biology and fat metabolism. Molecular and Cellular Endocrinology (2012); 350(2) 281-288.
30. Gomez-Sanchez, E. P. Brain mineralocorticoid receptors: orchestrators of hypertension and end-organ disease. Current Opinion in Nephrology and Hypertension (2004); 13,191–196.
31. Fuller, P. J., & Young, M. J. Mechanisms of mineralocorticoid action. Hypertension. (2005); 46,1227–1235.
32. Rickard, A. J., Morgan, J., Tesch, G., Funder, J. W., Fuller P. J., & Young, M. J. Deletion of mineralocorticoid receptors from macrophages protects against deoxycorticosterone/salt-induced cardiac fibrosis and increased blood pressure. Hypertension (2009); 54, 537–543.
33. Fuller, J. P. Novel interactions of the mineralocorticoid receptor, Molecular and Cellular Endocrinology (2015); 408, 33-37.
34. Funder J. W. Why are mineralocorticoid receptors so nonselective? Current Hypertension Reports (2007); 9(2), 112–116.

35. Gomez-Sanchez, E. P. The mammalian mineralocorticoid receptor: tying down a promiscuous receptor. Experimental Physiology (2010); 95(1),13-8.
36. Edwards, C. R. W., Burt, D., McIntyre, M. A., De Kloet, E. R., Stewart, P. M., Brett, L., Sutanto, W. S., & Monder, C. Localisation of 11β-hydroxysteroid dehydrogenase-tissue specific protector of the mineralocorticoid receptor. American Journal of Physiology Lancet ii (1988), 986–989.
37. Farman, N., Rafestin-Oblin, M. Multiple aspects of mineralocorticoid selectivity. American Journal of Physiology - Renal Physiology (2001); 280 (2): F181-F192.
38. Binart, N., Lombes, M., & Baulieu, E. E. Distinct functions of the 90 kDa heat-shock protein (hsp90) in oestrogen and mineralocorticosteroid receptor activity: effects of hsp90 deletion mutants. Biochemical Journal (1995); 311 (Pt 3):797–804.
39. Rogerson, F. M., Yao Y. Z., Elsass, R. E., Dimopoulos, N., Smith, B. J., & Fuller P. J. A critical region in the mineralocorticoid receptor for aldosterone binding and activation by cortisol: evidence for a common mechanism governing ligand binding specificity in steroid hormone receptors. Molecular Endocrinology (2007); 21, 817–28.
40. Connell, J. M. C., & Davies, E. New biology of aldosterone. Journal of Endocrinology (2005); 186(1), 1-20.
41. Yang, J., Young, M. J. The mineralocorticoid receptor and its coregulators. Journal of Molecular Endocrinology (2009); 43(2), 53-64.
42. Faresse, N. Post-translational modifications of the mineralocorticoid receptor: How to dress the receptor according to the circumstances? The Journal of Steroid Biochemistry and Molecular (2014); 143, 334-342.
43. Faresse, N., Vitagliano, J.J., & O. Staub. Differential ubiquitylation of the mineralocorticoid receptor is regulated by phosphorylation. The FASEB Journal (2012); 22, 4373–4382.
44. Yokota, K., Shibata, H., Kobayashi, S., Suda, N., Murai, A., Kurihara, I., Saito, I., & Saruta T. Proteasome-mediated mineralocorticoid receptor degradation attenuates transcriptional response to aldosterone. Endocrine Research (2004); 30, 611–616.

45. Jeong, Y., Xie, Y., Xiao, G., Behrens, C., Girard, L., Witsuba, I. I., Minna, J. D., & Mangelsdorf, D.J. Nuclear receptor expression defines a set of prognostic biomarkers for lung cancer. PLoS Medicine (2010); 7(12):e1000378
46. Nie, H., Li, J., Yang, X. M., Cao, Q. Z., Feng, M. X., Xue, F., Wei, L., Qin, W., Gu, J., Xia, Q., & Zhang, Z. G. Mineralocorticoid Receptor Suppresses Cancer. Progression and the Warburg Effect by Modulating the miR-338-3p-PKLR Axis in Hepatocellular Carcinoma. Hepatology (2015); 62(4), 1145-59.
47. Tiberio, L., Nascimbeni, R., Villanacci, V., Casella, C., Fra, A., Vezzoli, V., & et al. The Decrease of Mineralcorticoid Receptor Drives Angiogenic Pathways in Colorectal Cancer. PLoS ONE (2013); 8(3).
48. Di Fabio, F., Alvarado, C., Majdan, A., Gologan, A., & et al. Underexpression of Mineralocorticoid Receptor in Colorectal Carcinomas and Association with VEGFR-2 Overexpression. Journal Gastrointestinal Surgery (2007); 11: 1521. doi:10.1007/s11605-007-0234-8
49. Conde, I., Paniagua, R., Fraile, B., Lucio, J., Arenas, M. I. Glucocorticoid receptor changes its cellular location with breast cancer development. Histology and Histopathology (2008); 23(1):77-85.
50. Hollenberg S. M., Weinberger C., Ong E. S., Cerelli, G., & et al. Primary structure and expression of a functional human glucocorticoid receptor cDNA. Nature (1985); 318, 635–641.
51. Zhou, J., Cidlowski, J. A. The human glucocorticoid receptor: one gene, multiple proteins and diverse responses. Steroids (2005); 70 (5–7), 407–17.
52. Breslin, M. B., Geng, C. D., Vedeckis, W. V. Multiple promoters exist in the human GR gene, one of which is activated by glucocorticoids. Molecular Endocrinology (2001); 15:1381–1395
53. Turner, J. D., & Muller, C. P. Structure of the glucocorticoid receptor (NR3C1) gene 5′ untranslated region: identification, and tissue distribution of multiple new human exon 1. Journal of Molecular Endocrinology (2005); 35, 283–292.
54. Sapolsky, R. M., Romero, L. M., & Munck, A. U. How Do Glucocorticoids Influence Stress Responses? Integrating Permissive, Suppressive, Stimulatory, and Preparative Actions. Endocrine Reviews (2000); 21(1), 55–89.
55. Barnes, P. J. Anti-inflammatory Actions of Glucocorticoids: Molecular Mechanisms. Clinical Science (1998); 94(6), 557–572.

56. Pratt, W. B. The role of heat shock proteins in regulating the function, folding, and trafficking of the glucocorticoid receptor. The Journal of Biological Chemistry (1993); 268(29), 21455–8.
57. Bamberger, C. M., Schulte, & H. M., Chrousos, G. P. Molecular determinants of glucocorticoid receptor function and tissue sensitivity to glucocorticoids. Endocrine Reviews (1996); 17(3), 245–61.
58. Yudt, M. R., & Cidlowski, J. A. The glucocorticoid receptor: coding a diversity of proteins and responses through a single gene. Molecular Endocrinology (2002); 16(8), 1719–26.
59. Nicolaides, N. C., Galata, Z., Kino, T., Chrousos, G. P., & Charmandari, E. The human glucocorticoid receptor: Molecular basis of biologic function. Steroids (2010); 75(1), 1–12.
60. Gottlicher, M., Heck, S., & Herrlich, P. Transcriptional crosstalk, the second mode of steroid hormone receptor action. Journal of Molecular Medicine (1998); 76, 480–9.
61. De Bosscher, K., Vanden Berghe, W., Haegeman, G. The interplay between the glucocorticoid receptor and nuclear factor-kappaB or activator protein-1: molecular mechanisms for gene repression. Endocrine Reviews (2003); 24, 488–522.
62. Bruna, A., Nicolàs, M., Muñoz, A., Kyriakis, J. M., & Caelles, C. Glucocorticoid receptor–JNK interaction mediates inhibition of the JNK pathway by glucocorticoids. The EMBO Journal (2003); 22(22), 6035–6044.
63. Leo, J. C. L., Guo, C., Woon, C. T., Aw, S. E., & Lin, V. C. L. Glucocorticoid and Mineralocorticoid Cross-Talk with Progesterone Receptor to Induce Focal Adhesion and Growth Inhibition in Breast Cancer Cells. Endocrinology (2004); 145(3), 1314–1321.
64. Karmakar, S., Jin, Y., & Nagaich, A. K. Interaction of Glucocorticoid Receptor (GR) with Estrogen Receptor (ER) α and Activator Protein 1 (AP1) in Dexamethasone-mediated Interference of ERα Activity. Journal of Biological Chemistry (2013); 288 (33), 24020–24034.
65. West, D. C., Pan, D., Tonsing-Carter, E. Y., Hernandez, K. M., Pierce, C. F., Styke, S. C., Conzen, S. D. GR and ER Coactivation Alters the Expression of Differentiation Genes and Associates with Improved ER + Breast Cancer Outcome. Molecular Cancer Research (2016); 14(8), 707 LP – 719.

66. McKay, L. I., Cidlowski, J. A. Corticosteroids in the Treatment of Neoplasms. Holland-Frei Cancer Medicine (6th Edition) (2003).
67. Moran, T. J., Gray, S., Mikosz C. A., Conzen S. D. The glucocorticoid receptor mediates a survival signal in human mammary epithelial cells. Cancer Research (2000); 60(4), 867–872.
68. Harris, R. A., Hiles, I. D., Page, M. J., & O'Hare, M. J. The induction of apoptosis in human mammary luminal epithelial cells by expression of activated c-neu and its abrogation by glucocorticoids. British Journal of Cancer (1995); 72(2), 386–392.
69. Mikosz, C. A., Brickley, D. R., Sharkey, M. S., Moran, T. W., & Conzen, S. D. Glucocorticoid Receptor-mediated Protection from Apoptosis Is Associated with Induction of the Serine/Threonine Survival Kinase Gene, SGK1. Journal of Biological Chemistry (2001); 276(20), 16649–16654.
70. Buxant, F., Kindt, N., Laurent, G., Noï J., & Saussez, S. Antiproliferative effect of dexamethasone in the MCF-7 breast cancer cell line. Molecular Medicine Reports (2015); (10), 4051–4054.
71. Conde, I., Paniagua, R., Fraile, B., Lucio, J., & Arenas, M. I. Glucocorticoid receptor changes its cellular location with breast cancer development. Histology and Histopathology (2008); 23(1), 77–85.
72. Matthews, L. C., Berry, A. A., Morgan, D. J., Poolman, T. M., Bauer, K., Kramer, F. Ray, D. W., & et al. Glucocorticoid receptor regulates accurate chromosome segregation and is associated with malignancy. Proceedings of the National Academy of Sciences (2015); 112(17), 5479–5484.
73. Pan, D., Kocherginsky, M., & Conzen, S. D. Activation of the glucocorticoid receptor is associated with poor prognosis in estrogen receptor-negative breast cancer. Cancer Research (2011); 71: 6360–6370.
74. Webster, M. K., Goya, L., Ge, Y., Maiyar, A. C., & Firestone, G. L. Characterization of sgk, a novel member of the serine/threonine protein kinase gene family which is transcriptionally induced by glucocorticoids and serum. Molecular and Cellular Biology (1993); 13(4), 2031–2040.
75. Kobayashi, T., Deak, M., Morrice, N., & Cohen, P. Characterization of the structure and regulation of two novel isoforms of serum and glucocorticoid-induced protein kinase. Biochemical Journal (1999); 344: 189–197.

76. Arencibia, J. M., Pastor-Flores, D., Bauer, A. F., Schulze, J. O., & Biondi, R. M. AGC protein kinases: From structural mechanism of regulation to allosteric drug development for the treatment of human diseases. Biochimica et Biophysica Acta (BBA) - Proteins and Proteomics (2013); 1834(7), 1302–1321.

77. Bhargava, A., Fullerton, M. J., Myles, K., Purdy, T. M., Funder, J. W., Pearce, D., & Cole, T. J. The serum- and glucocorticoid-induced kinase is a physiological mediator of aldosterone action. Endocrinology (2001); 142: 1587–1594.

78. Firestone, G. L., Giampaolo, J. R., and O'Keeffe, B. A. Stimulus-dependent regulation of the serum and glucocorticoid inducible protein kinase (Sgk) transcription, subcellular localization and enzymatic activity. Cellular Physiology and Biochemistry (2003); 13: 1–12.

79. Park, J., Leong, M. L., Buse, P., Maiyar A. C., Firestone, G. L., Hemmings, B. A. Serum and glucocorticoid-inducible kinase (SGK) is a target of the PI 3-kinase-stimulated signalling pathway. The EMBO Journal (1999); 18:3024–3033.

80. Chen, S. Y., Bhargava, A., Mastroberardino, L., Meijer, O. C., Wang, J., Buse, P., Pearce, D., & et al. Epithelial sodium channel regulated by aldosterone-induced protein sgk. Proceedings of the National Academy of Sciences of the United States of America (1999); 96(5), 2514–9.

81. Waldegger S., Barth P., Raber G., & Lang F. Cloning and characterization of a putative human serine/threonine protein kinase transcriptionally modified during anisotonic and isotonic alterations of cell volume. Proceedings of the National Academy of Sciences of the USA (1997); 94:4440–4445.

82. Brunet, A., Park, J., Tran, H., Hu, L. S., Hemmings, B. A., & Greenberg, M. E. Protein kinase SGK mediates survival signals by phosphorylating the forkhead transcription factor FKHRL1 (FOXO3a). Molecular and Cellular Biology (2001); 21(3), 952–65.

83. Adeyinka, A., Emberley, E., Niu, Y., Snell, L., Murphy, L. C., Sowter, H., Watson, P. H., & et al. Analysis of gene expression in ductal carcinoma in situ of the breast. Clinical Cancer Research (2002); 8(12), 3788–3795.

84. Sommer, E. M., Dry, H., Cross, D., Guichard, S., Davies, B. R., & Alessi, D. R. Elevated SGK1 predicts resistance of breast cancer cells to Akt inhibitors. The Biochemical Journal (2013); 452(3), 499–508.
85. Anan, T., Nagata, Y., Koga, H., Honda, Y., Yabuki, N., Miyamoto, C., Nakao, M., & et al. Human ubiquitin-protein ligase Nedd4: Expression, subcellular localization and selective interaction with ubiquitin-conjugating enzymes. Genes to Cells (1998); 3(11), 751–763.
86. Kumar, S., Harvey, K. F., Kinoshita, M., Copeland, N. G., Noda, M., & Jenkins, N. A. cDNA cloning, expression analysis and mapping of the mouse Nedd4 gene. Genomics (1997); 40, 435–443.
87. Umemura, M., Ishigami, T., Tamura, K., Sakai, M., Miyagi, Y., Nagahama, K., & et al. Transcriptional diversity and expression of NEDD4L gene in distal nephron. Biochemical and Biophysical Research Communications (2006); 339, 1129–1137.
88. Kimura, T., Kawabe, H., Jiang, C., Zhang, W., Xiang, Y. Y., Lu, C., Salter, M. W., Brose, N., Lu, W. Y., & Rotin, D. Deletion of the ubiquitin ligase Nedd4L in lung epithelia causes cystic fibrosis-like disease. Proceedings of the National Academy of Sciences of the U.S.A. (2011); 108, 3216–3221.
89. Staub, O., Dho, S., Henry, P., Correa, J., Ishikawa, T., McGlade, J., & Rotin, D. WW domains of Nedd4 bind to the proline-rich PY motifs in the epithelial Na+ channel deleted in Liddle's syndrome. The EMBO Journal (1996); 15(10), 2371–2380.
90. Cao, X. R., Lill, N. L., Boase, N., Shi, P. P., Croucher, D. R., Shan, H., Qu, J., Sweezer, E. M., Place, T., Kirby, P. A., Daly, R. J., Kumar, S., & Yang, B. Nedd4 controls animal growth by regulating IGF-1 signalling. Science Signaling (2008); 1 (38):ra5.
91. Zou, X., Levy-Cohen, G., & Blank, M. Molecular functions of NEDD4 E3 ubiquitin ligases in cancer. Biochimica et Biophysica Acta (BBA) - Reviews on Cancer (2015); 1856(1), 91–106.
92. Voilley, N., Lingueglia, E., Champigny, G., Mattéi, M. G., Waldmann, R., Lazdunski, M., & Barbry, P. The lung amiloride-sensitive Na+ channel: biophysical properties, pharmacology, ontogenesis, and molecular cloning. Proceedings of the National Academy of Sciences of the United States of America (1994); 91(1), 247–251.

93. Canessa, C. M., Schild, L., Buell, G., Thorens, B., Gautschi, I., Horisberger, J. D., & Rossier, B. C. Amiloride-sensitive epithelial Na+ channel is made of three homologous subunits. Nature (1994); 367:463–467.
94. Waldmann, R., Champigny, G., Bassilana, F., Voilley, N., & Lazdunski, M. Molecular cloning and functional expression of a novel amiloride-sensitive Na+ channel. Journal of Biological Chemistry (1995); 270, 27411–27414.
95. Benos, D. J., & Stanton, B. A. Functional domains within the degenerin/epithelial sodium channel (Deg/ENaC) superfamily of ion channels. The Journal of Physiology (1999); 520(Pt 3), 631–644.
96. Bentley P.J. Amiloride: a potent inhibitor of sodium transport across the toad bladder. The Journal of Physiology (1968); 195:317–330.
97. Garty H., & Palmer L.G. Epithelial sodium channels: function, structure, and regulation. Physiological Reviews (1997); 77:359–396.
98. Rotin, D., Kanelis, V., & Schild, L. Trafficking and cell surface stability of ENaC. American Journal of Physiology - Renal Physiology (2001); 281(3), F391 LP-F399.
99. Boyd, C., & Náray-Fejes-Tóth, A. Steroid-Mediated Regulation of the Epithelial Sodium Channel Subunits in Mammary Epithelial Cells. Endocrinology (2007); 148(8), 3958–3967.
100. Staub, O., Gautschi, I., Ishikawa, T., Breitschopf, K., Ciechanover, A., Schild, L. & Rotin, D. Regulation of stability and function of the epithelial Na+ channel (ENaC) by ubiquitination. The EMBO Journal (1997); 16: 6325–6336.
101. Hughey, R. P., Bruns, J. B., Kinlough, C. L., Harkleroad, K. L., Tong, Q., Carattino, M. D., Kleyman, T. R., & et al. Epithelial Sodium Channels Are Activated by Furin-dependent Proteolysis. Journal of Biological Chemistry (2004); 279(18), 18111–18114.
102. Bondarava M., Li T., Endl E., & Wehner F. α-ENaC is a functional element of the hypertonicity-induced cation channel in HepG2 cells and it mediates proliferation. Pflugers Archive European Journal of Physiology (2009); 458(4), 675–687.
103. Del M´onaco S. M., Marino G. I., Assef Y. A., Damiano A. E., & Kotsias B. A. Cell migration in BeWo cells and the role of epithelial sodium channels. Journal of Membrane Biology (2009); 232(1–3), 1–13.

104. H. Sontheimer, “Ion channels and amino acid transporters support the growth and invasion of primary brain tumours. Molecular Neurobiology (2004); 29(1), 61–71.
105. Amara S., Ivy M. T., Myles E. L., & Tiriveedhi, V. Sodium channel γENaC mediates IL-17 synergized high salt induced inflammatory stress in breast cancer cells. Cellular Immunology (2016); 302, 1–10.
106. Debonneville, C., Flores, S. Y., Kamynina, E., Plant, P. J., Tauxe, C., Thomas, M. A., Staub, O., & et. al. Phosphorylation of Nedd4-2 by Sgk1 regulates epithelial Na+ channel cell surface expression. The EMBO Journal (2001); 20(24), 7052–7059.
107. Staub, O., & Verrey, F. Impact of Nedd4 proteins and serum and glucocorticoid-induced kinases on epithelial Na+ transport in the distal nephron. Journal of the American Society of Nephrology: JASN (2005); 16(11), 3167–74.
108. Kuiper, G. G. J. M., Carlsson, B., Grandien, K., Enmark, E., Haggblad, J., Nilsson, S., & Gustafsson, J.-A. Comparison of the ligand binding specificity and transcript tissue distribution of estrogen receptors a and b. Endocrinology (1997); 138, 863–870.
109. Gosden, J. R., Middleton, P. G., & Rout, D. Localization of the human oestrogen receptor gene to chromosome 6q24–q27 by in situ hybridization. Cytogenetics and Cell Genetics (1986); 43, 218–220.
110. Kumar, V., Green, S., Stack, G., Berry, M., Jin, J.-R., & Chambon, P. Functional domains of the human estrogen receptor. Cell (1987); 51(6), 941–951.
111. Cong, B., Du, J., Zhu, X., Lu, J., & Ni, X. Estrogen enhancement of SGK1 expression induced by urocortin contributes to its cardioprotection against ischemia/reperfusion insult. International Journal of Cardiology (2015); Volume 178, 200 – 202.
112. Hall, B. A., Kim, T. Y., Skor, M. N., & Conzen, S. D. Serum and glucocorticoid-regulated kinase 1 (SGK1) activation in breast cancer: requirement for mTORC1 activity associates with ER-alpha expression. Breast Cancer Research and Treatment (2012); 135(2), 469–479.

113. Riazi S., Maric C., & Ecelbarger C. A. 17-beta Estradiol attenuates streptozotocin-induced diabetes and regulates the expression of renal sodium transporters. Kidney International (2006); 69:471-480.
114. Laube M., Küppers E., & Thome U. H. Modulation of sodium transport in alveolar epithelial cells by estradiol and progesterone. Pediatric Research (2011); 69:200-205.
115. Yang, G. Z., Nie, H. G., Lu, L., Chen, J., Lu, X. Y., Ji H. L., & Li, Q. N. Estrogen regulates the expression and activity of epithelial sodium channel in mouse osteoblasts. Cellular and Molecular Biology (2011); 57(Suppl), OL1480–OL1486.
116. Hamidi S. A., Dickman K. G., Berisha H., & Said S.I. 17β-estradiol protects the lung against acute injury: possible mediation by vasoactive intestinal polypeptide. Endocrinology (Dec, 2011); 152:4729–37.
117. Mueller, K. B., Lu, Q., Mohammad, N. N., Luu, V., McCurley, A., Williams, G. H., Adler, G. K., Karas, R. H., & Jaffe, I. Z. Estrogen Receptor Inhibits Mineralocorticoid Receptor Transcriptional Regulatory Function. Endocrinology (2014); 155(11), 4461–4472.
118. Masilamani, S., Kim, G.-H., Mitchell, C., Wade, J. B., & Knepper, M. A. Aldosterone-mediated regulation of ENaC α, β, and γ subunit proteins in rat kidney. Journal of Clinical Investigation (1999); 104(7), R19–R23.
119. Alnemri, E. S., Maksymowych, A. B., Robertson, N. M., & Litwack, G. Overexpression and characterization of the human mineralocorticoid receptor. Journal of Biological Chemistry (1991); 266(27), 18072–18081.
120. Fejes-Tóth, G., & Náray-Fejes-Tóth, A. Early aldosterone-regulated genes in cardiomyocytes: Clues to cardiac remodelling. Endocrinology (2007); 148(4), 1502–1510.
121. Jeong, Y., Xie, Y., Xiao, G., Behrens, C., Girard, L., Wistuba, I. I., Minna, J. D., & Mangelsdorf, D. J. Nuclear receptor expression defines a set of prognostic biomarkers for lung cancer. PLoS Medicine (2010); 7(12).
122. Carroll, J. S., Meyer, C. A., Song, J., Li, W., Geistlinger, T. R., Eeckhoute, J., Brown, M., & et al. Genome-wide analysis of estrogen receptor binding sites. Nature Genetics (2006); 38(11), 1289–1297.

123. Coser, K. R., Chesnes, J., Hur, J., Ray, S., Isselbacher, K. J., & Shioda, T. Global analysis of ligand sensitivity of estrogen inducible and suppressible genes in MCF7/BUS breast cancer cells by DNA microarray. Proceedings of the National Academy of Sciences of the United States of America (2003); 100(24), 13994–9.

124. Rae, J. M., Johnson, M. D., Scheys, J. O., Cordero, K. E., Larios, J. M., & Lippman, M. E. GREB1 is a critical regulator of hormone dependent breast cancer growth. Breast Cancer Research and Treatment (2005); 92(2), 141–149.

125. Moggs, J. G., Murphy, T. C., Lim, F. L., Moore, D. J., Stuckey, R., Antrobus, K., Kimber, I., & Orphanides, G. Anti-proliferative effect of estrogen in breast cancer cells that re-express ERα is mediated by aberrant regulation of cell cycle genes. Journal of Molecular Endocrinology (2005); 34(2), 535–551.

126. Neve, R. M., Chin, K., Fridlyand, J., Yeh, J., Baehner, F. L., Fevr, T., Gray, J. W., & et al. A collection of breast cancer cell lines for the study of functionally distinct cancer subtypes. Cancer Cell (2006); 10(6), 515–527.

127. Dunn, D. M., Ishigami, T., Pankow, J., von Niederhausern, A., Alder, J., Hunt, S. C., Leppert, M. F., Lalouel, J., & Weiss, R. B. Common variant of human NEDD4L activates a cryptic splice site to form a frameshifted transcript. Journal of Human Genetics (2002); 47(12), 665–676.

128. Náray-Fejes-Tóth, A., Boyd C., & Fejes-Tóth G. Regulation of epithelial sodium transport by promyelocytic leukemia zinc finger protein. American Journal of Physiology Renal Physiology (Jul, 2008); 295(1): F18-26.

129. Snyder P. M., Olson D. R., & Thomas B. C. Serum and glucocorticoid-regulated kinase modulates Nedd4-2-mediated inhibition of the epithelial Na+ channel. The Journal of Biological Chemistry (Jan 4, 2002); 277(1):5-8.

130. Briet, M., & Schiffrin, E. L. Aldosterone: effects on the kidney and cardiovascular system. Nature Reviews Nephrology (2010); 6(5), 261–273.

131. Minghua Li, Zhi-Gang Xiong. Ion channels as targets for cancer therapy. Int J Physiol Pathophysiol Pharmacol (2011);3(2):156-166

132. Siguang Xu et. al. Potential Roles of Amiloride-Sensitive Sodium Channels in Cancer Development. BioMed Research International (2016), Article ID 2190216, 6 pages

133. Briet, M. & Schiffrin, E. L. Aldosterone: effects on the kidney and cardiovascular system. Nat. Rev. Nephrol. (2010) 6, 261–273.

134. Yamil R. Yusef, Warren Thomas, Brian J. Harvey. Estrogen increases ENaC activity via PKCδ signaling in renal cortical collecting duct cells. Physiological Reports May 2014, 2 (5) e12020.
135. Tingzhong Wang, Andrew Hogan-Cann et. al. Muscarinic Receptor Modulation of hERG Channels. Molecular Pharmacology June 1, 2014, 85 (6) 877-886
136. Minegishi, S., Ishigami, T., Kino, T., Chen, L., Nakashima-Sasaki, R., Araki, N., Umemura, S. An isoform of Nedd4-2 is critically involved in the renal adaptation to high salt intake in mice. Scientific Reports (2016), 6, 27137.
137. Shi-Xun Zhong, Guo-Hua Hu, Zhao-Hua Liu. Expression of ENaC, SGK1 and Nedd4 isoforms in the cochlea of guinea pig. Folia Histochemica et Cytobiologica (2014),Vol. 52, No. 2, pp. 144–148

Appendix

Appendix A: In silico results: E2 response of downstream targets of MR in ER (+) and ER (-) breast cancer cells

A)

Profile GDS3285 / 201739_at
Title Estrogen effect on breast cancer cell line: time course
Organism Homo sapiens

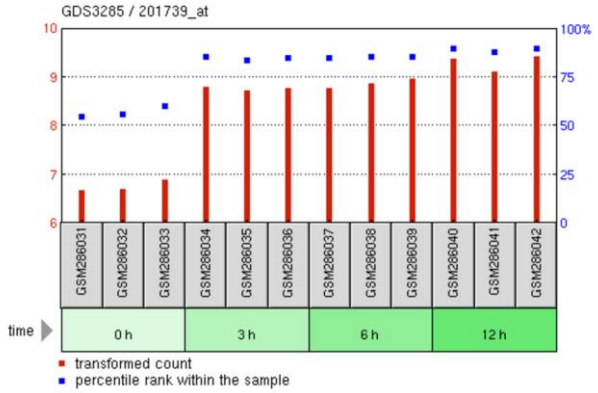

B)

Profile GDS3285 / 212445_s_at
Title Estrogen effect on breast cancer cell line: time course
Organism Homo sapiens

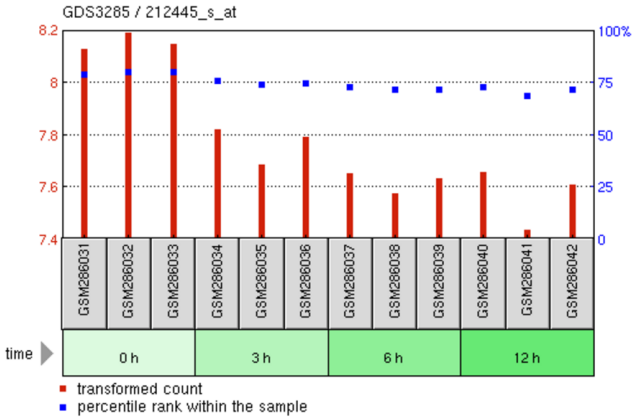

Appendix Figure 1: E2 effect on expression levels of SGK1 and NEDD4-2 mRNA in MCF-7 cells. **A.** Changes in SGK1 expression **B.** Changes in NEDD4-2 expression.

A)

Profile GDS2323 / 201739_at
Title Estrogen-starved breast cancer cell line: time course
Organism Homo sapiens

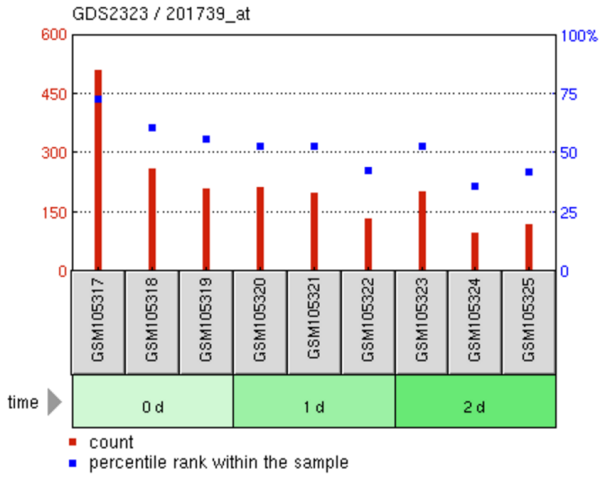

B)

Profile GDS2323 / 212445_s_at
Title Estrogen-starved breast cancer cell line: time course
Organism Homo sapiens

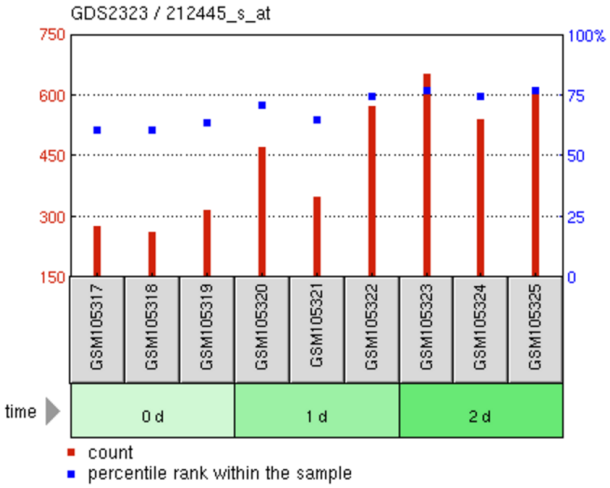

Appendix Figure 2: Changes in expression levels of SGK1 and NEDD4-2 mRNA in response to E2 starvation in MCF-7 cells. **A.** Changes in SGK1 expression **B.** Changes in NEDD4-2 expression.

A)

Profile GDS1549 / 201739_at

Title Estrogen effect on estrogen receptor alpha positive breast cancer cell lines

Organism Homo sapiens

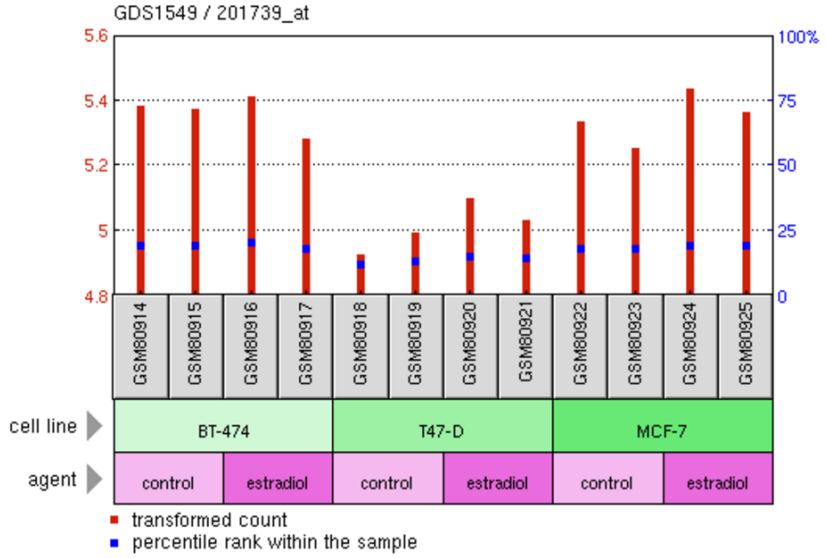

B)

Profile GDS1549 / 212445_s_at

Title Estrogen effect on estrogen receptor alpha positive breast cancer cell lines

Organism Homo sapiens

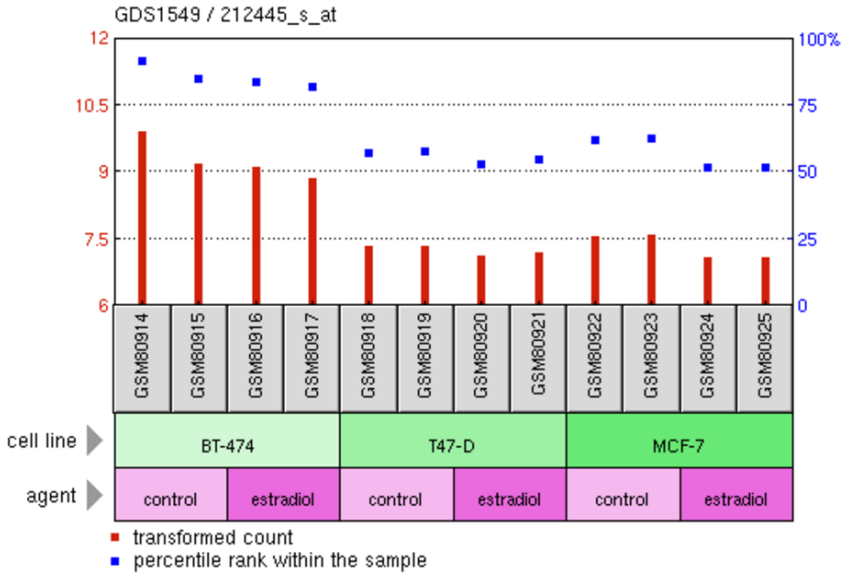

Appendix Figure 3: Changes in expression levels of SGK1 and NEDD4-2 in response to E2 in MCF-7, T-47D and BT-474 cells. **A.** SGK1 expression **B.** NEDD4-2 expression.

A)

Profile GDS3285 / 203453_at
Title Estrogen effect on breast cancer cell line: time course
Organism Homo sapiens

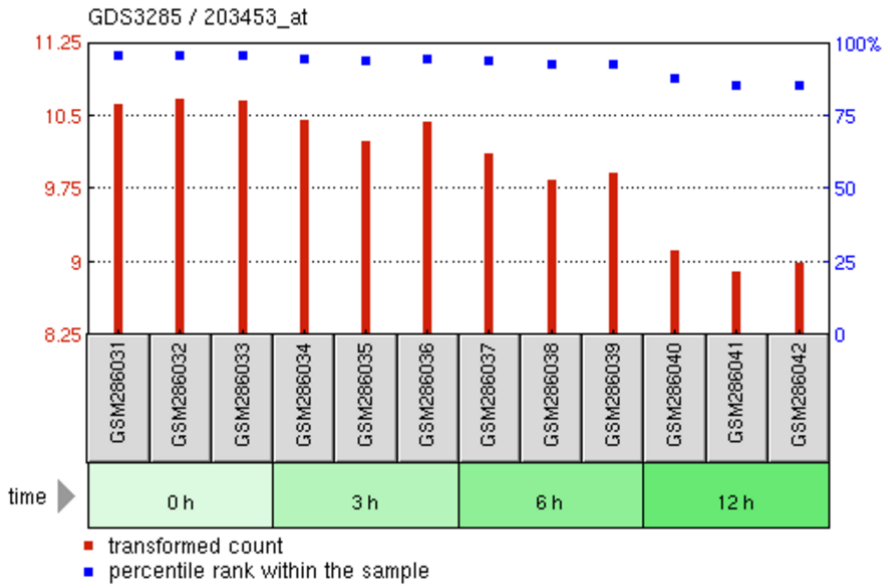

B)

Profile GDS3285 / 205464_at
Title Estrogen effect on breast cancer cell line: time course
Organism Homo sapiens

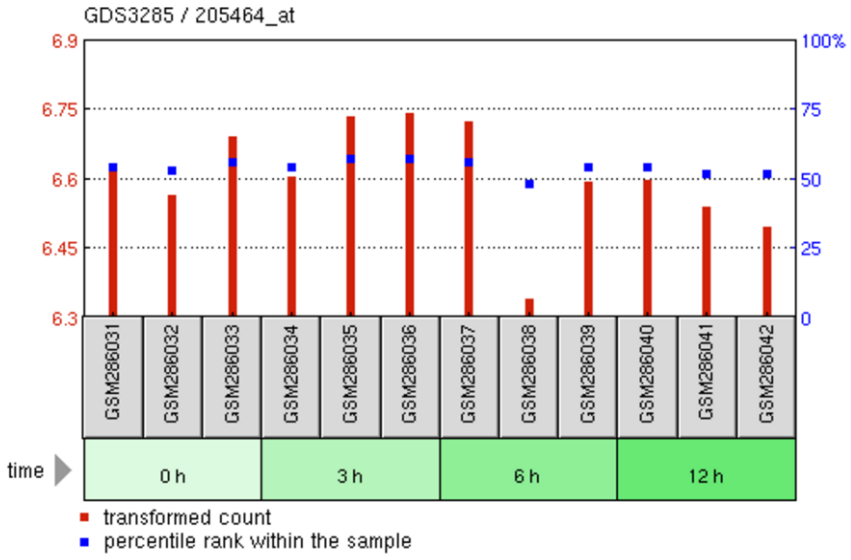

C)

Profile GDS3285 / 207295_at
Title Estrogen effect on breast cancer cell line: time course
Organism Homo sapiens

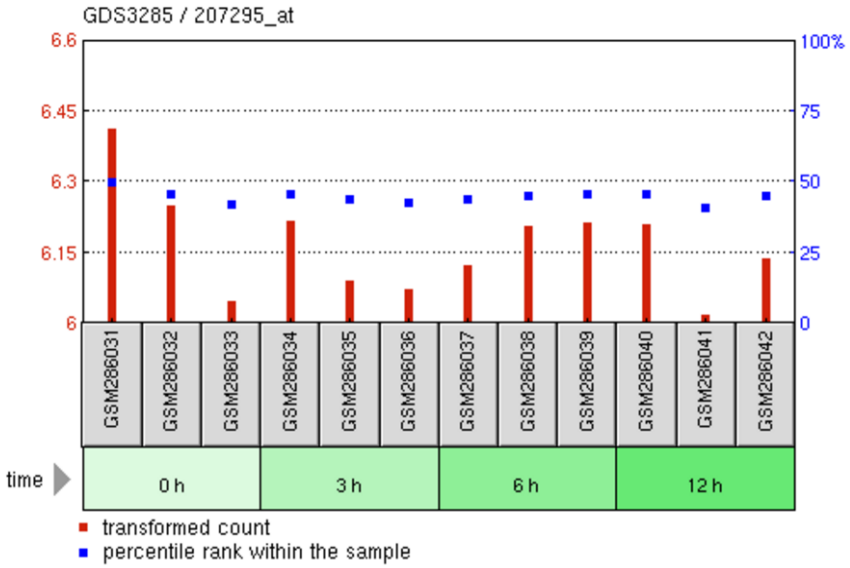

Appendix Figure 4: E2 effect on expression levels of ENaC subunits (namely α, β and γ) mRNA in MCF-7 cells. **A.** αENaC expression **B.** βENaC expression **C.** γENaC expression

A)

Profile GDS2323 / 203453_at
Title Estrogen-starved breast cancer cell line: time course
Organism Homo sapiens

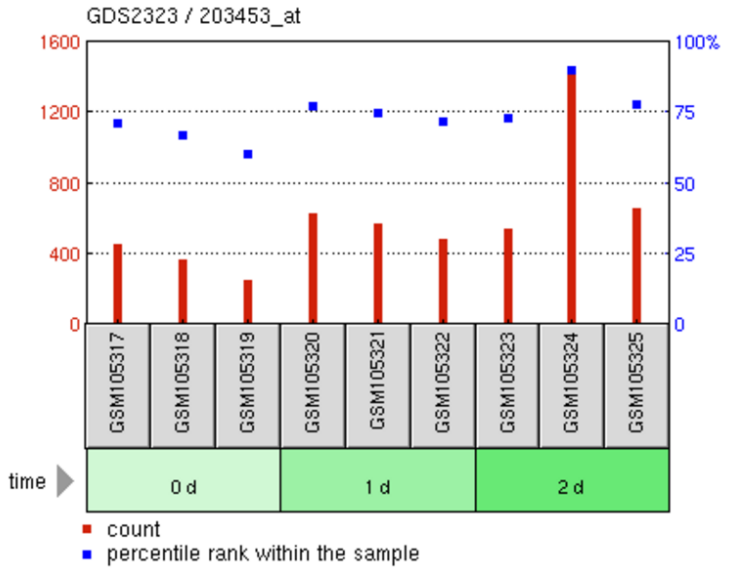

B)

Profile GDS2323 / 205464_at
Title Estrogen-starved breast cancer cell line: time course
Organism Homo sapiens

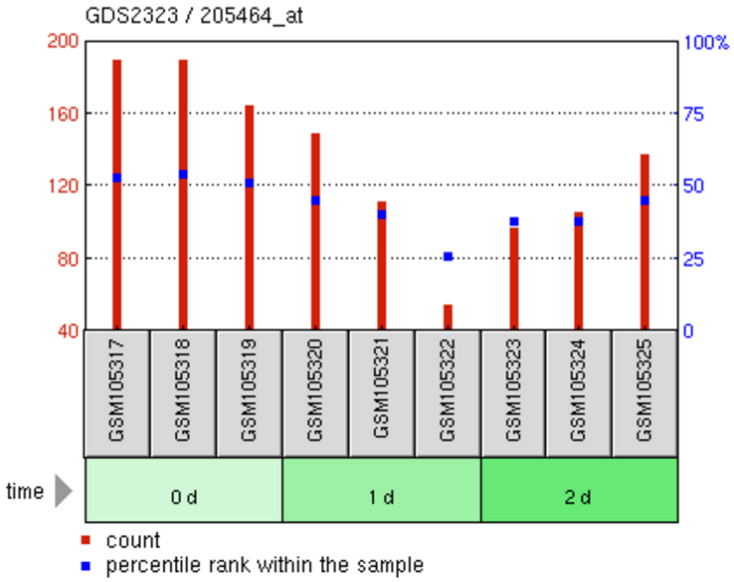

C)

Profile GDS2323 / 207295_at
Title Estrogen-starved breast cancer cell line: time course
Organism Homo sapiens

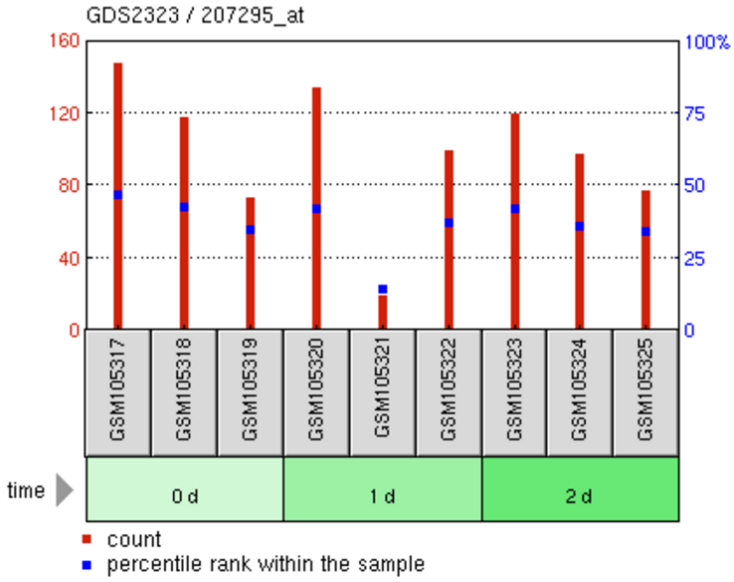

Appendix Figure 5: Changes in expression levels of ENaC subunits (α, β and γ) mRNA in response to E2 starvation in MCF-7 cells. **A.** αENaC expression **B.** βENaC expression **C.** γENaC expression

A)

Profile GDS1549 / 203453_at
Title Estrogen effect on estrogen receptor alpha positive breast cancer cell lines
Organism Homo sapiens

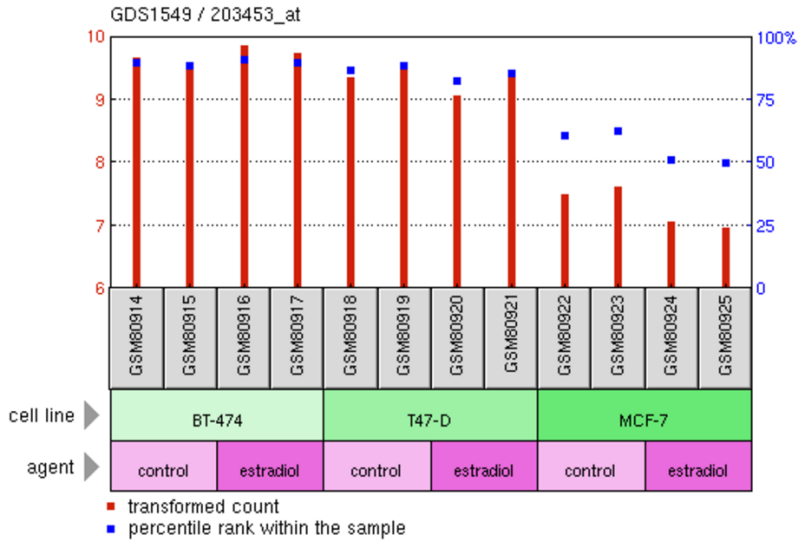

B)

Profile GDS1549 / 205464_at

Title Estrogen effect on estrogen receptor alpha positive breast cancer cell lines

Organism Homo sapiens

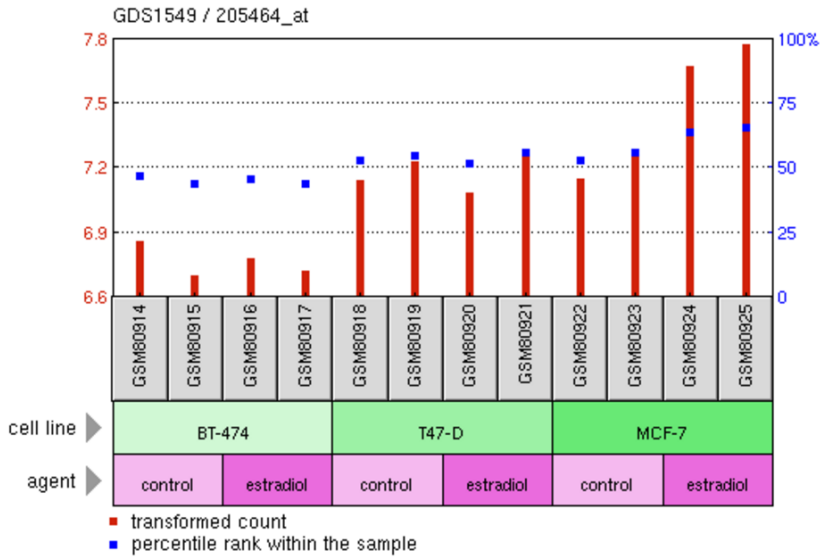

C)

Profile GDS1549 / 207295_at

Title Estrogen effect on estrogen receptor alpha positive breast cancer cell lines

Organism Homo sapiens

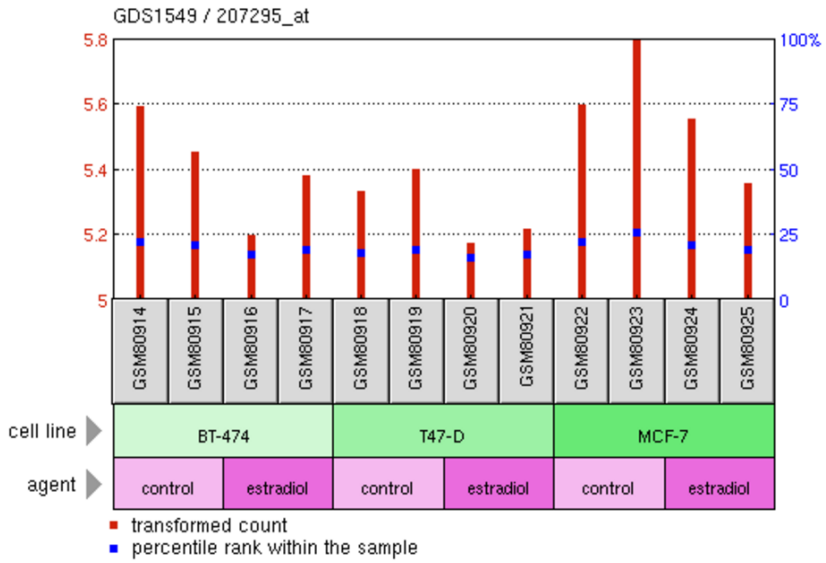

Appendix Figure 6: Changes in expression levels of ENaC subunits (α, β and γ) mRNA in response to E2 in MCF-7, T-47D and BT-474 cells. **A.** αENaC expression **B.** βENaC expression **C.** γENaC expression

A)

Profile GDS1326 / 201739_at

Title Breast cancer cells reexpressing estrogen receptor alpha response to 17beta-estradiol

Organism Homo sapiens

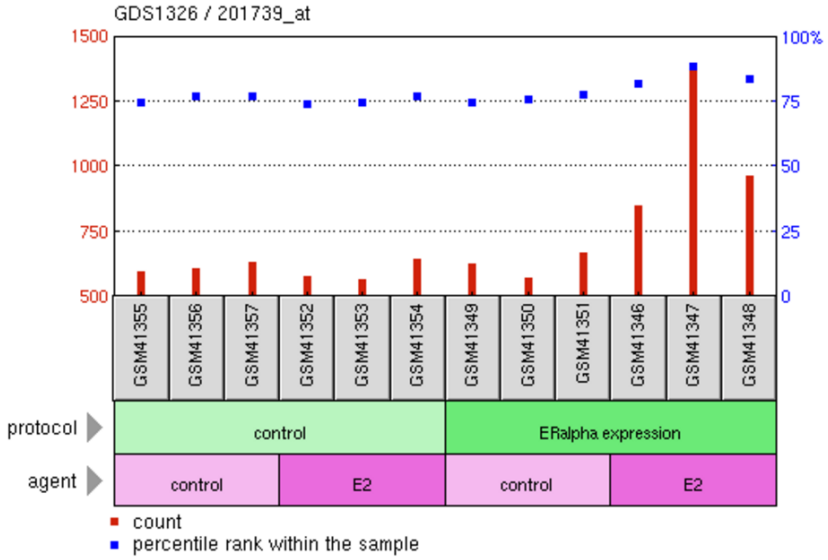

B)

Profile GDS1326 / 212445_s_at

Title Breast cancer cells reexpressing estrogen receptor alpha response to 17beta-estradiol

Organism Homo sapiens

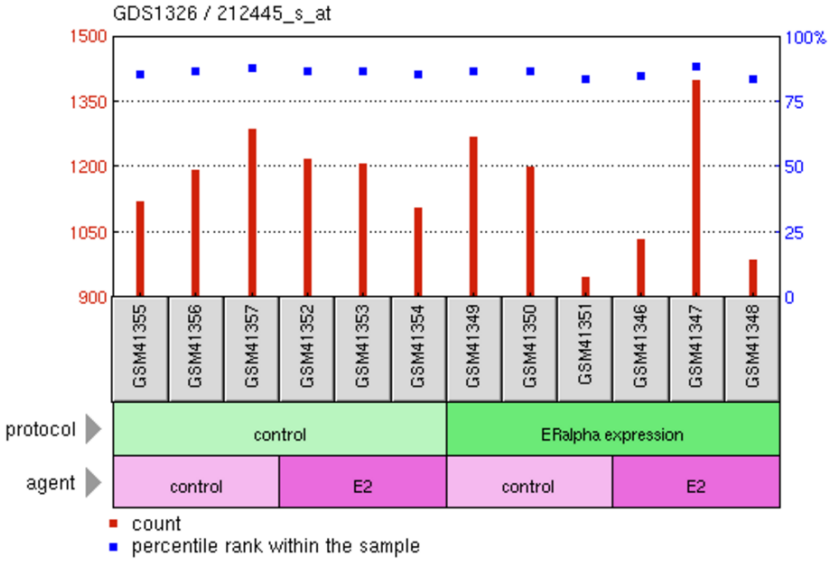

Appendix Figure 7: Changes in expressions of SGK1 and NEDD4-2 in MDA-MB-231 cells treated with 10 nM E2 for 48 hrs. **A.** SGK1 expression **B.** NEDD4-2 expression.

A)

Profile GDS1326 / 203453_at

Title Breast cancer cells reexpressing estrogen receptor alpha response to 17beta-estradiol

Organism Homo sapiens

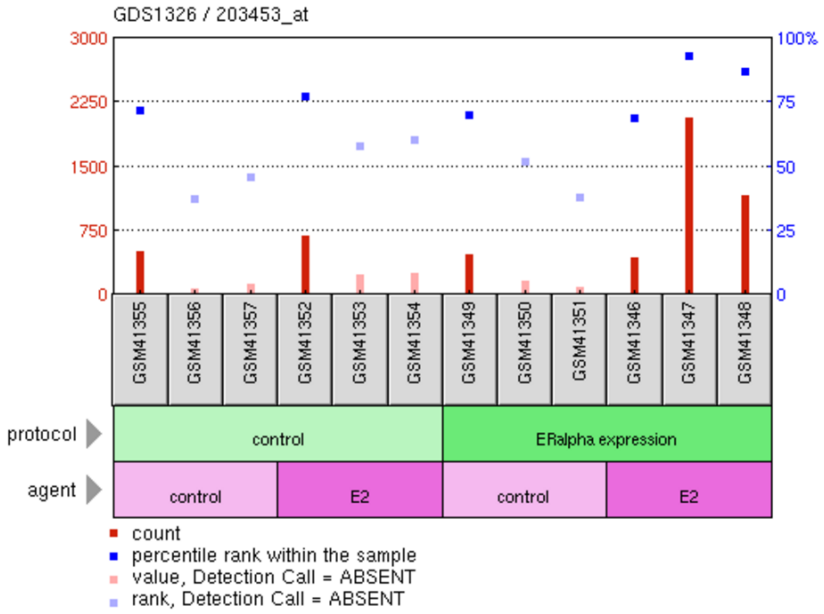

B)

Profile GDS1326 / 205464_at

Title Breast cancer cells reexpressing estrogen receptor alpha response to 17beta-estradiol

Organism Homo sapiens

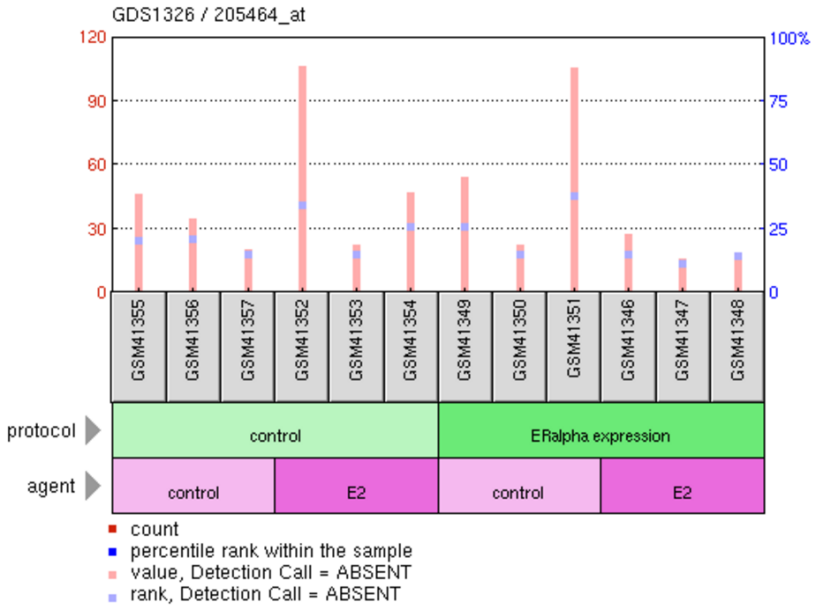

C)

Profile GDS1326 / 207295_at

Title Breast cancer cells reexpressing estrogen receptor alpha response to 17beta-estradiol

Organism Homo sapiens

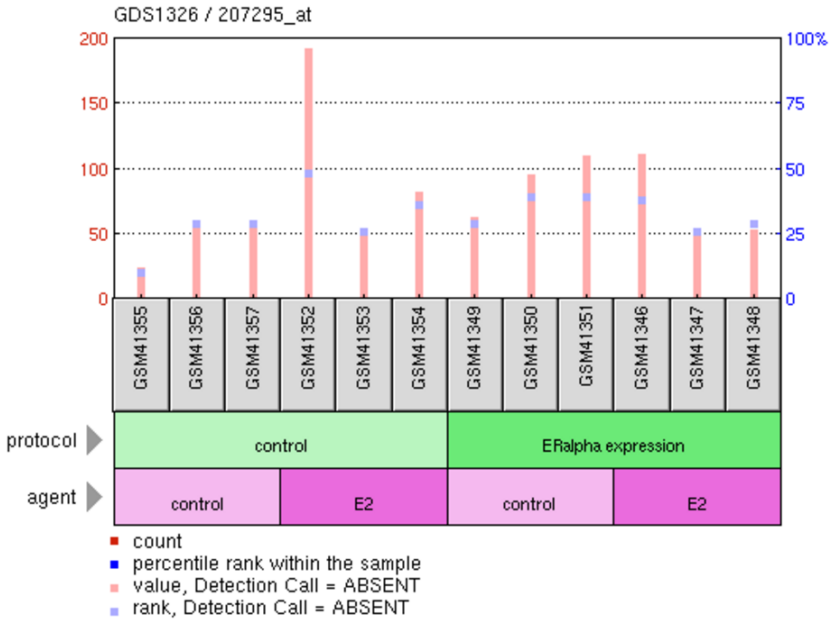

Appendix Figure 8: Changes in expression levels of ENaC subunits (α, β and γ) mRNA in response to E2 in MDA-MB-231 cells. **A.** αENaC expression **B.** βENaC expression **C.** γENaC expression

Appendix B: Copyright Permissions

No copyright permissions were required for Figure 1.1 and Table 1.2.

Copyright permission for Figure 1.2

NATURE PUBLISHING GROUP LICENSE TERMS AND CONDITIONS

Nov 06, 2016

This Agreement between bircan coban ("You") and Nature Publishing Group ("Nature Publishing Group") consists of your license details and the terms and conditions provided by Nature Publishing Group and Copyright Clearance Center.

License Number	3983181452977
License date	Nov 06, 2016
Licensed Content Publisher	Nature Publishing Group
Licensed Content Publication	Nature Reviews Drug Discovery
Licensed Content Title	Present and future drug treatments for chronic kidney diseases: evolving targets in renoprotection
Licensed Content Author	Norberto Perico, Ariela Benigni and Giuseppe Remuzzi
Licensed Content Date	Oct 10, 2008
Licensed Content Volume Number	7
Licensed Content Issue Number	11
Type of Use	reuse in a dissertation / thesis
Requestor type	academic/educational
Format	print and electronic
Portion	figures/tables/illustrations
Number of figures/tables/illustrations	1
High-res required	no
Figures	Figure 2: Mechanisms of aldosterone-induced kidney damage
Author of this NPG article	no
Your reference number	
Title of your thesis / dissertation	Regulation of Mineralocorticoid Receptor and its downstreamtargets by Estrogen and Aldosterone in breast cancer
Expected completion date	Nov 2016
Estimated size (number of pages)	150
Requestor Location	bircan coban Bilkent University Main Campus MBG department Bilkent, Cankaya Ankara, 06800 Turkey Attn: Bircan COBAN
Billing Type	Invoice
Billing Address	bircan coban Bilkent University Main Campus MBG department Bilkent Cankaya Ankara, Turkey 06800 Attn: Bircan COBAN
Total	0.00 USD

Copyright permission for Figure 1.3.

NATURE PUBLISHING GROUP LICENSE TERMS AND CONDITIONS

Nov 06, 2016

This Agreement between bircan coban ("You") and Nature Publishing Group ("Nature Publishing Group") consists of your license details and the terms and conditions provided by Nature Publishing Group and Copyright Clearance Center.

License Number	3983190339636
License date	Nov 06, 2016
Licensed Content Publisher	Nature Publishing Group
Licensed Content Publication	Nature Reviews Nephrology
Licensed Content Title	Aldosterone: effects on the kidney and cardiovascular system
Licensed Content Author	Marie Briet and Ernesto L. Schiffrin
Licensed Content Date	Mar 16, 2010
Licensed Content Volume Number	6
Licensed Content Issue Number	5
Type of Use	reuse in a dissertation / thesis
Requestor type	academic/educational
Format	print and electronic
Portion	figures/tables/illustrations
Number of figures/tables/illustrations	1
High-res required	no
Figures	Figure 1: Regulation of ENaC by aldosterone.
Author of this NPG article	no
Your reference number	
Title of your thesis / dissertation	Regulation of Mineralocorticoid Receptor and its downstreamtargets by Estrogen and Aldosterone in breast cancer
Expected completion date	Nov 2016
Estimated size (number of pages)	150
Requestor Location	bircan coban Bilkent University Main Campus MBG department Bilkent, Cankaya Ankara, 06800 Turkey Attn: Bircan COBAN
Billing Type	Invoice
Billing Address	bircan coban Bilkent University Main Campus MBG department Bilkent Cankaya Ankara, Turkey 06800 Attn: Bircan COBAN
Total	0.00 USD